

ENGINEERING RESEARCH INSTITUTE
THE UNIVERSITY OF MICHIGAN
ANN ARBOR

Report No. AFSWP-704

DIFFRACTION OF A MACH STEM SHOCK OVER A SQUARE BLOCK

Eugene B. Turner
Walter R. Johnson
Donald L. Upham
Robert D. Burgess
John A. Green

Otto Laporte
Supervisor

Project 2241

OFFICE OF NAVAL RESEARCH, U. S. NAVY DEPARTMENT
CONTRACT NO. Nonr-1224 (04)

January 1956

TABLE OF CONTENTS

	Page
LIST OF FIGURES	iii
OBJECTIVE	iv
I. INTRODUCTION	1
II. MACH REFLECTION	3
III. DIFFRACTION	5
IV. EXPERIMENTS	8
V. DATA REDUCTION	10
APPENDIX	14

LIST OF FIGURES

Fig.	Page
1. Shock tube.	1
2. Mach reflection at the wedge tip.	2
3a. Sound reflection.	4
3b. Shock reflection.	4
4. Regions where regular reflection may and may not occur.	5
5. Sound waves produced for interaction with Mach stem initially twice the height of block.	6
6. Interaction for Mach stem initially one-half block height.	7
7. Monochromatic no-flow fringes.	10
8. Monochromatic flow fringes, $y = 1.2$, 75° angle of incidence, 1/2-in. Mach stem.	11
9. White-light fringe picture, taken simultaneously with picture in Fig. 8.	11

OBJECTIVE

The research work on this project is concerned with the experimental determination of the density fields around a model at various times after it is struck by a shock wave. The shock waves are produced in a shock tube and the density fields are determined from Mach-Zehnder interferometer photographs. The problems to be studied were requested by the Armed Forces Special Weapons Project; they are the diffraction of Mach stem shocks and regular shock reflections over a square block.

I. INTRODUCTION

This report describes the results of experiments done with the University of Michigan 2" x 7" shock at the request of the Armed Forces Special Weapons Project. These experiments were concerned with the effect of a "Mach" shock-wave configuration striking an object of square cross section.

The method of generating the Mach configuration, the diffraction pattern observed when this configuration interacts with the block, and the interpretation of this pattern will be described briefly below and in more detail later in the report.

The Mach configuration is generated by placing a wedge in the observing section of the shock tube. When the diaphragm separating the high- and low-pressure chambers of the tube is broken, a plane shock wave travels down the tube and strikes the wedge (see Fig. 1). If the angle of incidence

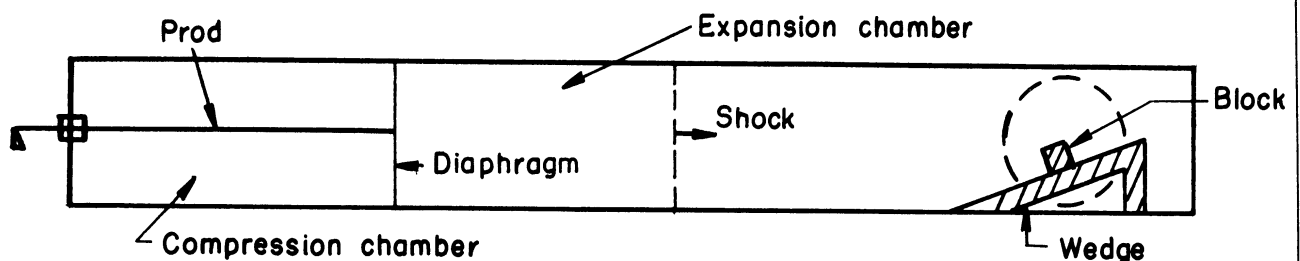


Fig. 1. Shock tube.

(angle between normal to shock and normal to wedge face) is sufficiently near 90° , the shock wave will break into a three-shock configuration commonly called a Mach configuration. This shock-wave configuration may be described as follows: The incident shock does not extend to the wedge, but at a point above the wedge, the triple point, it branches into two shocks. One of these, the Mach stem, extends down to the wedge and meets it normally, while the other, the reflected shock, extends from the triple point into the region behind the incident shock. There is also a density discontinuity which extends from the triple point into the region between the reflected shock and the Mach stem (see Fig. 2).

The pattern described above grows linearly in time about a point,

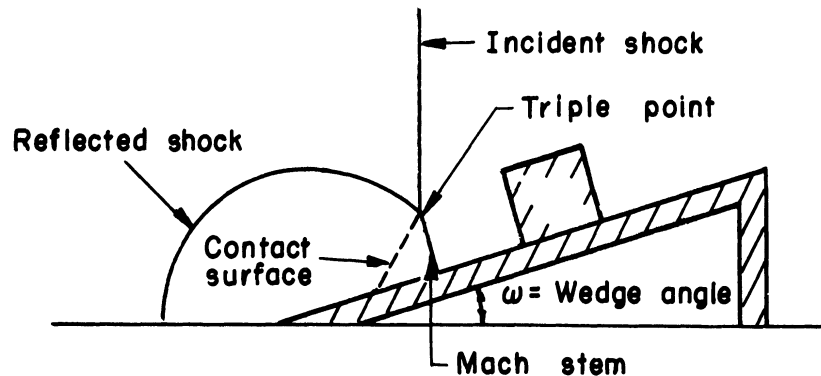


Fig. 2. Mach reflection at the wedge tip.

called the center of similarity. The center of similarity is, of course, not stationary but moves downstream with the gas behind the shock.

The experiments which were performed on the shock tube were not concerned directly with the generation of such a configuration, but with the interaction of the configuration with a block mounted on the wedge. Since the face of the block lies on the wedge surface, and since the Mach stem is normal to the wedge surface, the Mach stem will be parallel to the other block face. The incident shock on the other hand will make a small angle (90° angle of incidence) with the same block face. As the various shock waves which make up the Mach configuration strike the block, reflected shock waves will be generated which will interact with the other shock waves present as well as the block. This leads to a complicated situation which is difficult to predict, but which may be interpreted after the experiments have been performed.

The diffraction pattern is recorded with schlieren photographs and a Mach-Zehnder interferometer. The monochromatic fringe pattern is photographed before the shock tube is fired. The shock tube is then fired and pictures of the monochromatic fringes and the white-light fringes are simultaneously taken of the resulting shock-wave diffraction pattern.

When the two monochromatic interference patterns are carefully superimposed and observed over a light table, lines of constant fringe shift may be observed. Because of the relation between the fringe shift and the density, these lines are also lines of constant density, isopycnics, of the diffraction pattern. The white-light fringes allow one to determine the absolute fringe shift across the shock waves and thus the absolute density in the various regions of the field. Hence, one is able to measure experimentally the densities in the various regions of the diffraction pattern.

II. MACH REFLECTION

In these experiments we are considering the effect of a Mach configuration of shock waves interacting with a block. In order to determine what results are to be expected it is necessary to know something about the structure of the Mach configuration.

Before we discuss the shock-wave patterns it might be appropriate to discuss the behavior of a sound pulse striking the wedge, and to see in what fashion this behavior must be modified to account for the nonlinear nature of the shock wave. In other words, we would like to deduce qualitatively the behavior of a shock wave striking a wedge from the corresponding behavior of a sound wave.

The theory of the behavior of a sound wave striking a wedge is due to Keller and Blank and appears in Comm. in Pure and Applied Math, 4, 75 (1951).

Huygen's principle is applied to the sound pulse at the time the pulse strikes the wedge in order to determine the subsequent behavior. The result is that a circle of radius ct is generated about the wedge point, where c is the sound speed and t is the time. The incident sound pulse extends down to the wedge, where it is met by another sound pulse which makes an angle equal to the angle of incidence with the normal to the wedge. This pulse will be tangent to the circular pulse. This pattern expands in time about the wedge tip (see Fig. 3a).

If it is assumed that the relative pressure change across the incident pulse is of order ϵ , then the relative pressure change across the reflected shock will be equal to this, whereas there will be no discontinuity in pressure across the circular pulse.

Hence, the pressure is known in the field except for the interior of the circular wave, where it may be found by solving the wave equation. Keller and Blank solved this equation in their paper and found the pressure in this region.

If the initial pulse is finite in amplitude we will have to deal with shock waves instead of sound waves. The nonlinearity of the corresponding equations makes the solution of the problem very difficult. It is clear that for sufficiently weak shock waves the solution of the problem should be close to the sound-wave solution.

The first result to be noticed is that the shock wave induces a flow in the gas it passes over. This flow will cause the circular pattern to

move forward relative to the shock wave, and if the angle of incidence is sufficiently small the circular wave will actually intersect the incident wave. The part of the incident shock wave which lies below the point of intersection will become distorted since it is joining a region of constant pressure and density to a nonuniform region. This wave will be the Mach shock. It will evidently meet the wedge normally, since it must cause the disturbed flow velocity at the wedge to be parallel to the wedge. This shock is ordinarily approximated by a straight shock from the intersection to the wedge, normal to the wedge.

The circular wave is also disturbed. It becomes a finite shock wave which meets the incident and Mach shocks at the triple point. This leads to a configuration of three shocks meeting at a point, which is not possible according to hydrodynamic theory. Thus, it is necessary to introduce another discontinuity in the flow. The only possible place for this to occur is in the disturbed region between the circular shock and the wedge. This is called the contact surface (see Fig. 3b).

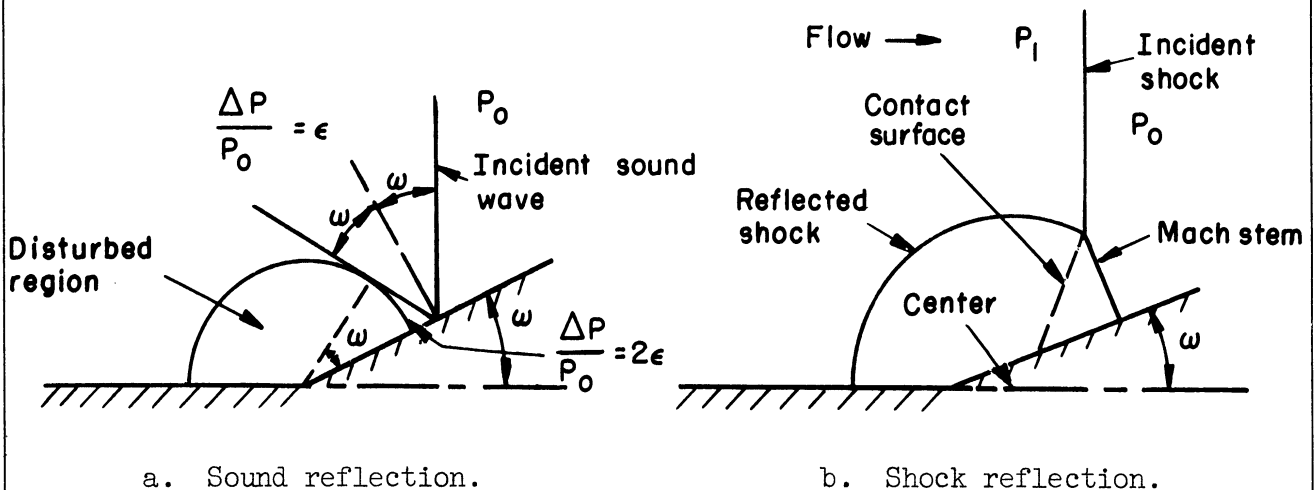


Fig. 3.

Thus, we have the ordinarily observed Mach configuration. The theory of Mach reflection of shock waves for small angles appears in the paper of M. J. Lighthill, Proceedings of the Royal Society, A198, 454 (1949).

In a sufficiently small region surrounding the triple point we may treat the various waves as if they were straight. In this case the problem may be completely solved giving the local behavior of the waves and gas in the vicinity of the triple point. The results appear in Courant and Freidrichs, Supersonic Flow and Shock Waves, Chapter IV. The most important result of such a study is that Mach reflection is not possible for any combination of angles and shock strengths but is limited as shown in Fig. 4.

From Fig. 4 it is seen that Mach reflection is limited to small wedge angles, and as the shock becomes weaker the angle of incidence necessary to produce Mach reflection becomes larger.

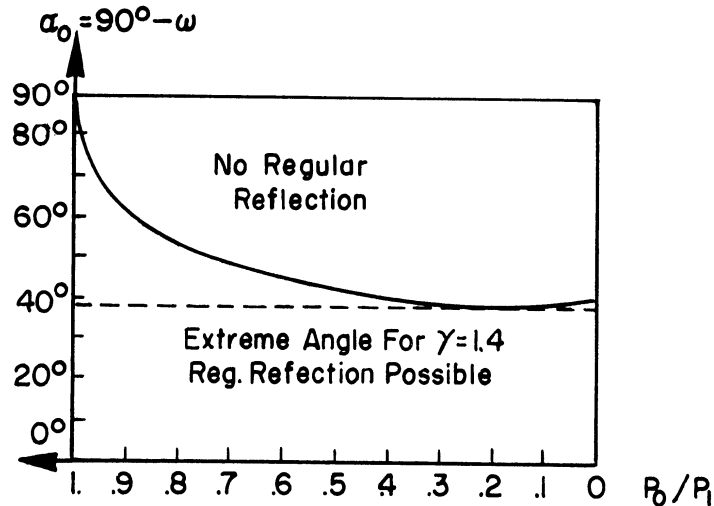


Fig. 4. Regions where regular reflection may and may not occur (Fig. 54, Courant-Freidrichs).

III. DIFFRACTION

In the experiments performed on the diffraction of the Mach configuration, the incident shock was relatively weak except in the case of the 30° wedge where $p_1/p_0 = 2$. If we omit this case from our considerations temporarily we may interpret the remaining patterns in terms of sound waves. In particular, we will neglect the contact surface and treat the other waves as linear.

For the 15° wedge and weak shocks there are two essentially different types of behavior. First is the behavior when the Mach stem is one-half the block height upon contact. The other case is when the Mach stem is either one or two times the block height.

Let us treat the latter case first, as it is the simpler. Let τ denote the distance of the triple point from the initial block face, in units of the block thickness, measured parallel to the wedge. For $\tau < 0$ there will be no interaction, and at $\tau = 0$ the interaction begins.

For $0 < \tau < 1$ the Mach stem which is the only wave to interact with the block will split into two parts. One will be reflected and the other transmitted. If we treat these as sound waves their speeds will be the same, but for shock waves the reflected wave will travel faster. A circular wave will be generated at $\tau = 0$. This wave will be tangent to both the incident and reflected waves. In the linear case this wave will have its center on the initial corner of the block, and in the case of finite shock waves the center of this wave will be blown downstream with the flow.

At $\tau = 1$ the Mach stem generates a circular wave upon interacting with the trailing edge of the block. The lower edge of the circular wave is reflected from the wedge surface and upon reflection generates another small circular wave from the corner between the wedge and block.

For $\tau > 1$ the waves produced thus far interact with the wedge and block and the wave pattern may be calculated by means of Huygen's principle (see Fig. 5).

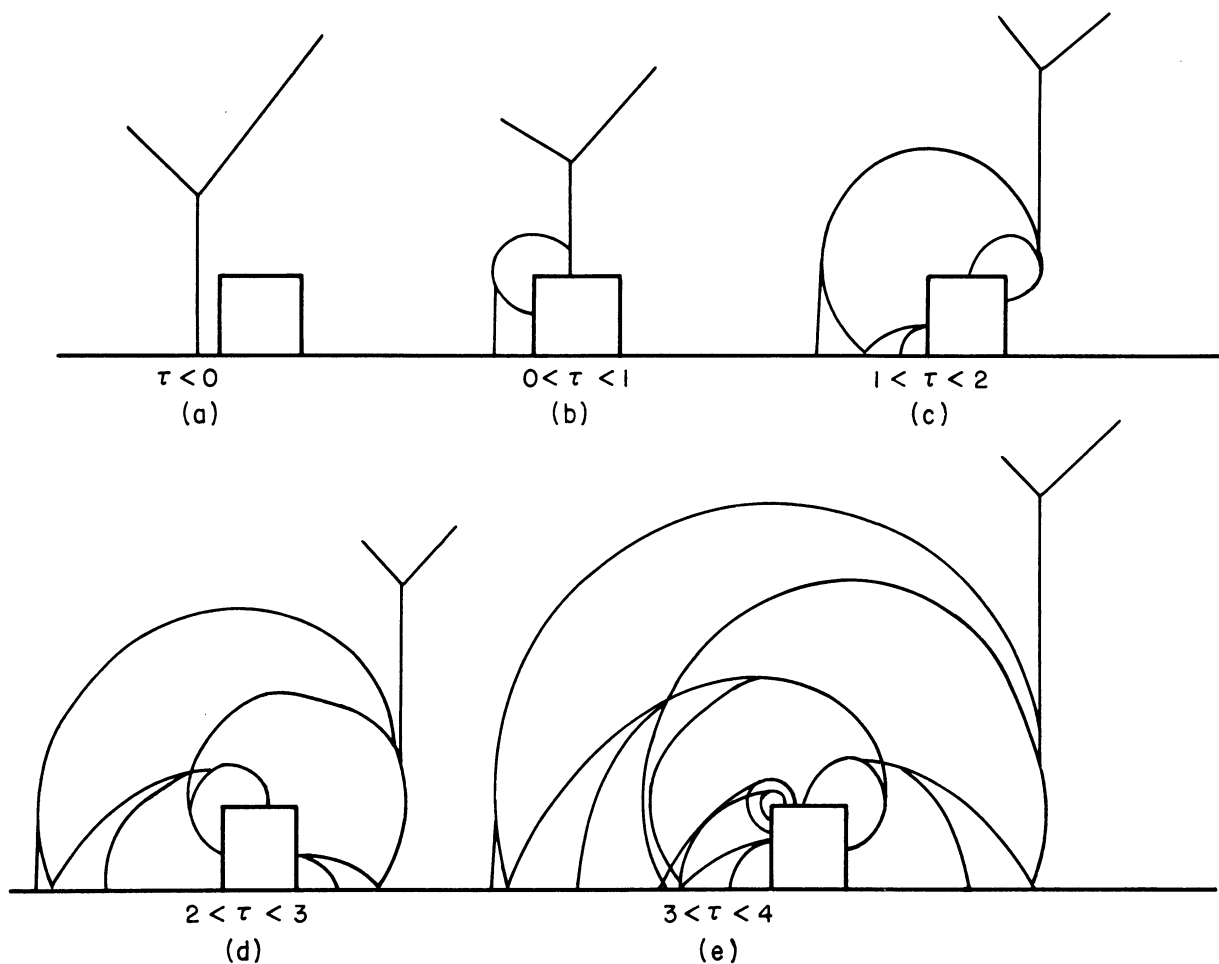


Fig. 5. Sound waves produced for interaction with Mach stem initially twice the height of block.

If we now consider the case of the Mach stem of one-half the block height at $\tau = 0$ interacting with the block, we see that the situation will be somewhat more complicated.

The incident shock will in this case be the first to strike the block. We will get the same Mach pattern at the top of the block as was observed when the shock struck the wedge, since the top surface of the block is parallel to the wedge surface. The pattern observed on the front surface of the block should be one of regular reflection.

For $\tau > 0$ the following will be observed. The Mach wave will move backward after reflection from the block. It will be joined at the top by a wave reflected from the reflected shock of the original configuration. The circular wave generated by the incident shock will continue to grow and join these other waves as shown in Fig. 6. For $\tau > 1$ these waves will interact according to Huygen's principle with the edges of the block and the wedge.

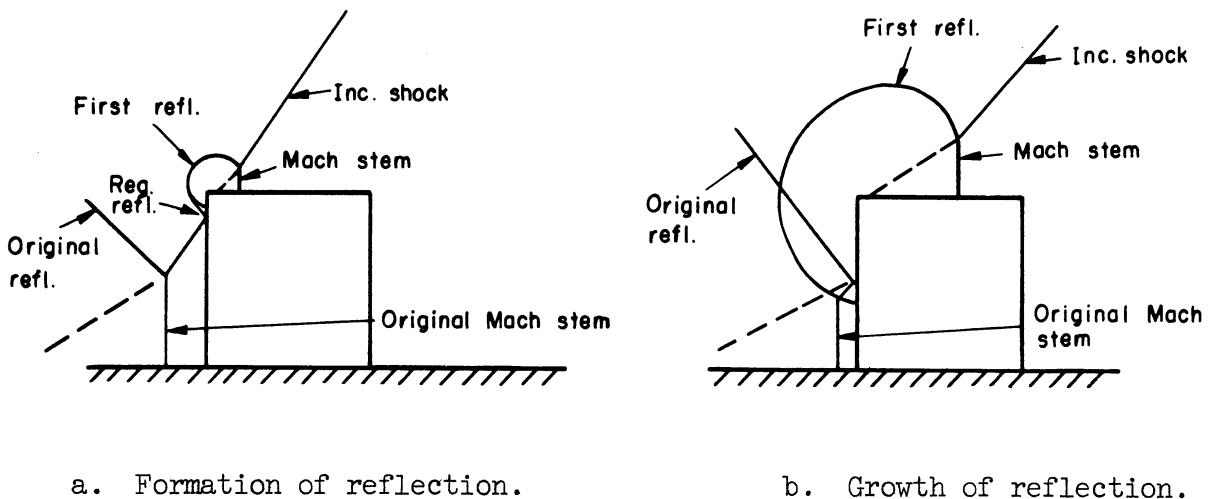


Fig. 6. Interaction for Mach stem initially one-half block height.

We might now mention the case of the 30° wedge in which case the shock strength p_1/p_0 of the initial wave equals 2. In this case the contact surface is evident. The shock is so strong in this case that a linear treatment is unreasonable.

Several features of this case might be pointed out though. First, it should be noted that a Mach configuration is generated when the incident shock strikes the block as above. The reflected shock of this configuration again interacts with the reflected shock of the original configuration as well as the contact surface. Second, it should be noted that temperature differences can be detected in various regions of the flow by noting the relative

speeds of a particular wave in several regions, e.g., on either side of the contact surface.

The detailed behavior of the gas in the various regions has not as yet been calculated theoretically, but the waves generated when a sound wave strikes the wedge can, of course, be treated by means of Huygen's principle as above. No progress at all has been made theoretically for such problems.

IV. EXPERIMENTS

The experiments consisted of nine series of shots. For each series we have included four schlieren pictures and several tracings of the isopycnics. All but one of these series was performed using a 15° wedge giving a 75° angle of incidence. The last series was performed using a 30° wedge. Table I gives the data for the various series including the block size, incident shock strength, and the height of the Mach stem at $\tau = 0$.

TABLE I

Series	Angle of Incidence, degree	Block Height, in.	Incident Pressure Ratio	Mach Stem Height, in.	Rel. Mach Stem Height, in.
I	75	1	1.17	1/2	1/2
II	75	1	1.17	1	1
III	75	1	1.22	1/2	1/2
IV	75	1	1.22	1	1
V	75	3/4	1.22	1-1/2	2
VI	75	1	1.33	1/2	1/2
VII	75	1	1.33	1	1
VIII	75	3/4	1.33	1-1/2	2
IX	60	1	2.05	1/2	1/2

For the 75° cases the maximum shock strength was 1.33 and thus these results should agree approximately with the linear theory. Series IX has a shock strength of 2 and thus should be less in agreement with linear theory.

The gases used in the expansion and compression chambers of the shock tube were nitrogen and hydrogen, respectively. These gases were at room temperature initially and the pressures were adjusted to give the desired shock strengths.

The desired shock strengths were 1.15, 1.2, 1.3, and 2. These strengths were computed by noting the time for the shock wave to move a fixed distance. The time was measured by means of an electronic scaler. In our experiments the scaler was found to have a 10-microsecond lag which caused all times to be approximately 10 microseconds too great. Thus, the shock strengths calculated were too small. This was taken into account in the final preparation of the report, and the adjusted shock strengths appear here.

After the shock strengths had been determined several test shots were taken to determine the manner in which the Mach stem grew with time. The block was then mounted on the wedge at such a position that the relative height of the Mach stem at $\tau = 0$ was as desired. For the 1/2 and 1 ratios, a 1-in. block was used. For the 2 ratio it was necessary to use a 3/4-in. block in order to keep the flow within the field of the shock tube windows.

For the 30° wedge only a 1/2-in. Mach stem could be produced, this is shown in series IX.

In each series two types of photographs are included. First, a group of four schlieren photographs show the locations of the various shock waves at several different times during the interactions. Second, the remaining photographs in each series were interferograms. For each shot in this group three pictures were taken:

1. a monochromatic no-flow interferogram,
2. a monochromatic flow interferogram, and
3. a white-light flow picture.

The monochromatic no-flow interferogram was taken shortly before the shock tube was fired but after the pressure in the expansion chamber had been set. This picture gives a series of fringes which may be used for reference purposes. The shock tube is then fired and the monochromatic flow interferogram as well as the picture of the white-light fringes was taken.

The flow and no-flow interferograms were enlarged onto 8" x 10" Kodalith films. A contact print of the enlarged no-flow interferogram was made on another sheet of Kodalith film.

When the enlarged prints of the flow and no-flow interferograms were superimposed over a light table the regions in which the dark fringes in the one picture crossed the light fringes in the other could be easily seen and were traced on a sheet of frosted acetate placed over the two pictures. These regions represented regions of half-integral fringe shift. When the contact print of the enlarged no-flow interferogram was used instead of the original, the region of integral fringe shift could be traced.

The white-light fringe picture allowed one to measure the jump in

density at each shock wave, and in particular was used to check the incident shock strength. A typical no-flow monochromatic interferencegram is shown in Fig. 7, and the corresponding flow interferencegram is shown in Fig. 8. Figure 9 is the white-light interferencegram used to trace the density jumps across the shock waves.

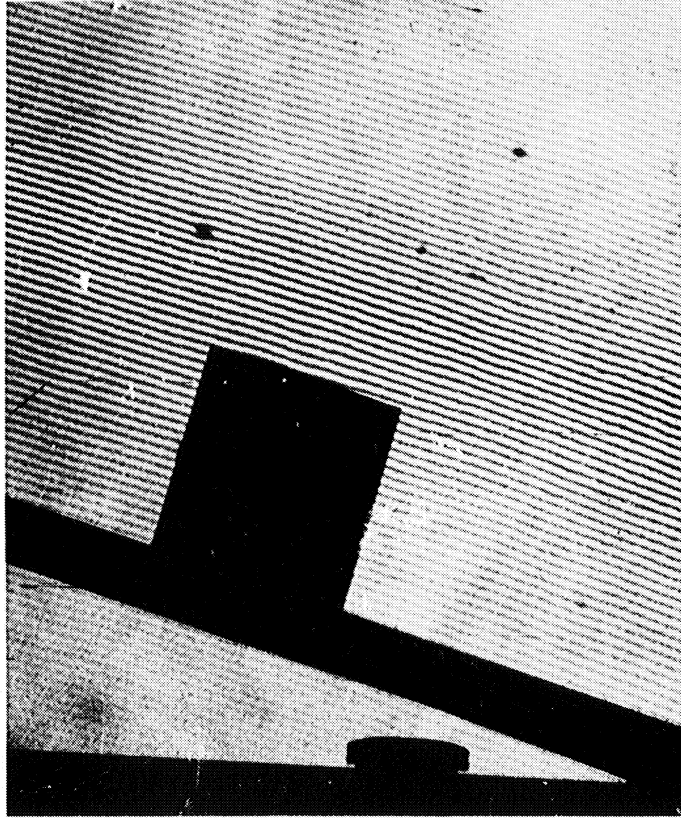


Fig. 7. Monochromatic no-flow fringes.

V. DATA REDUCTION

In order to make it possible for the reader to compute the densities and pressures in the flow field around the block, a brief account of the theory of fringe shifts will be given. The gas density and the index of refraction are related by

$$\eta = 1 + K \frac{\rho}{\rho_s} \quad (1)$$

where ρ_s is the density at 0°C and 760-mm Hg pressure, and K is known as the Gladstone-Dale constant. Before the shock tube is fired the density in the tube, which will be called ρ_0 , is known.

When the tube is fired a photograph is taken of the interferometer

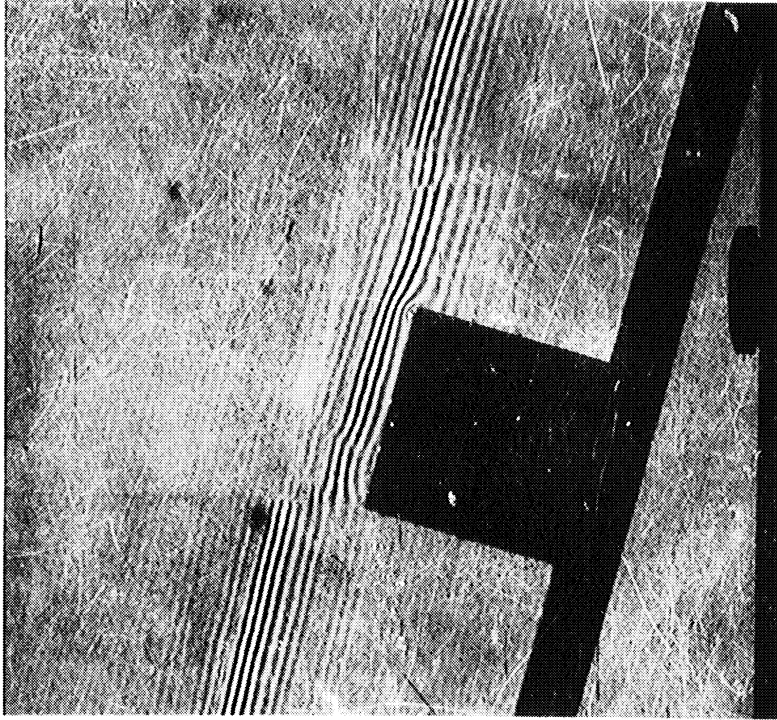


Fig. 9. White-light fringe picture, taken simultaneously with picture in Fig. 8.



Fig. 8. Monochromatic flow fringes, $\gamma = 1.2$, 75° angle of incidence, 1/2-in. Mach stem.

fringes, which are now shifted. The density in the test section, and hence the index of refraction, are no longer constant but vary from point to point. The index of refraction is related to the variable density ρ by the above equation. The increase in optical path length at a particular point in the field* due to the change in the index of refraction is $(\eta - \eta_0)L$, where L is the thickness of the test section and η_0 is the index of refraction corresponding to ρ_0 . According to Equation 1 this increase in optical path length is then given by

$$\frac{KL}{\rho_s} (\rho - \rho_0) .$$

The phase shift of the light corresponding to this increase is

$$2\pi/\lambda \text{ (increase in optical path length)}$$

where λ is the wavelength of the monochromatic light. The fringe shift, measured in units of the fringe spacing, is just the phase shift in units of 2π . The fringe shift at a particular point in the flow field will then be given by

$$n = \left(\frac{LK}{\lambda}\right) \frac{1}{\rho_s} (\rho - \rho_0) = \frac{LK}{\lambda} \cdot \frac{273}{760} \cdot \frac{p_0}{T_0} \left(\frac{\rho}{\rho_0} - 1\right) \quad (2)$$

or

$$n = C \left(\frac{\rho}{\rho_0} - 1\right) \quad \text{where} \quad C = \frac{LK}{\lambda} \cdot \frac{273}{760} \cdot \frac{p_0}{T_0} .$$

The lines of constant fringe shift, or isopycnics, are shown on the tracings, and they are numbered by the total fringe shift from the undisturbed gas of density ρ_0 . Therefore, by the above equation one may calculate the variable density ρ at any point in the flow field

The absolute numbering of the isopycnics could not be determined from the monochromatic fringe pictures alone. It is impossible to find the jump in fringes across a shock wave. This difficulty is overcome by taking a white-light fringe picture simultaneously with the monochromatic fringe picture. The central fringe in a white-light interferogram can be easily distinguished from the others so that across a shock wave the fringe jump, and therefore the density jump, can be found. Ideally, one would try to take the white-light interferograms in such a way that the central fringe passes across all

*The flow field is two-dimensional so a point refers to a narrow cross section across the width of the tube.

the shock waves present in the flow field. This is, of course, not possible in our case since there are so many shocks present. But one can place this central fringe so that it cuts the important shocks, i.e., incident and reflected shocks. The remaining shocks are weak enough so that the fringe shift is less than unity, and hence the shift can be determined directly from the monochromatic interferograms.

As long as the shock waves are weak, the pressures may be determined fairly accurately by assuming the flow is isentropic behind the primary shock wave. The pressure ratio across the primary shock wave is given by the well-known Rankine-Hugoniot equation

$$\frac{p_1}{p_0} = \frac{1 - \left(\frac{\gamma + 1}{\gamma - 1} \cdot \frac{\rho_1}{\rho_0} \right)}{\frac{\rho_1}{\rho_0} - \frac{\gamma + 1}{\gamma - 1}} \quad (3)$$

where γ is defined as the ratio of the specific heat at constant pressure to the specific heat at constant volume. If, then, the flow behind the primary shock is assumed to be isentropic,

$$\frac{p}{p_0} = \frac{p_1}{p_0} \left(\frac{\rho}{\rho_1} \right)^\gamma = \frac{p_1}{p_0} \left(\frac{\rho_0}{\rho_1} \right)^\gamma \left(\frac{\rho}{\rho_0} \right)^\gamma = \frac{p_1}{p_0} \left(\frac{\rho_0}{\rho_1} \right)^\gamma \left(1 + \frac{n}{C} \right)^\gamma \quad (4)$$

But

$$C = \frac{1}{n_1} \left(\frac{\rho_1}{\rho_0} - 1 \right)$$

where n_1 is the fringe jump across the primary shock. Therefore,

$$\frac{p}{p_0} = \left(\frac{p_1}{p_0} \right) \left(\frac{\rho_0}{\rho_1} \right)^\gamma \left[1 + \frac{n}{n_1} \left(\frac{\rho_1}{\rho_0} - 1 \right) \right]^\gamma \quad (5)$$

The calculation of the pressures from the isopycnics when the reflected shocks are strong is a very complicated process. The entropy behind a strong curved shock, for example, is not constant throughout the field but only along a streamline. Because of the difficulties involved in such calculations, they will not be discussed in this report. For the information of the reader the following constants are listed:

- L = 5.10 cm, thickness of test section;
- λ = 5170 Å, wavelength of monochromatic light used; and
- K = 299×10^{-6} , Gladstone-Dale constant for nitrogen.

APPENDIX

SERIES I

Shock strength..... $\gamma = 1.17$

Mach stem height..... $1/2$

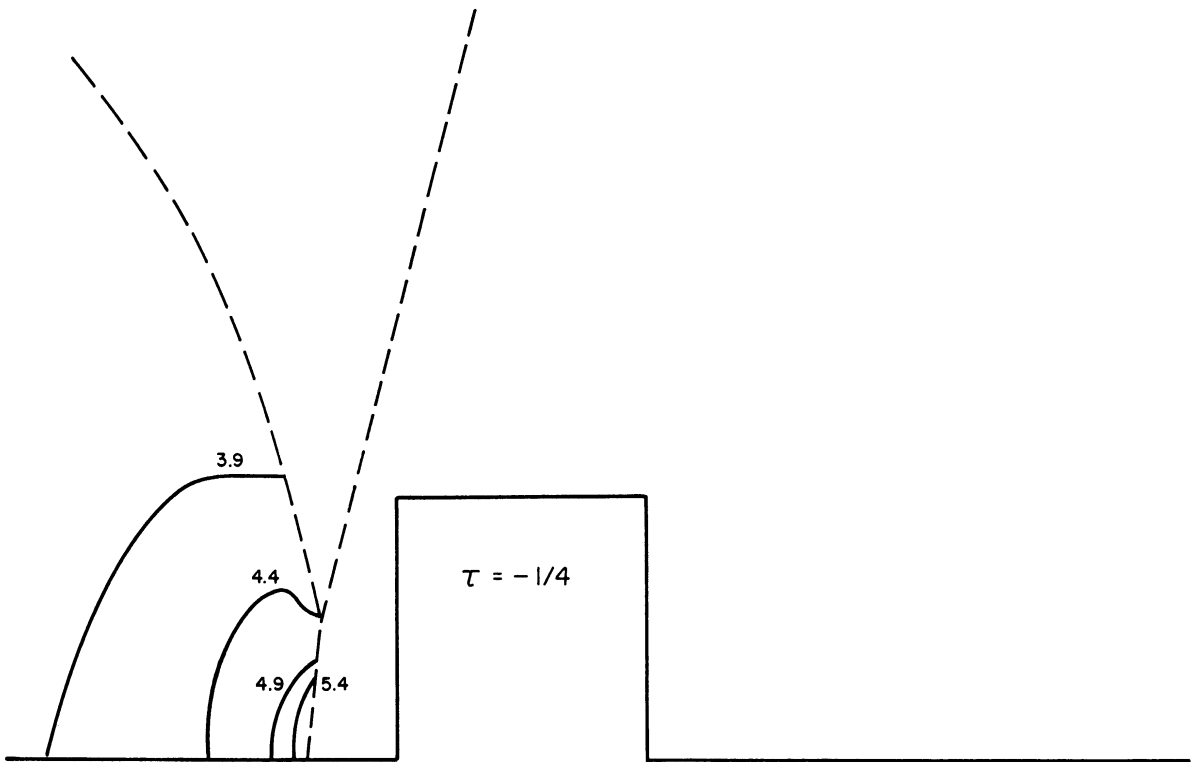
Block height..... 1

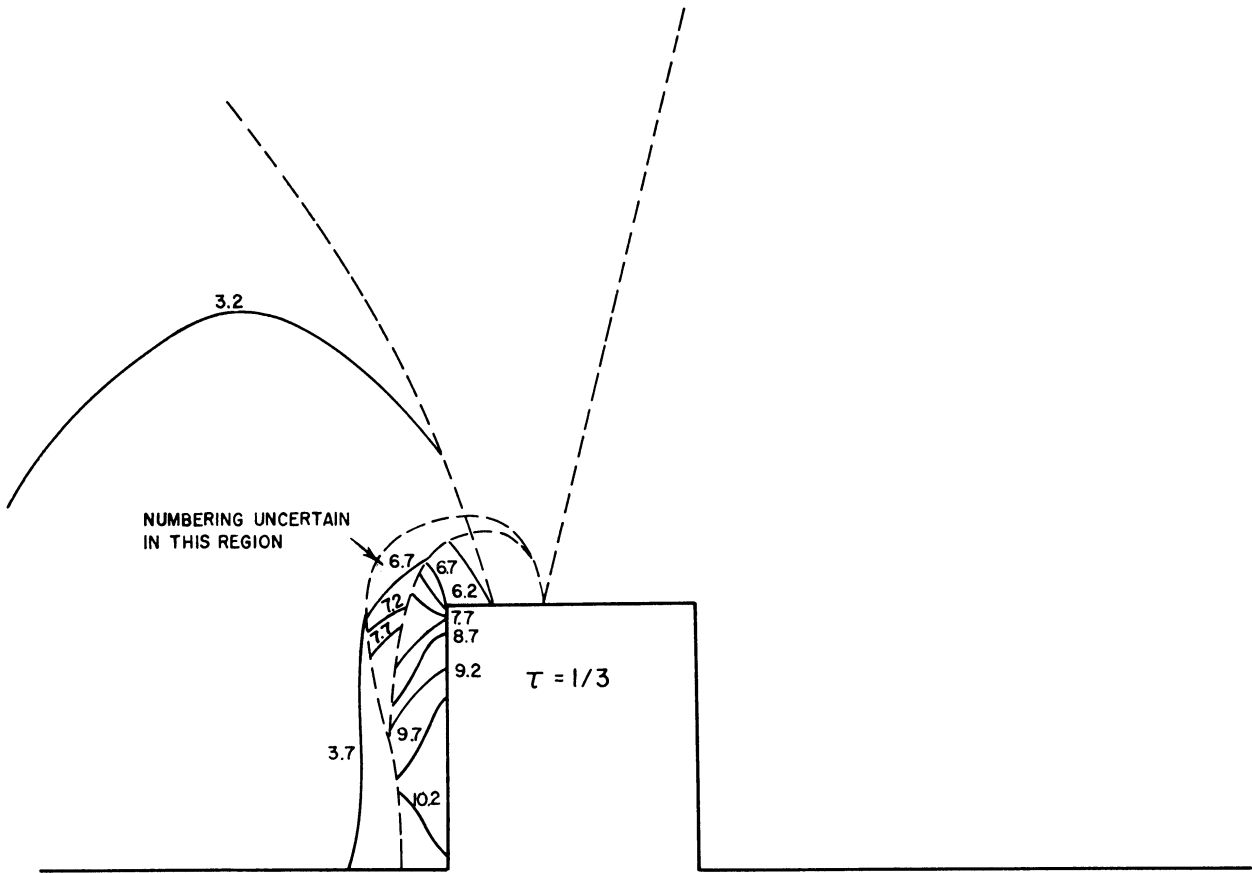
Angle of incidence..... 75°

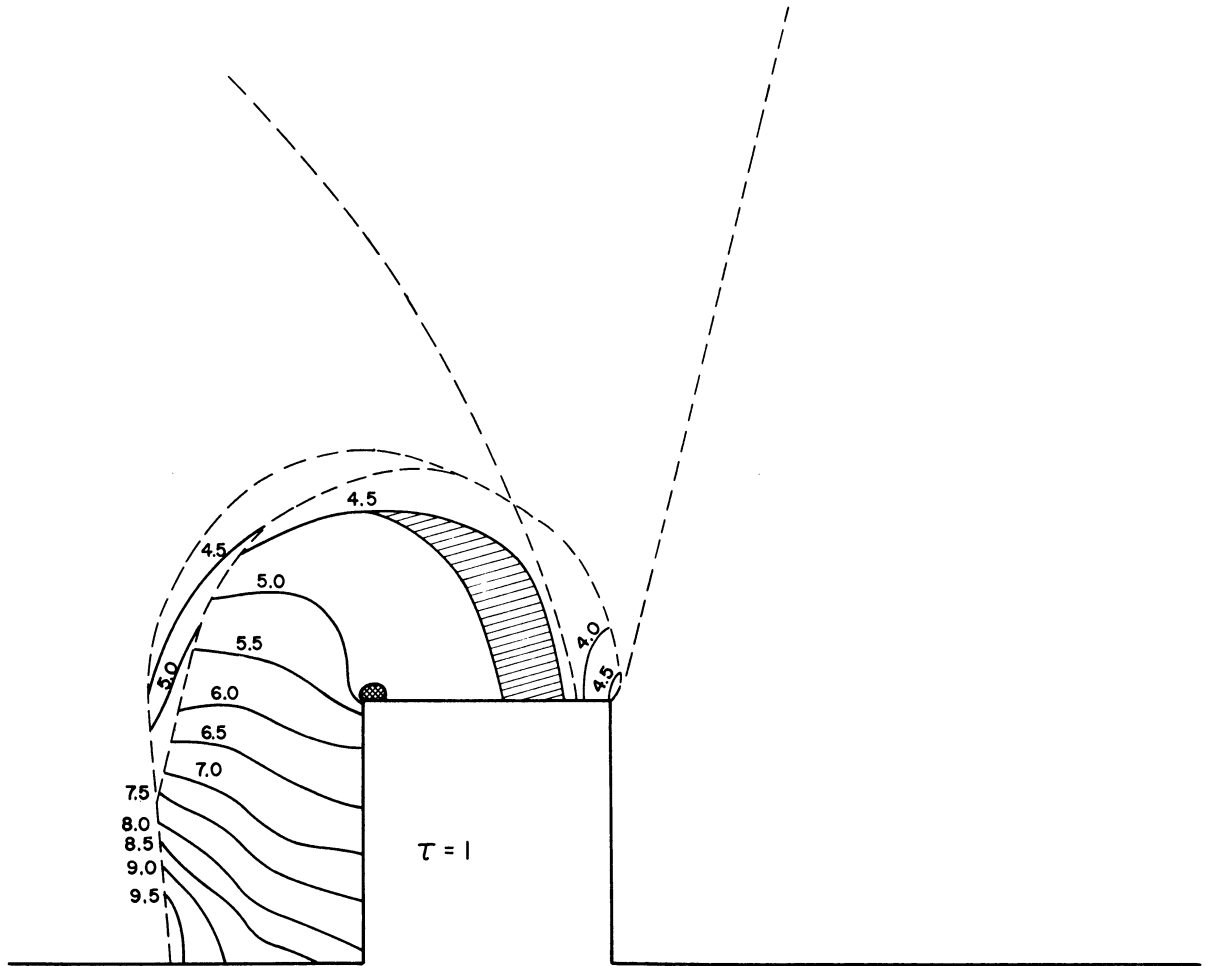
Density ratio..... $\frac{\rho_1}{\rho_0} = 1.118$

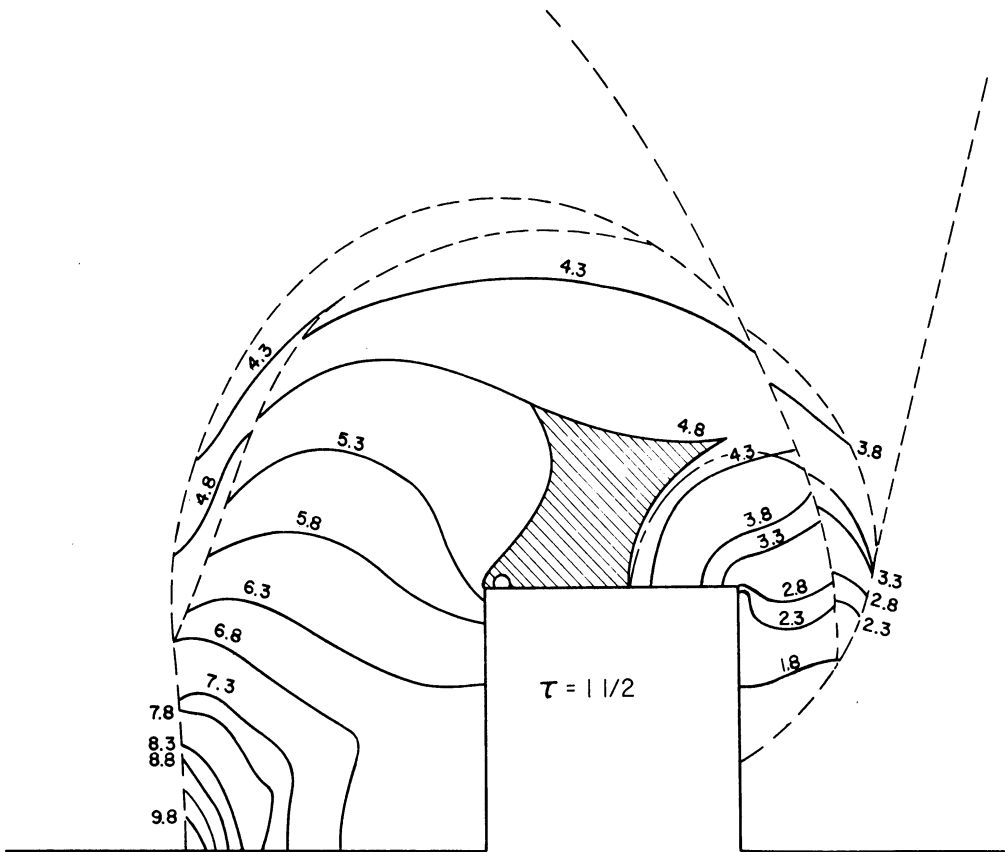
Pressure..... $P_0 = 741 \text{ mm Hg.}$

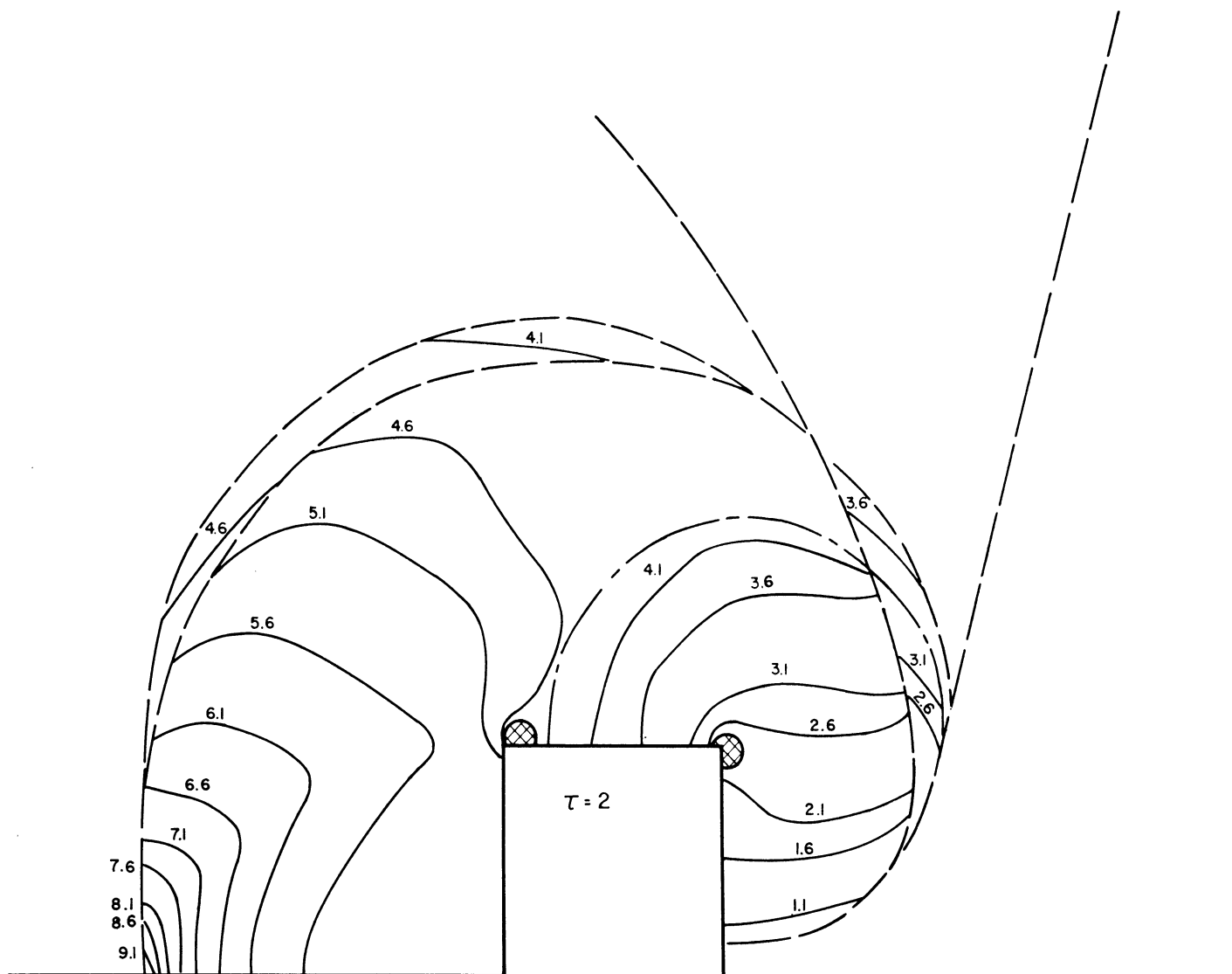
Shift across incident shock... $n_1 = 3.17$

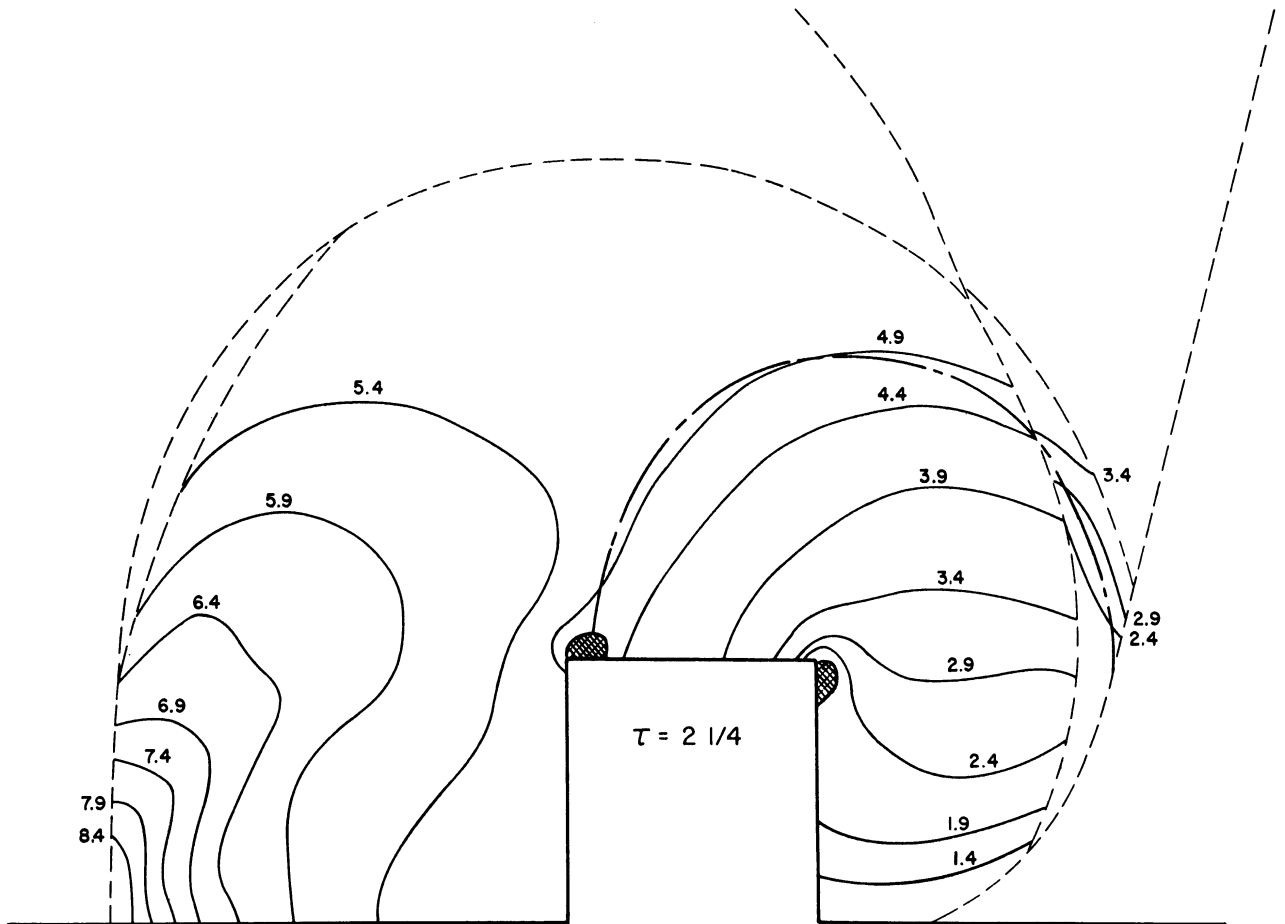


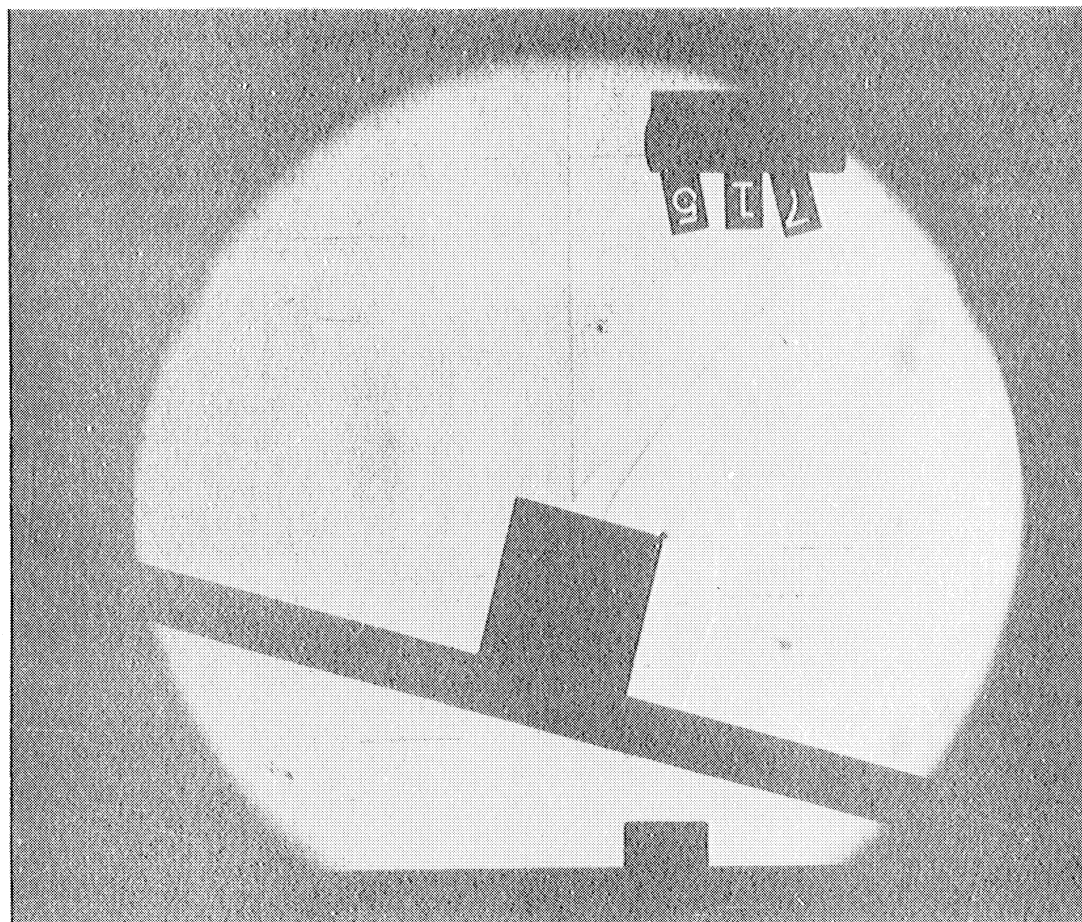
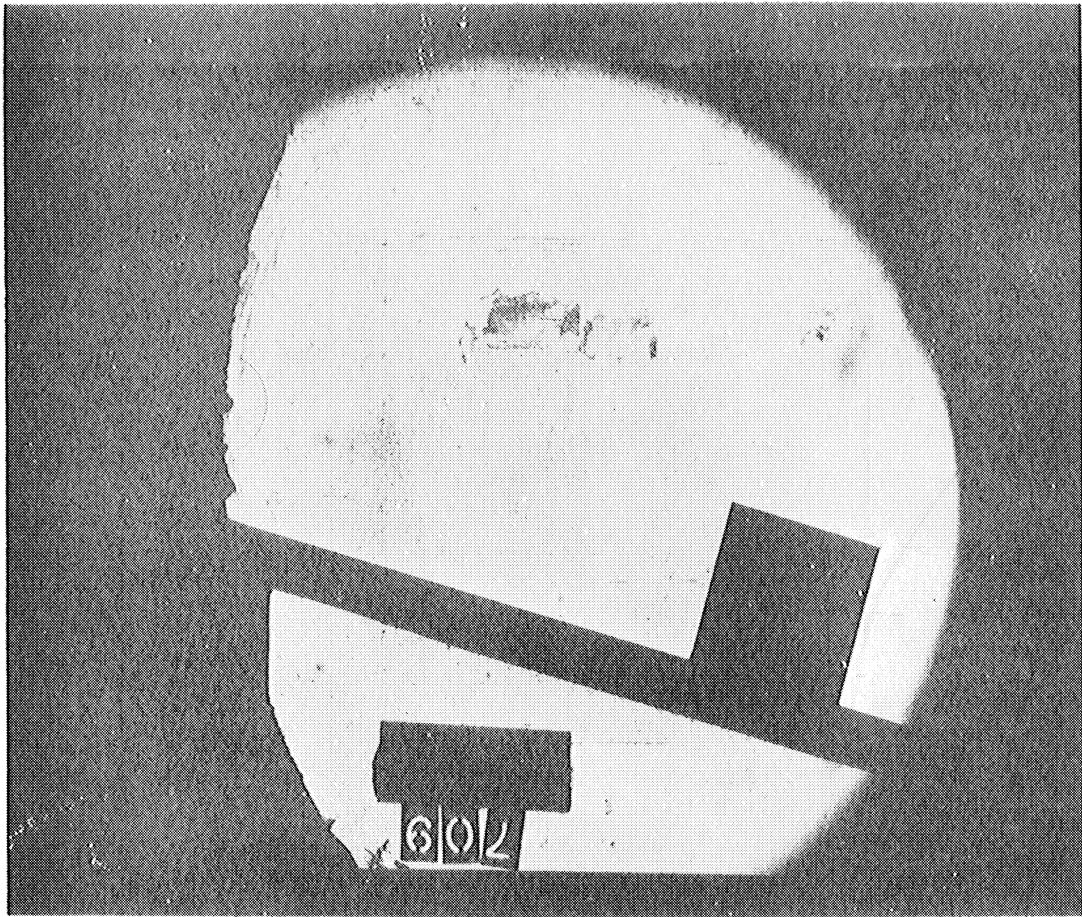


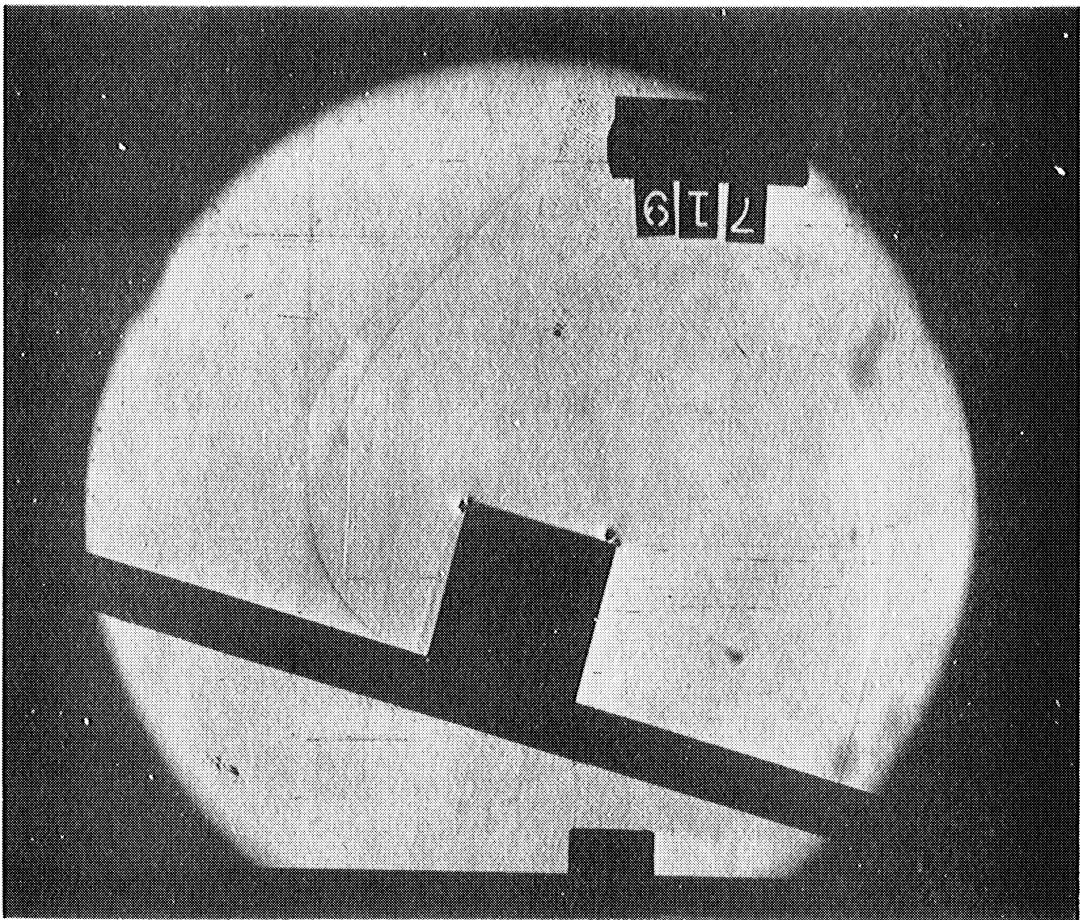
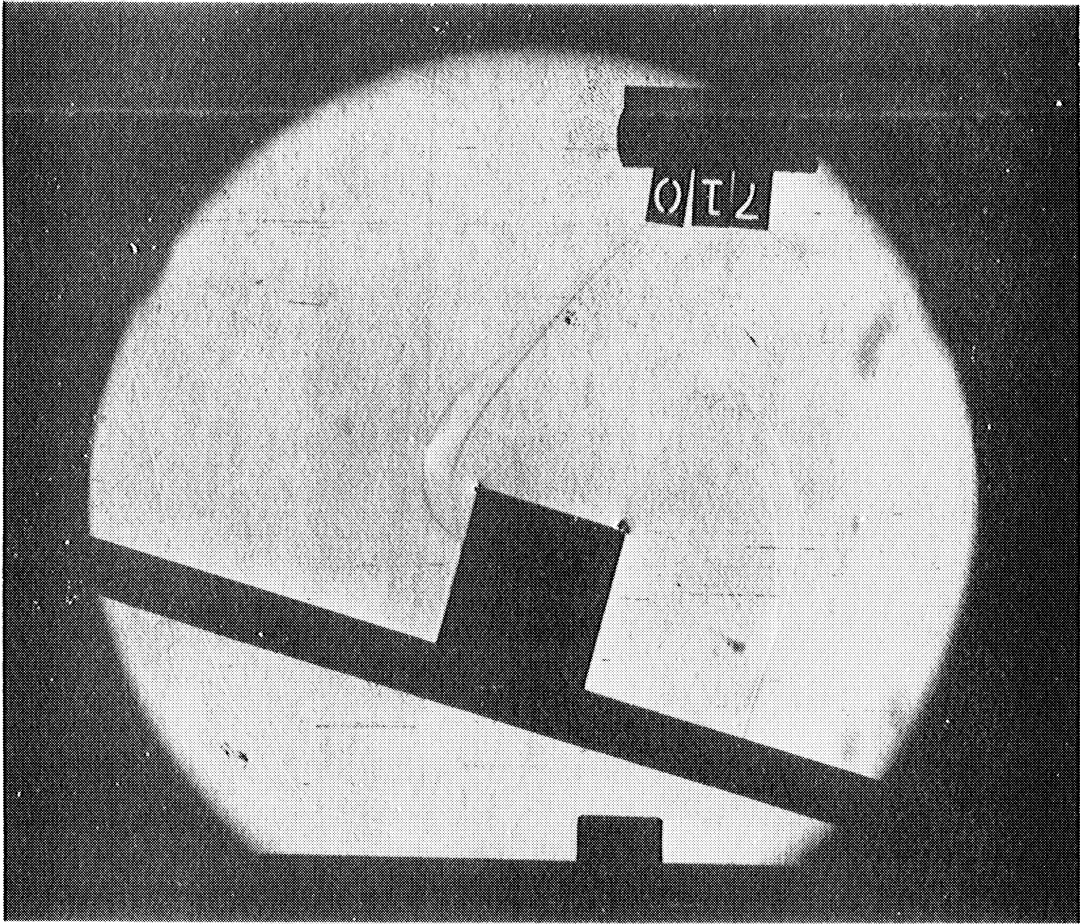












SERIES II

Shock strength..... $\gamma = 1.17$

Mach stem height..... 1

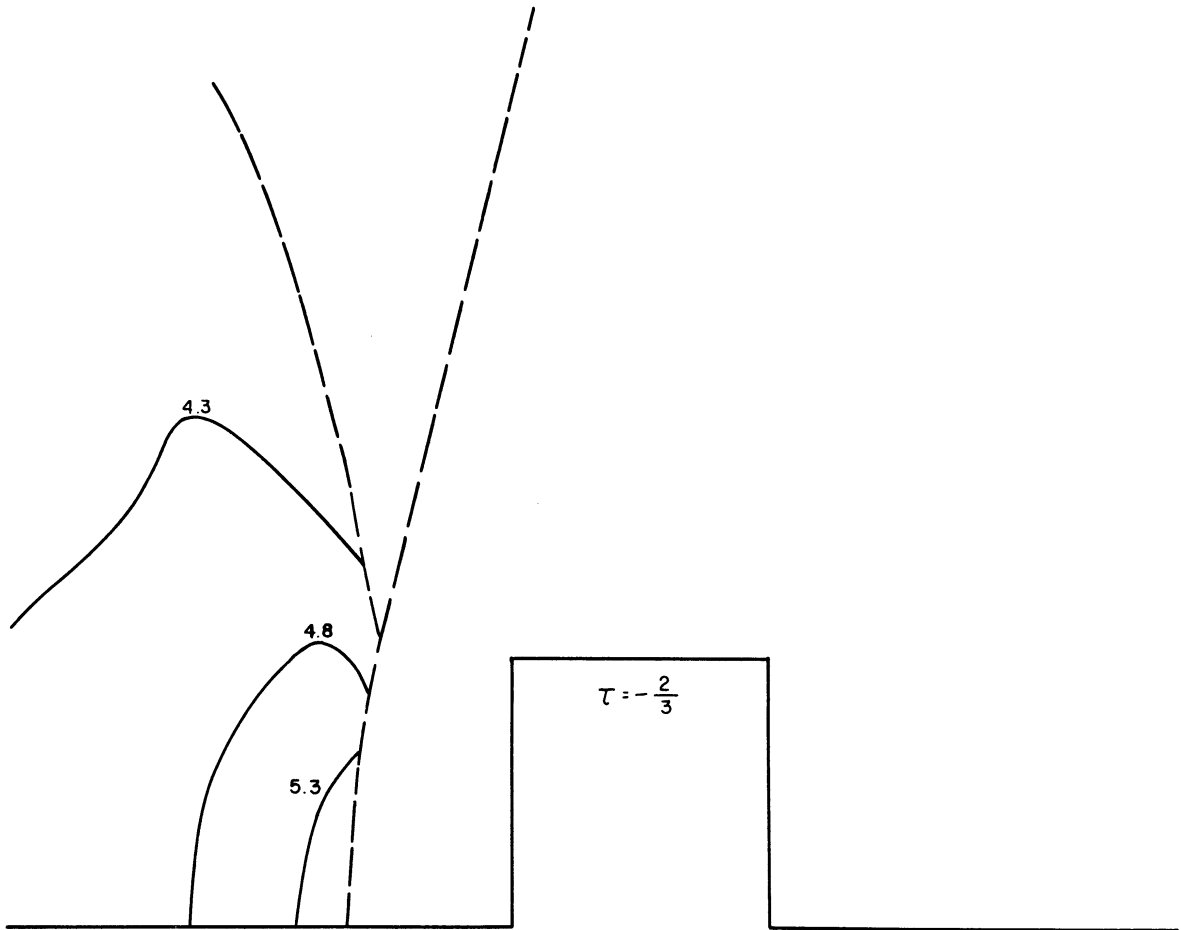
Block height..... 1

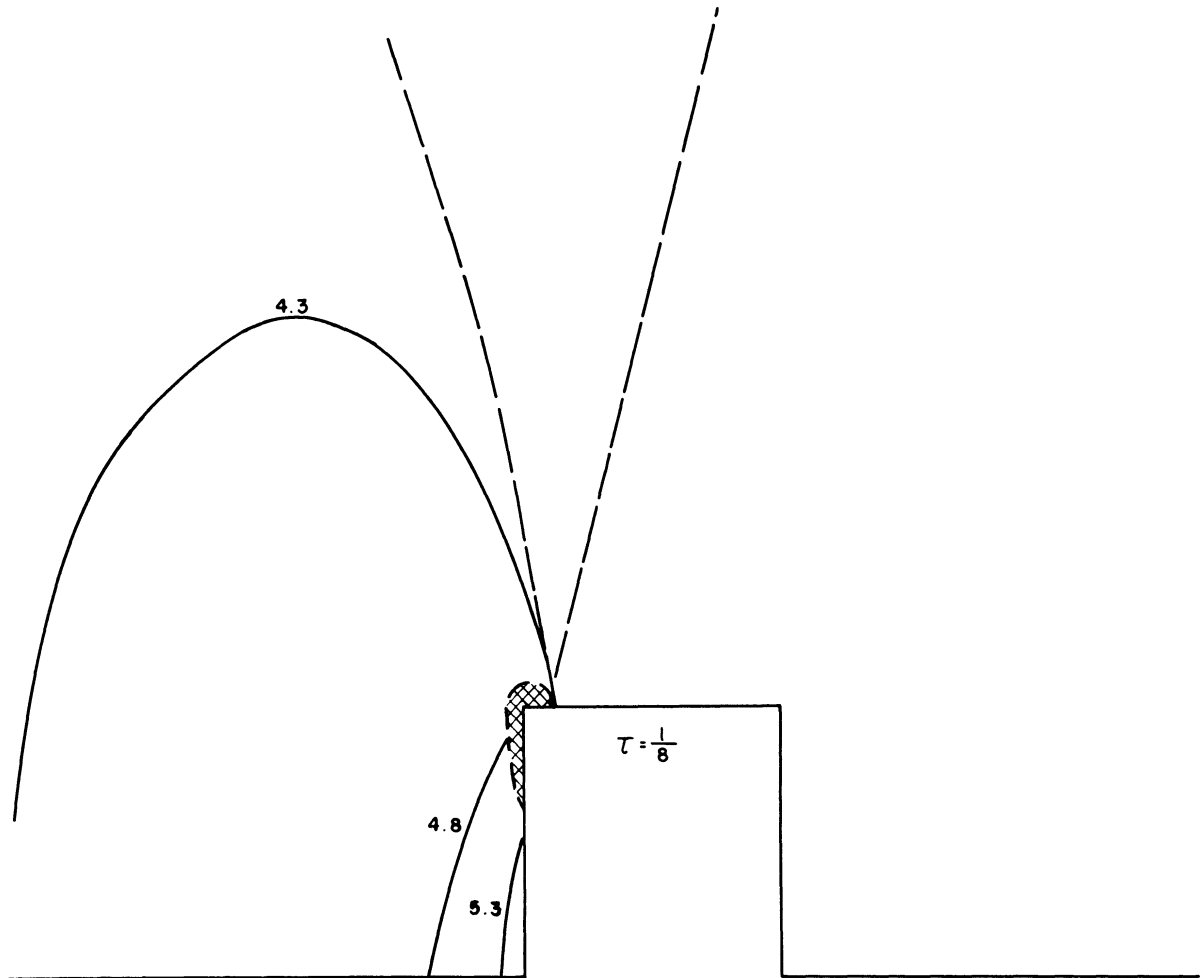
Angle of incidence..... 75°

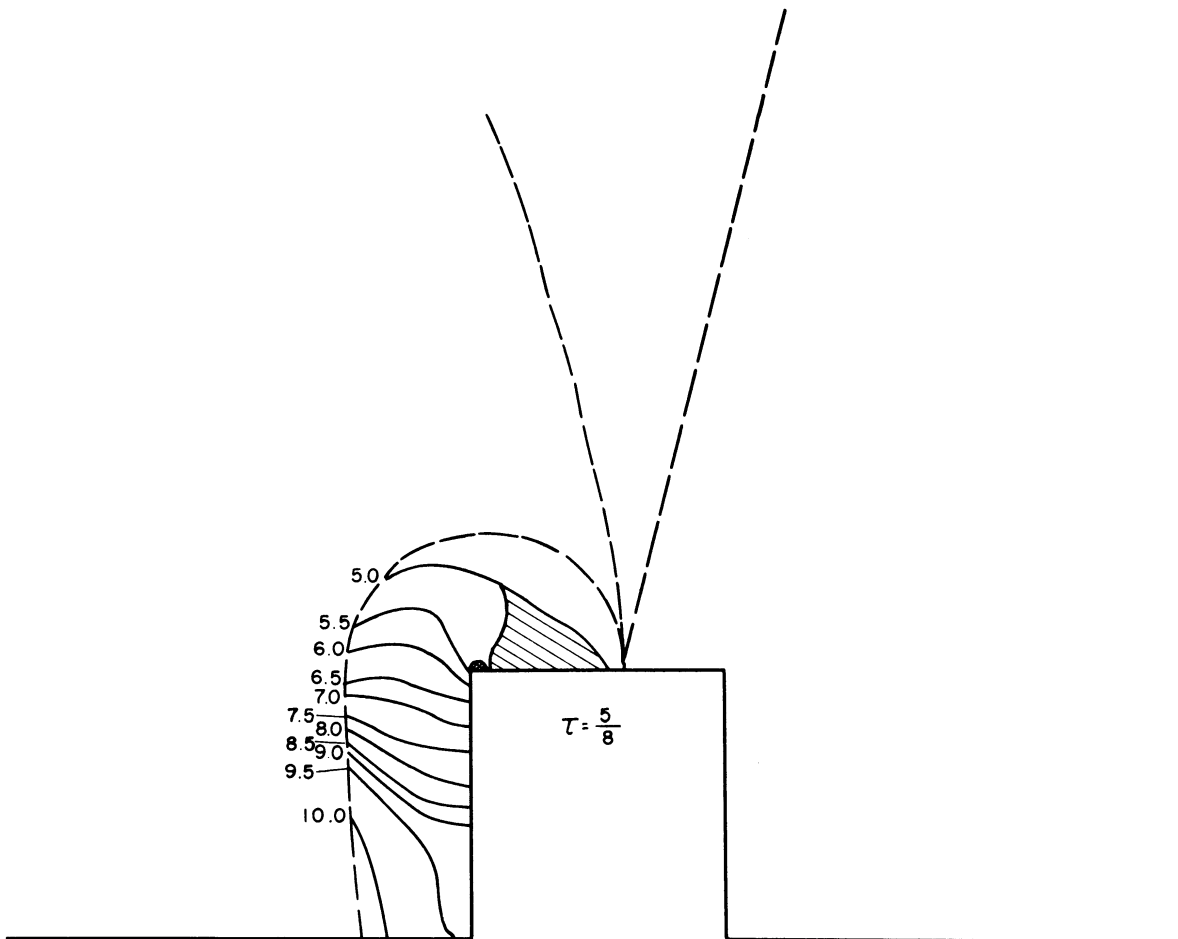
Density ratio..... $\frac{\rho_1}{\rho_0} = 1.118$

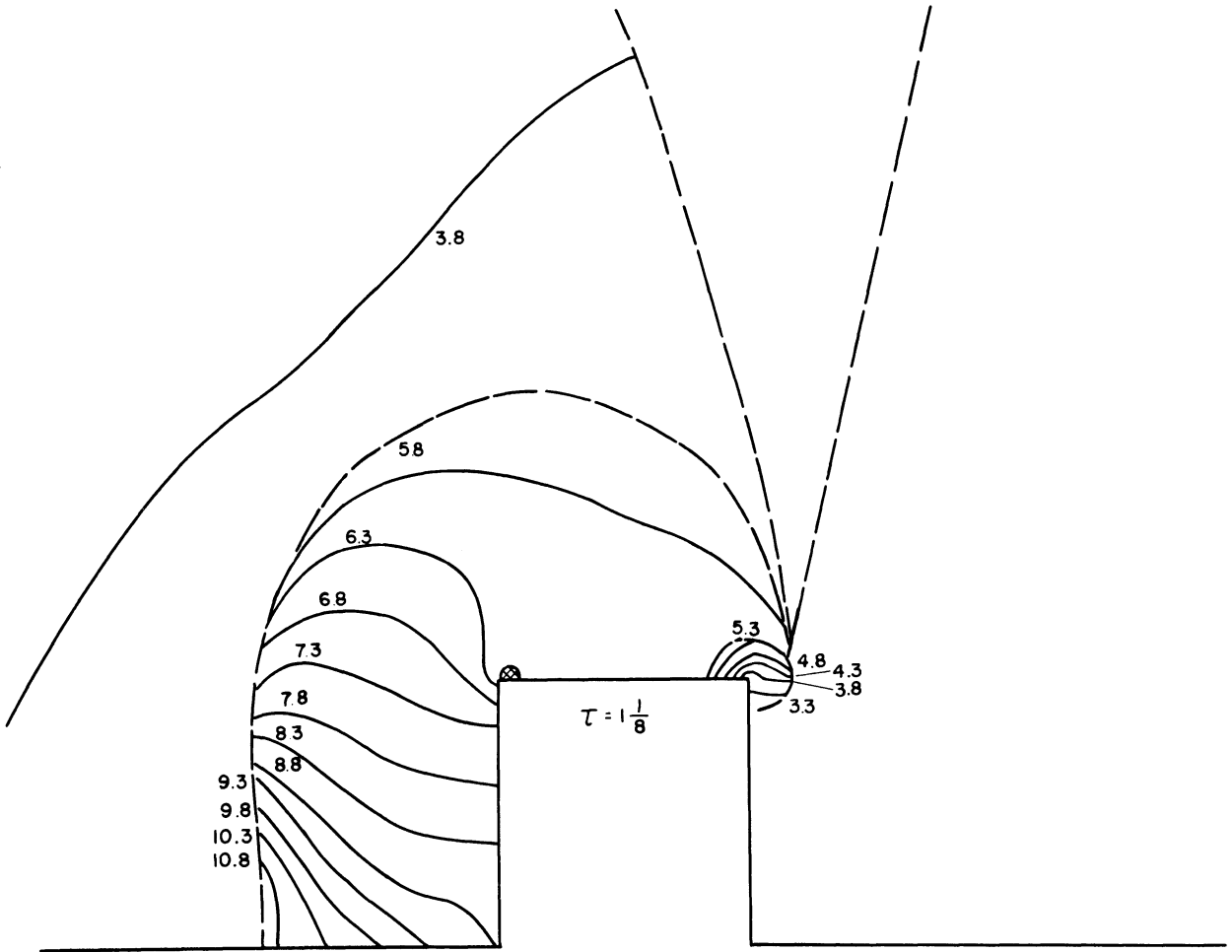
Pressure..... $P_0 = 739$ mm Hg.

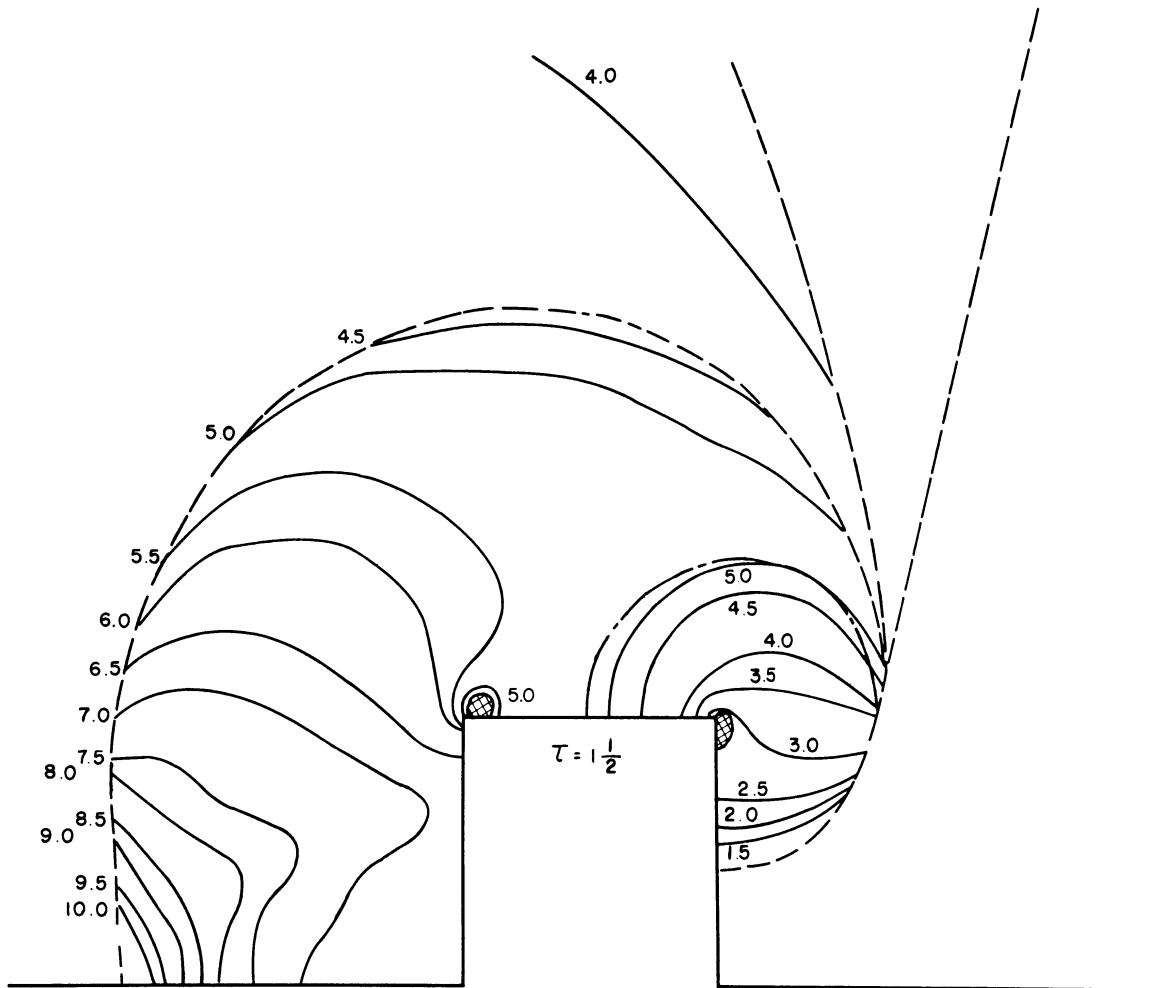
Shift across incident shock... $n_1 = 3.17$

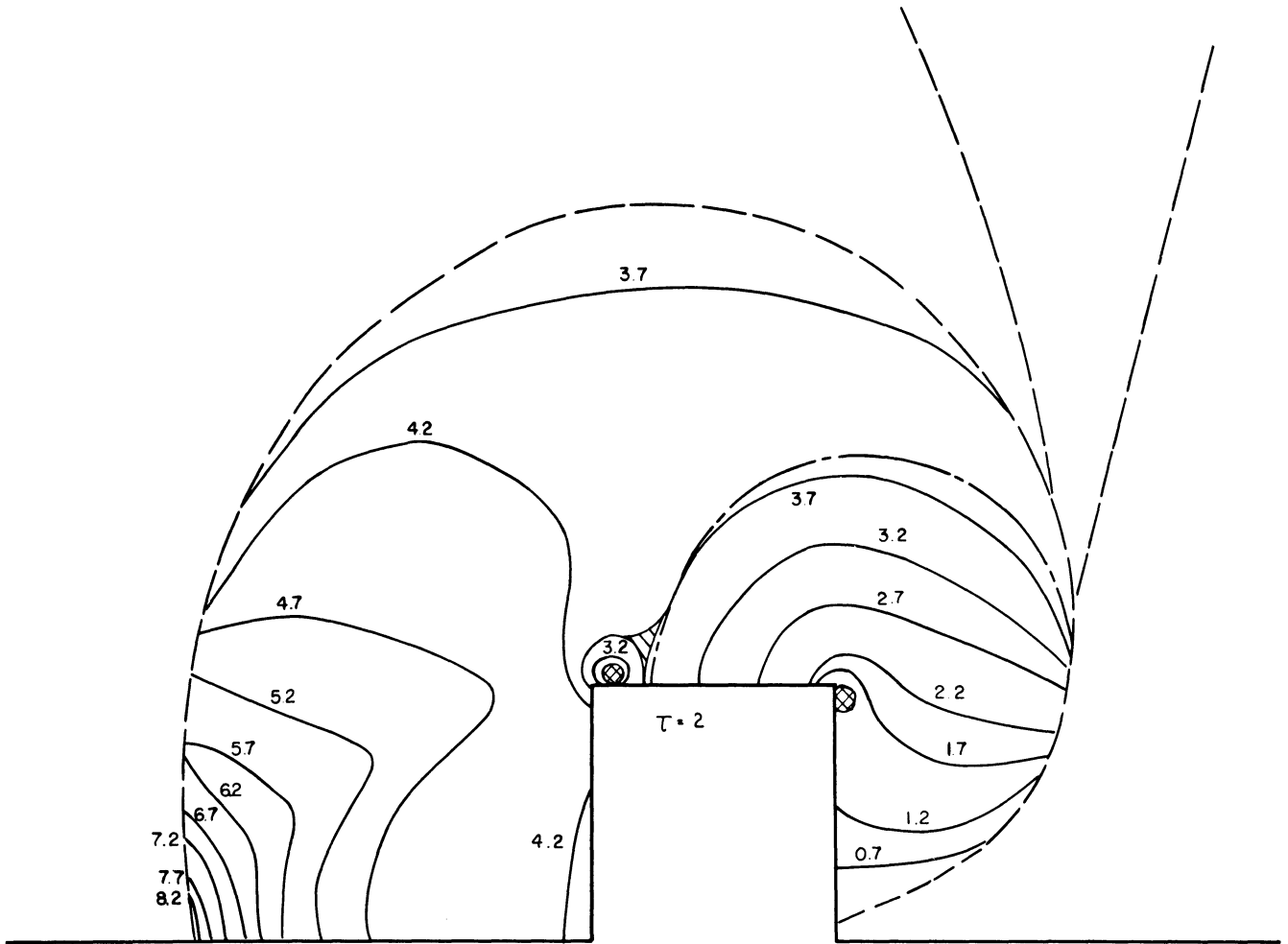


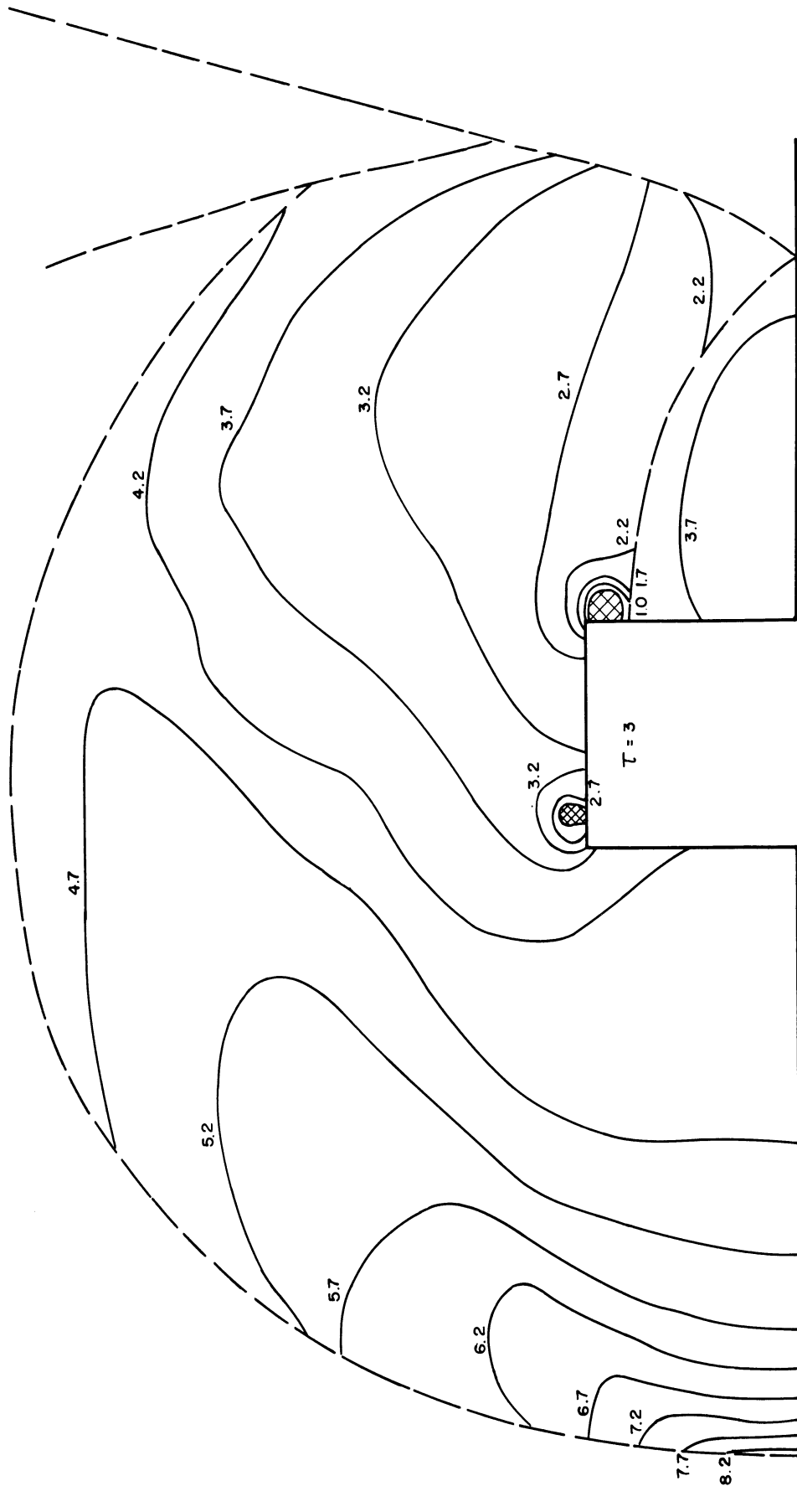


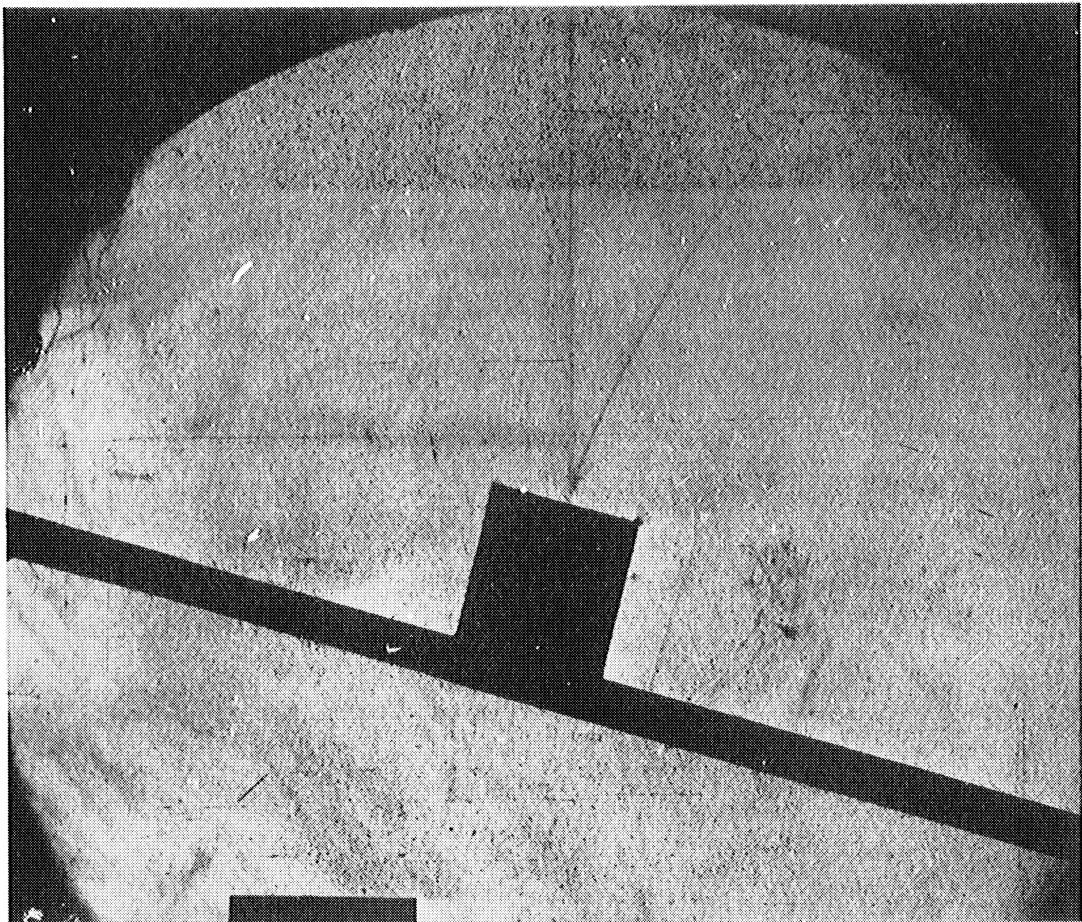
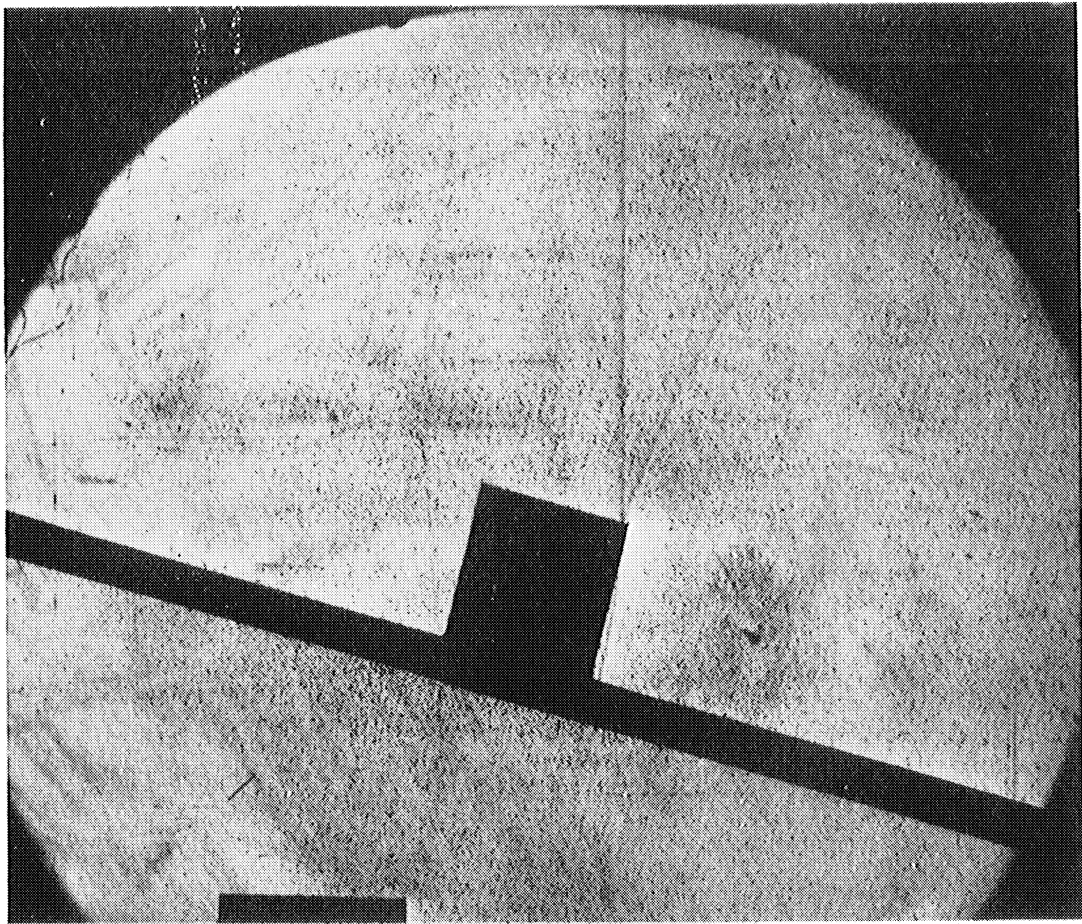


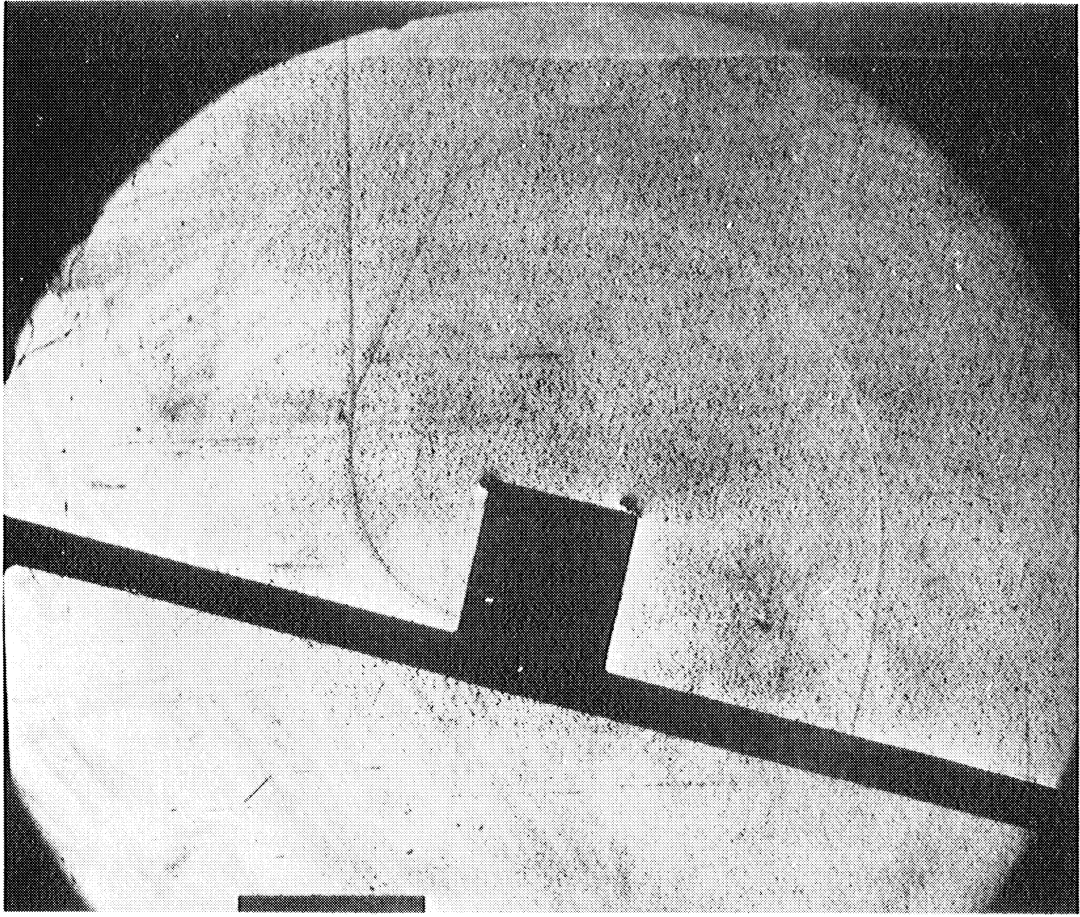












SERIES III

Shock strength..... $\gamma = 1.224$

Mach stem height..... $1/2$

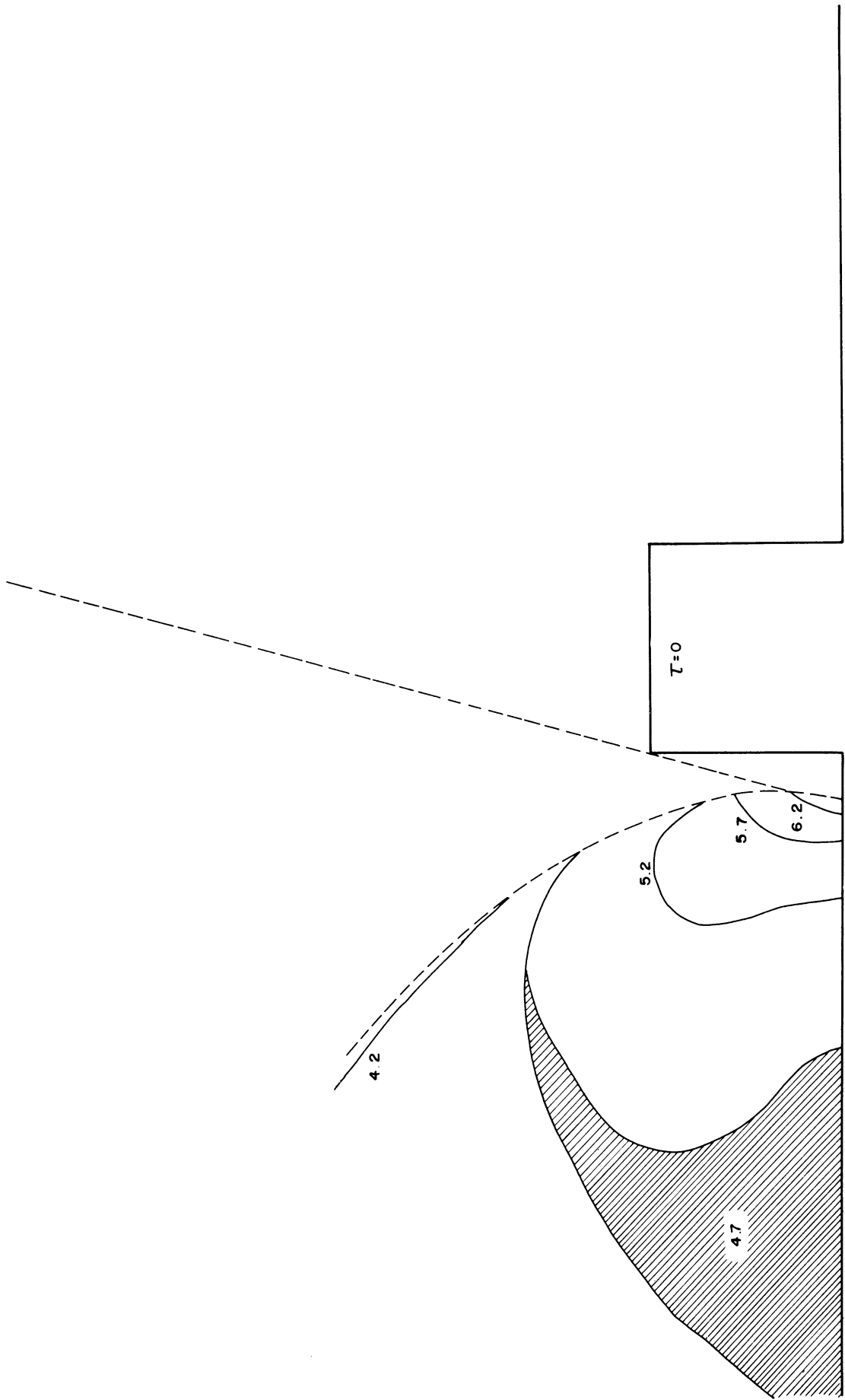
Block height..... 1

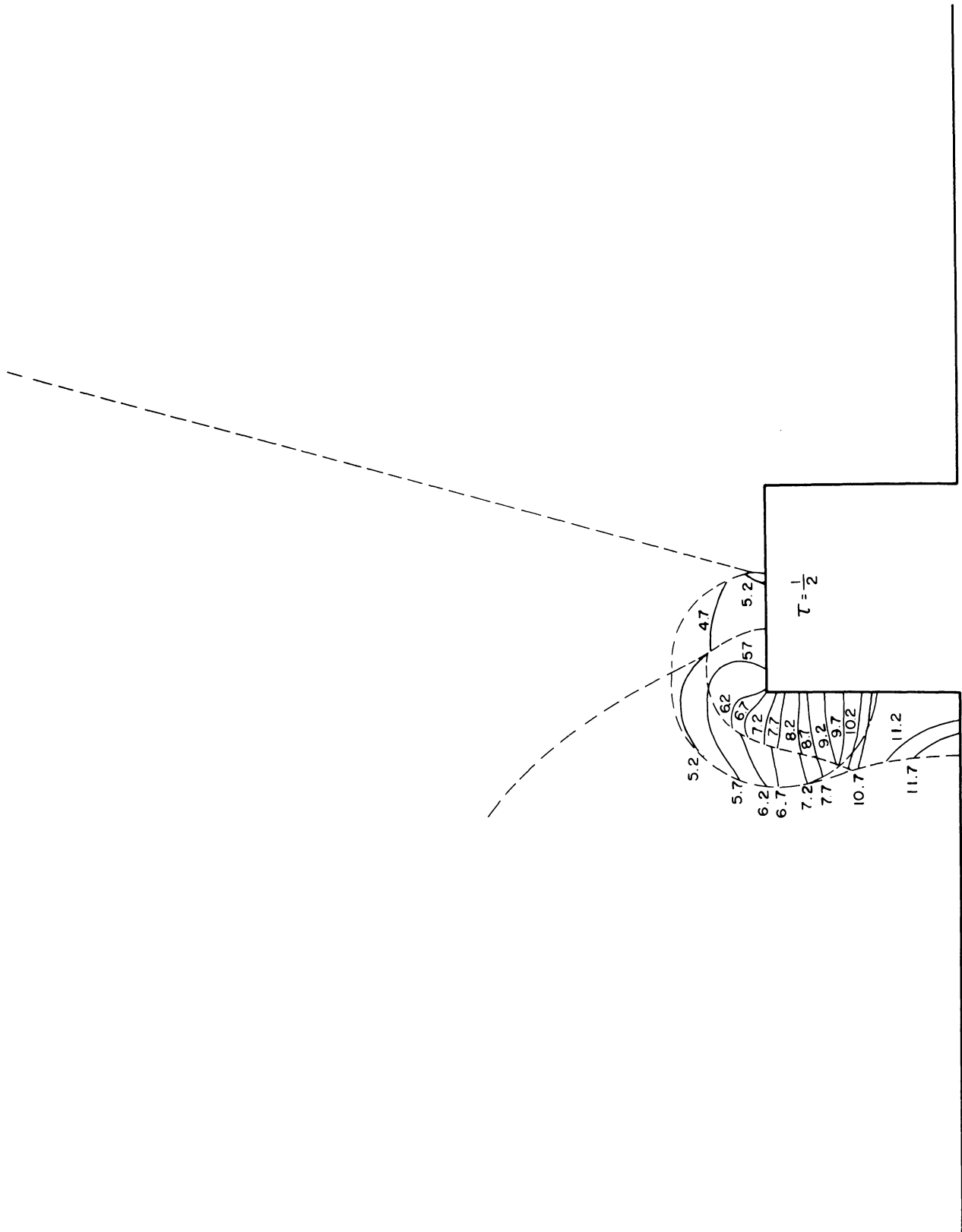
Angle of incidence..... 75°

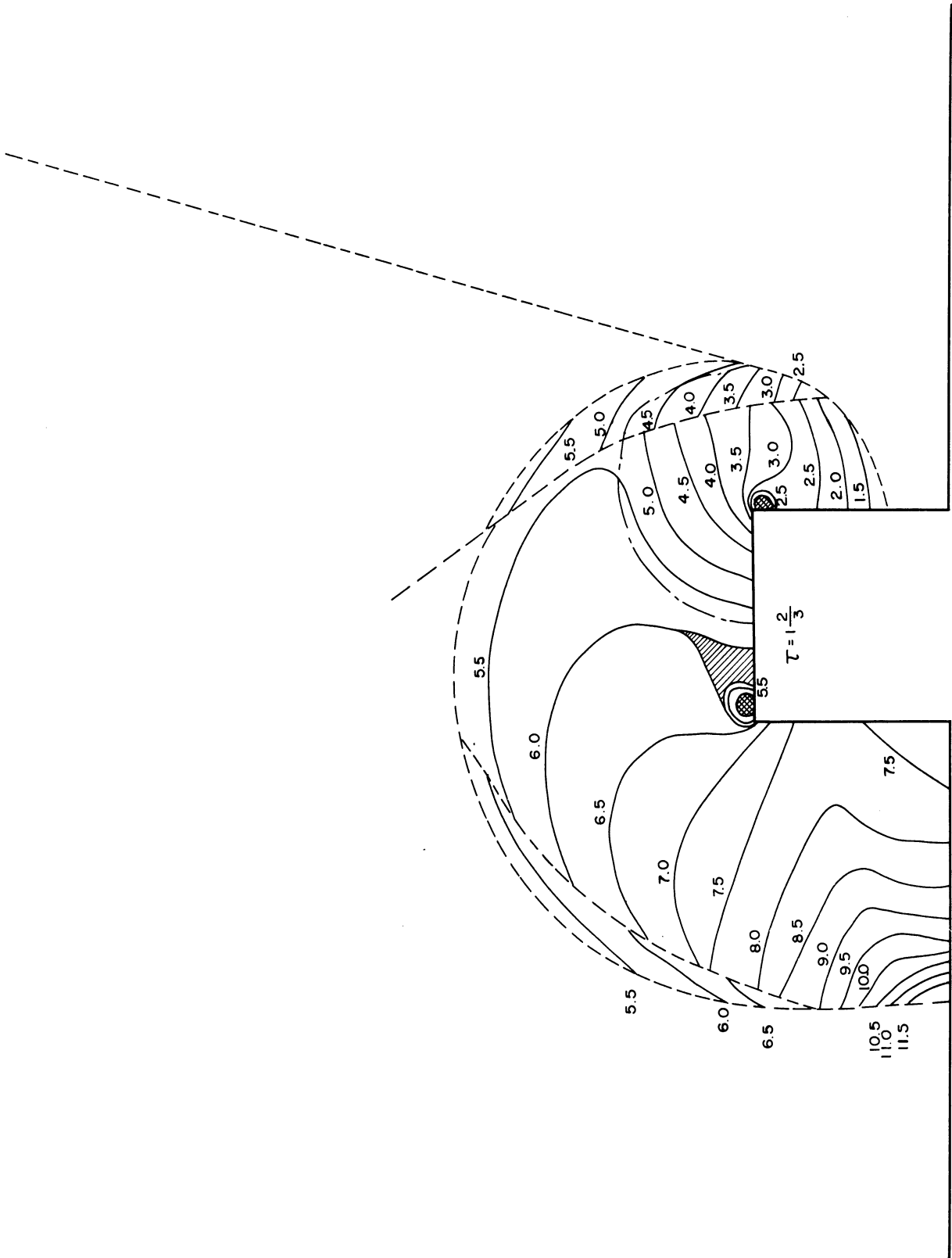
Density ratio..... $\frac{\rho_1}{\rho_0} = 1.154$

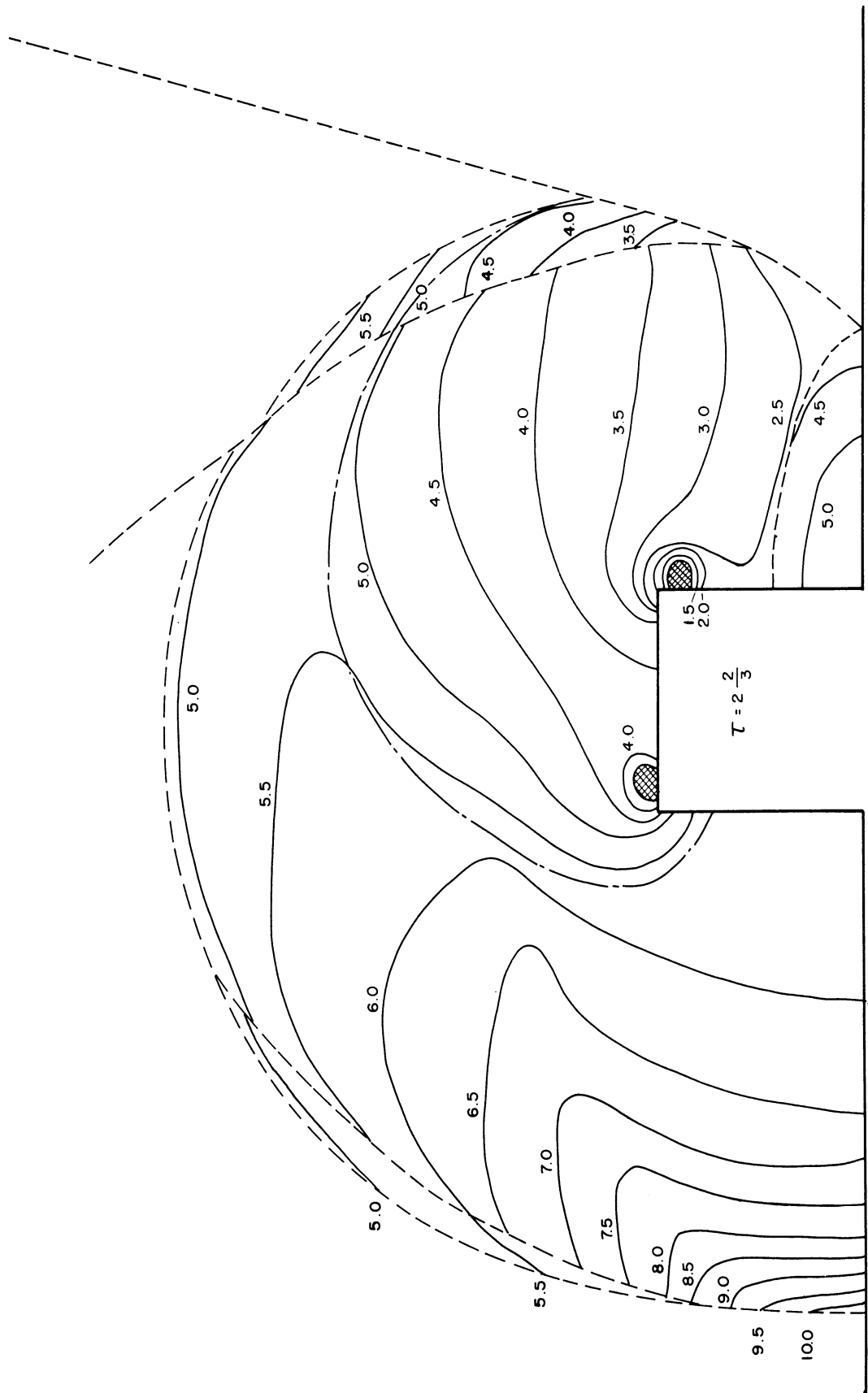
Pressure..... $P_0 = 738$ mm Hg.

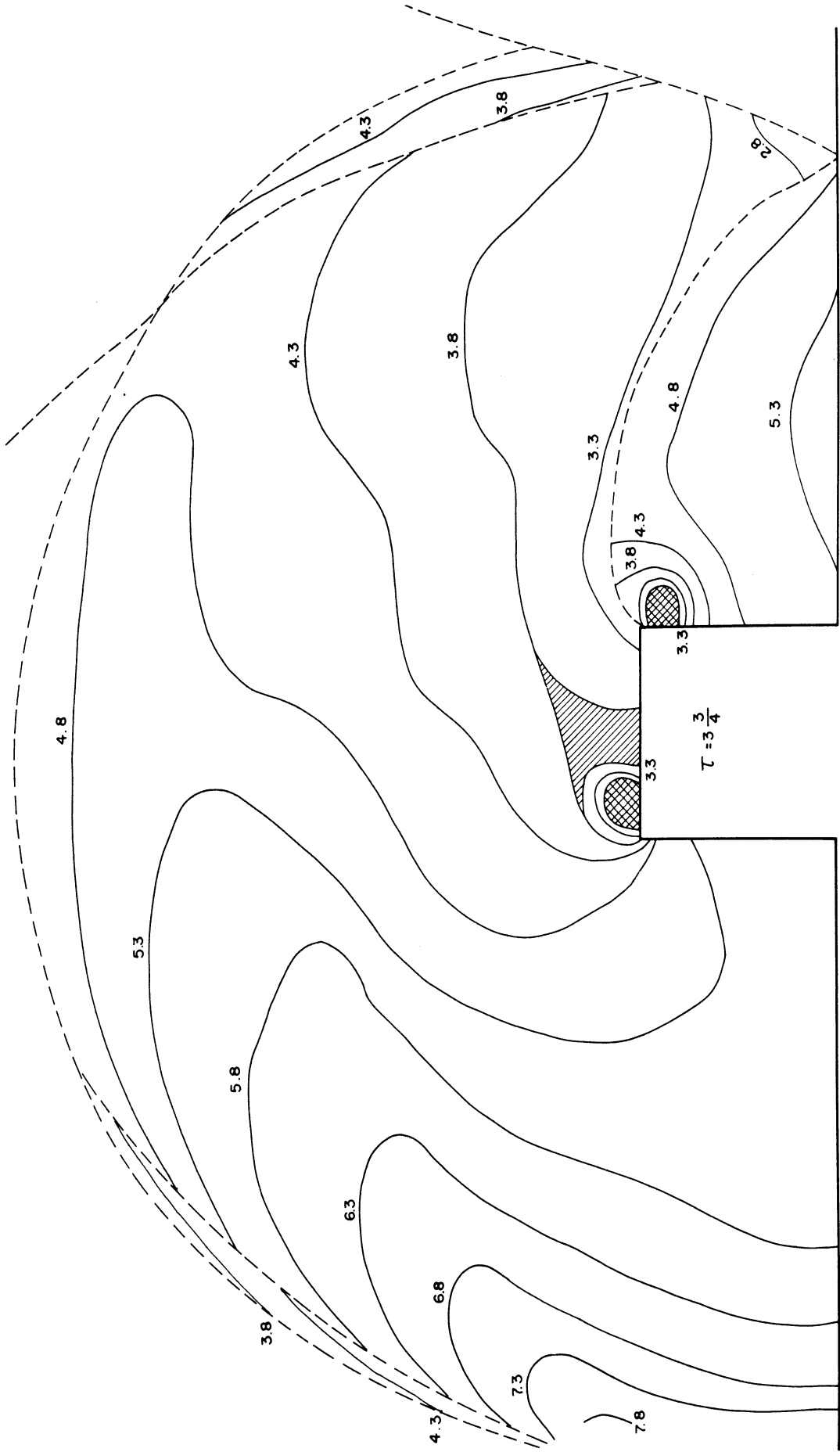
Shift across incident shock... $n_1 = 4.06$

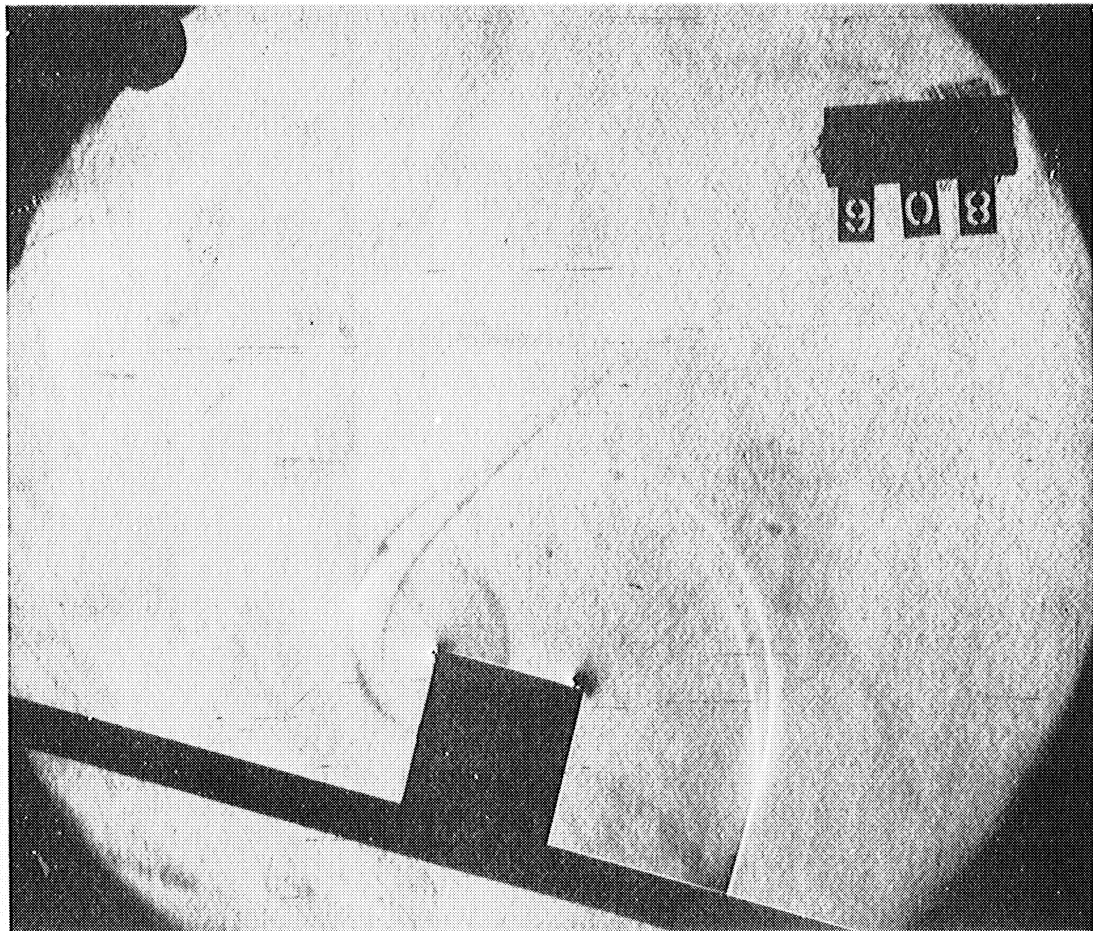
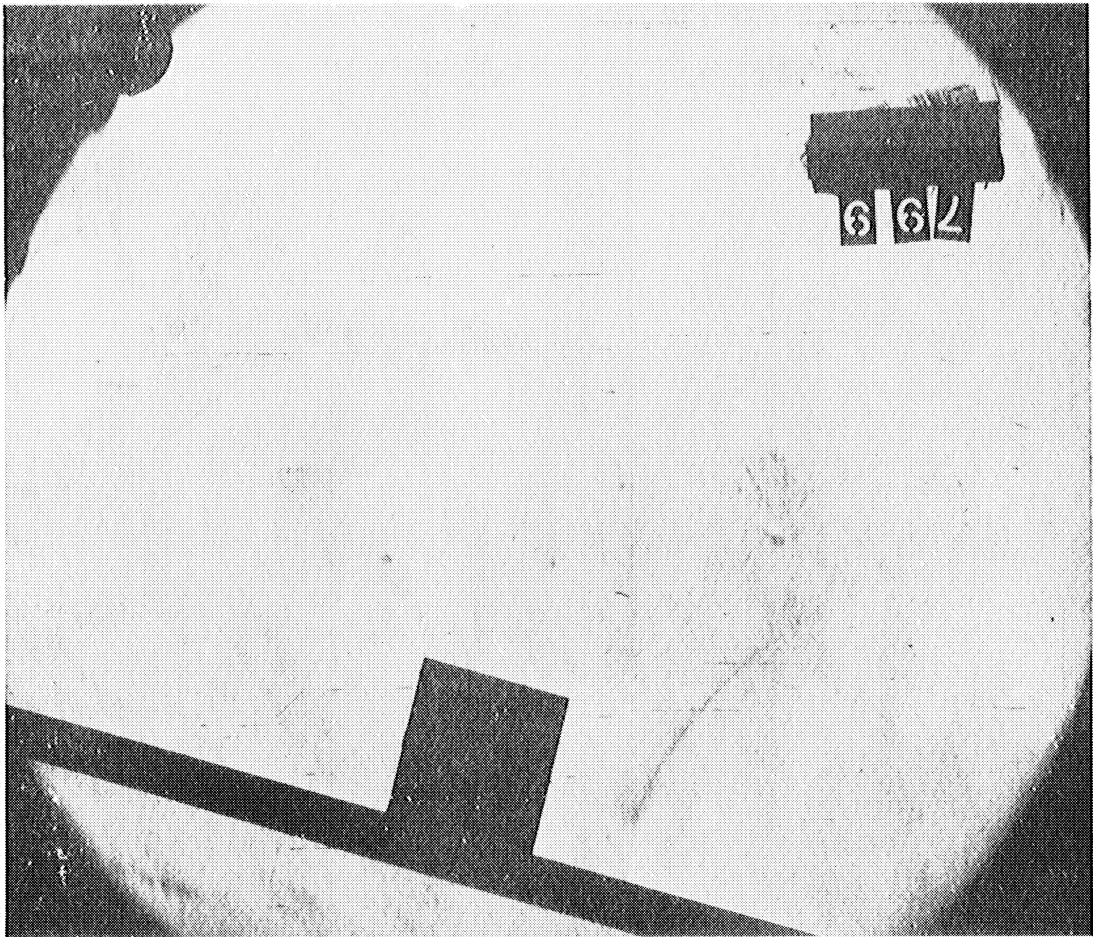


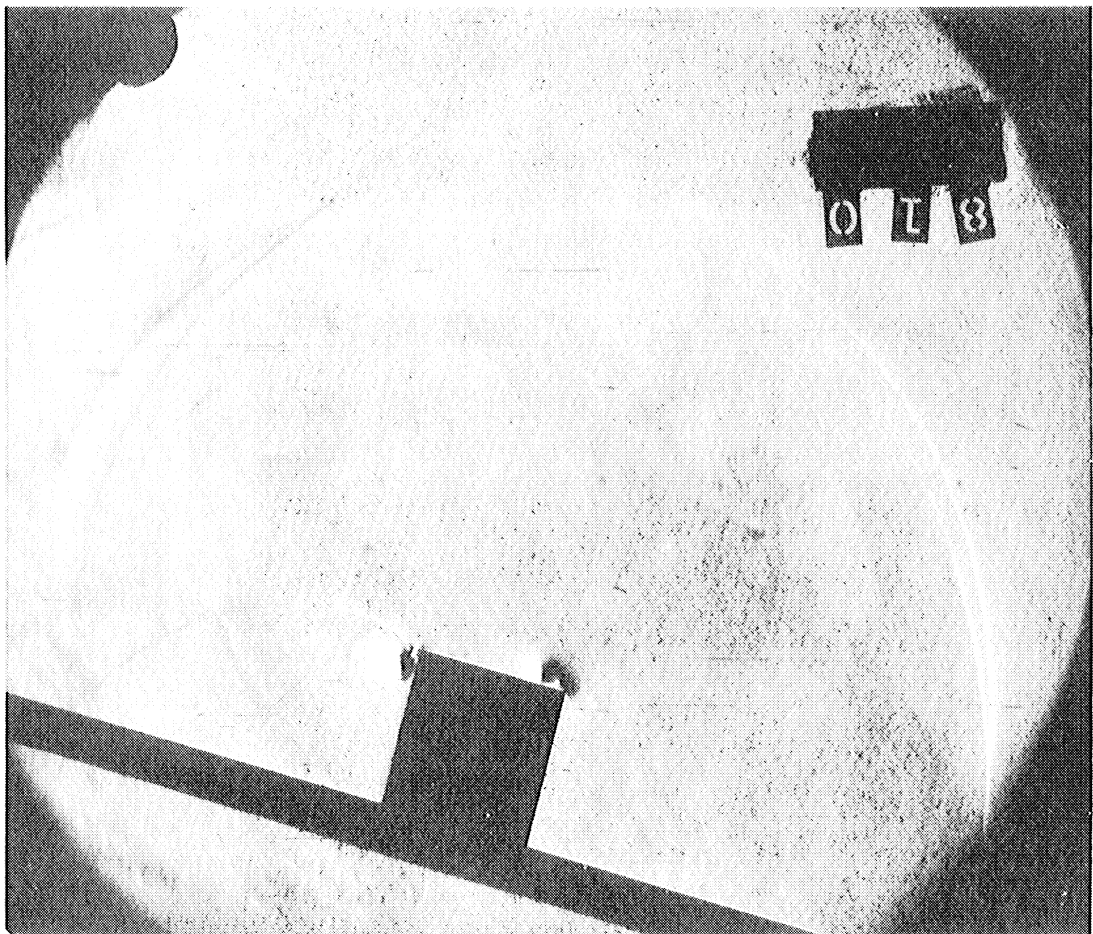
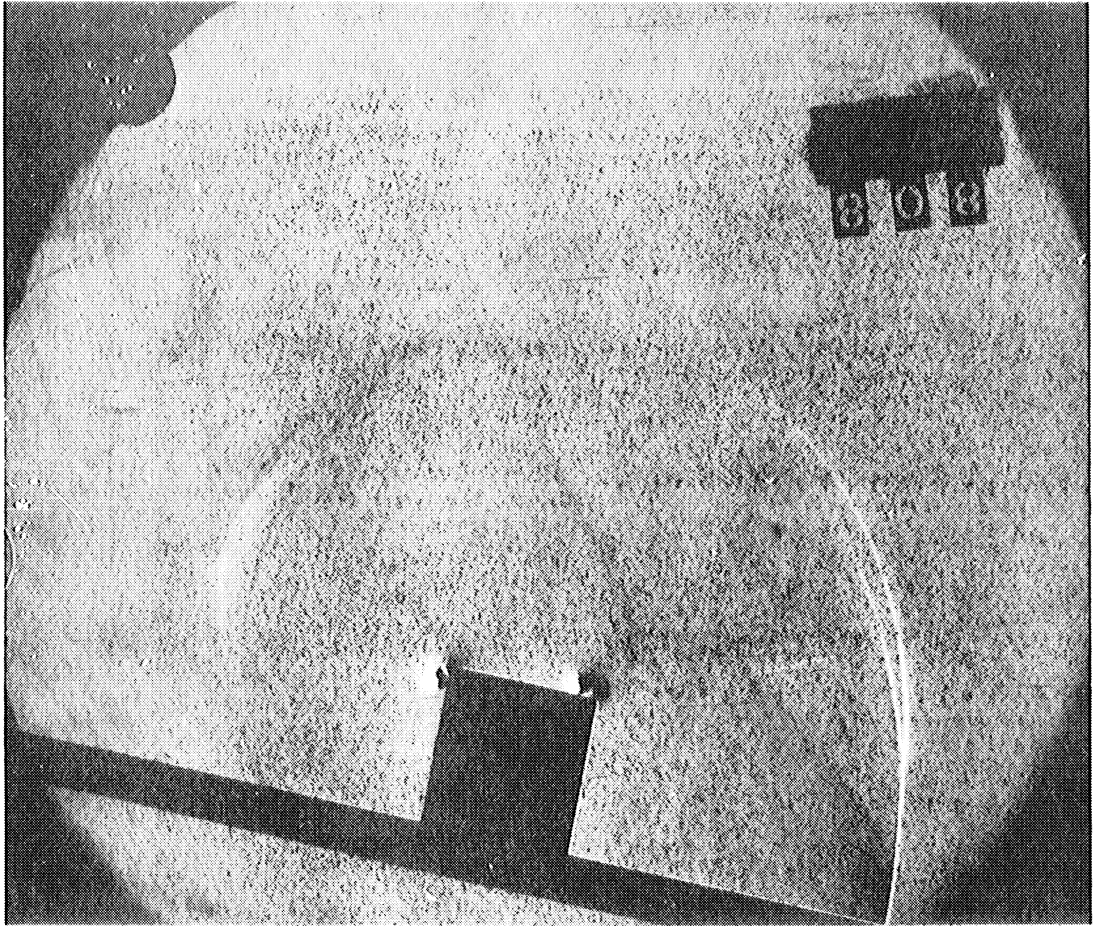












SERIES IV

Shock strength..... $\gamma = 1.224$

Mach stem height..... 1

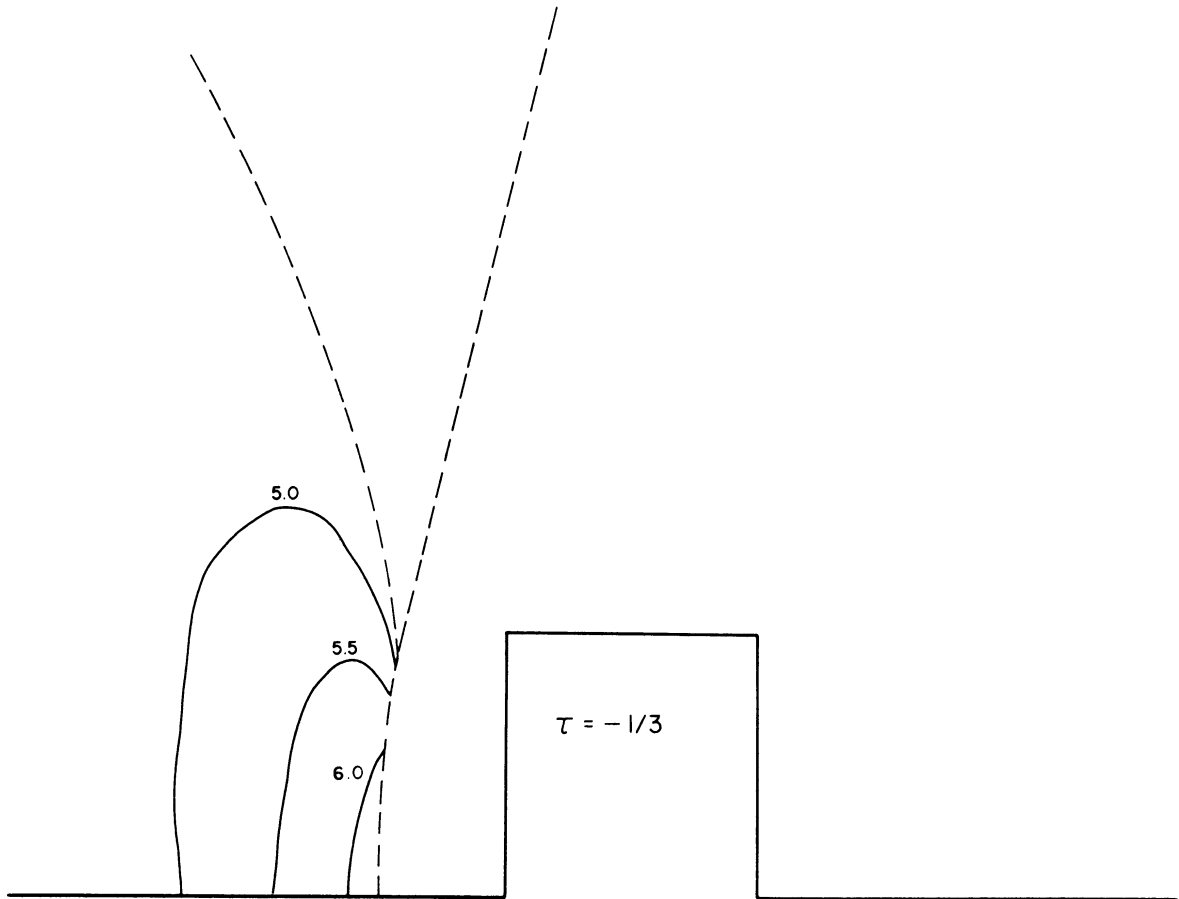
Block height..... 1

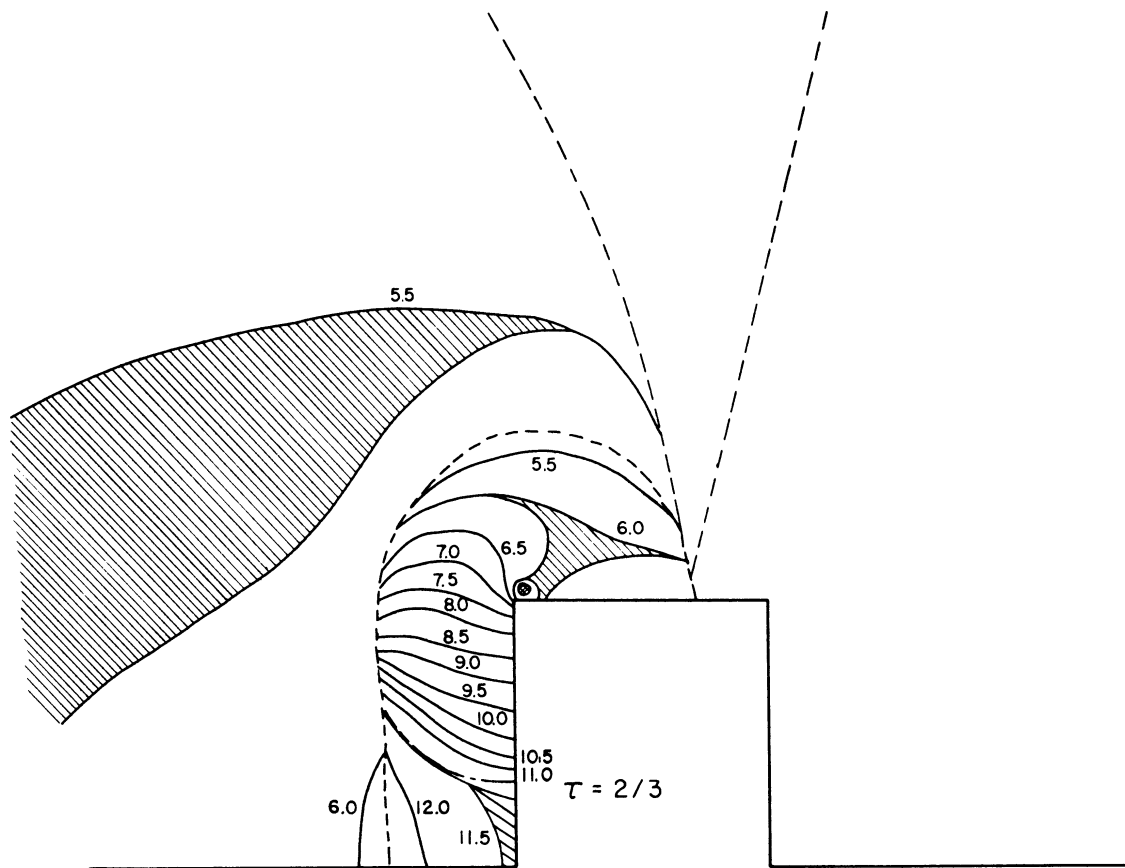
Angle of incidence..... 75°

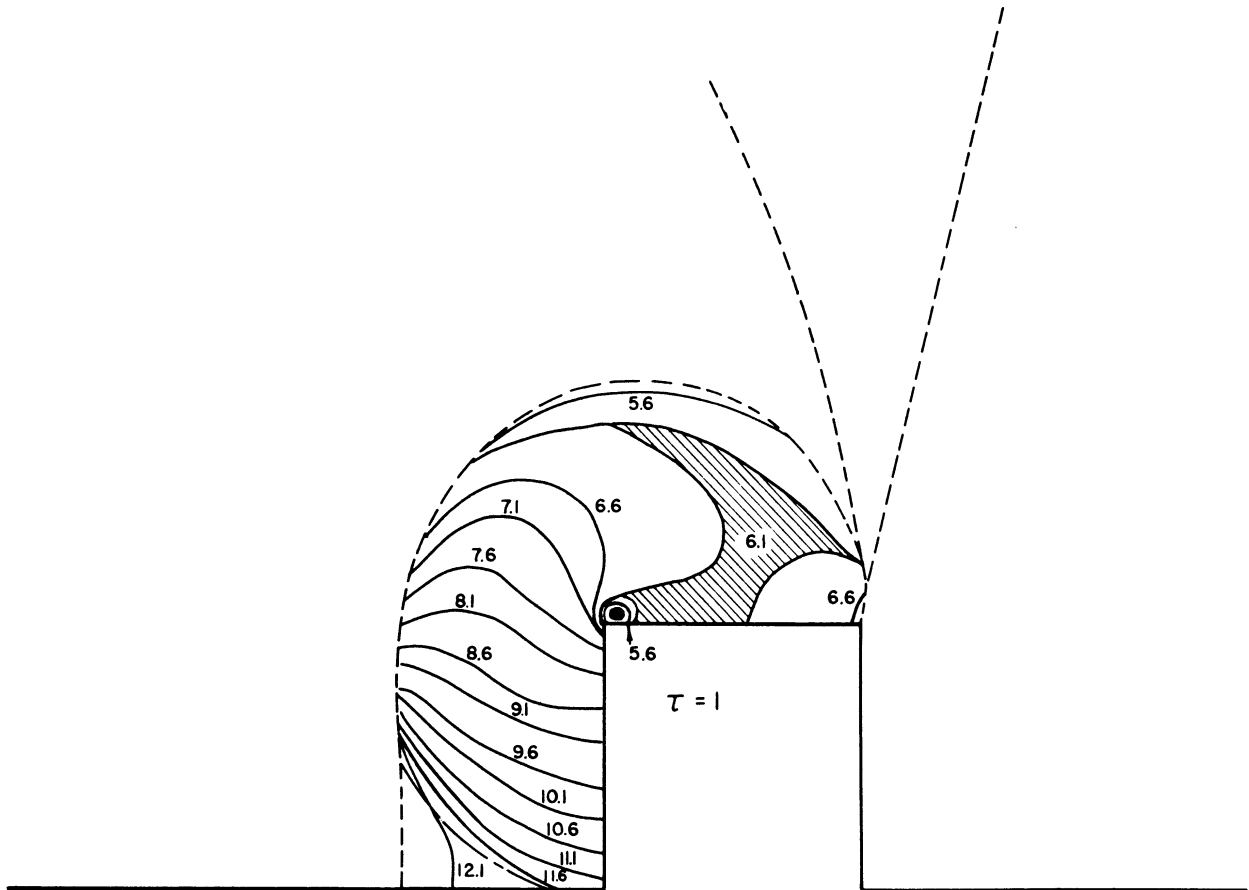
Density ratio..... $\frac{\rho_1}{\rho_0} = 1.154$

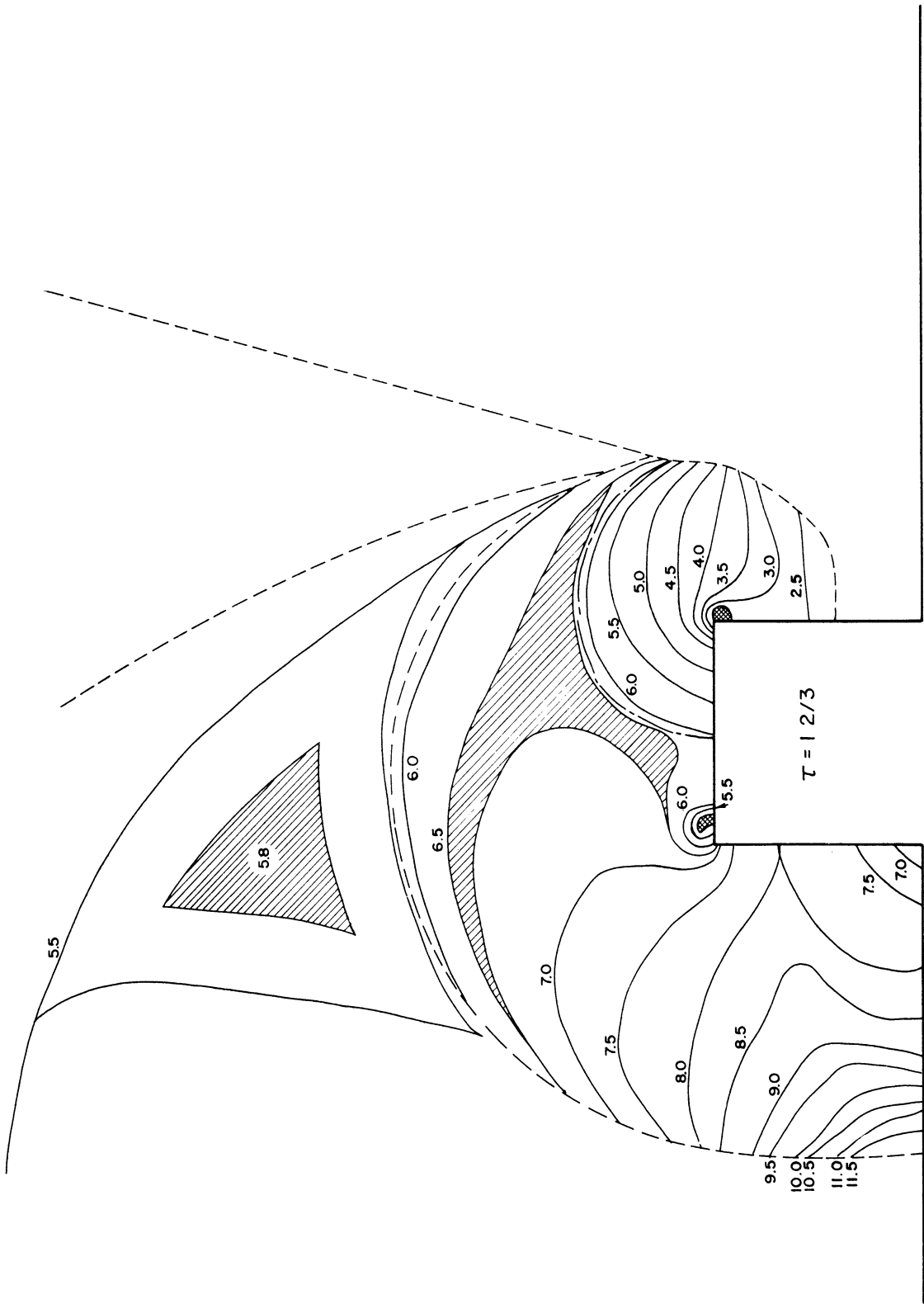
Pressure..... $P_0 = 739$ mm Hg.

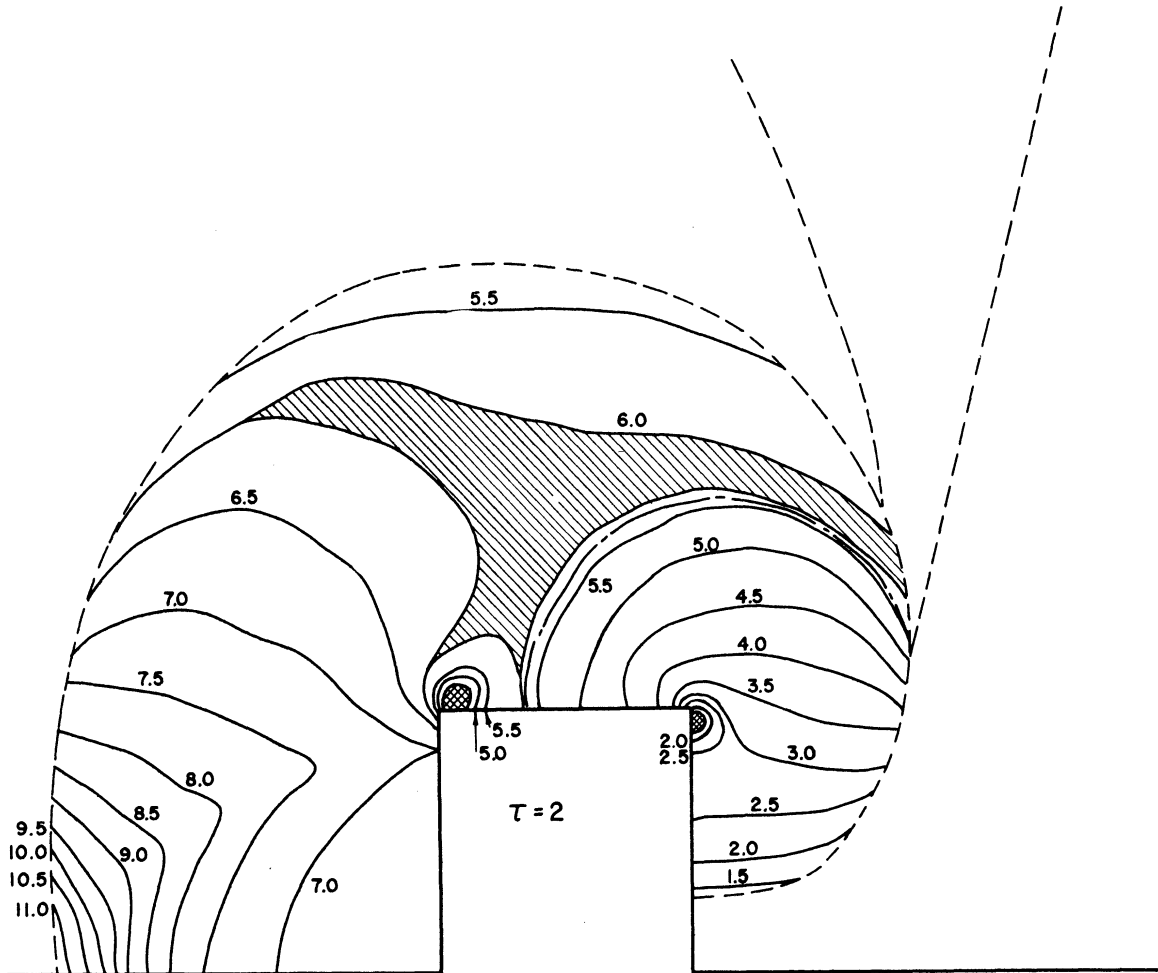
Shift across incident shock... $n_1 = 4.06$

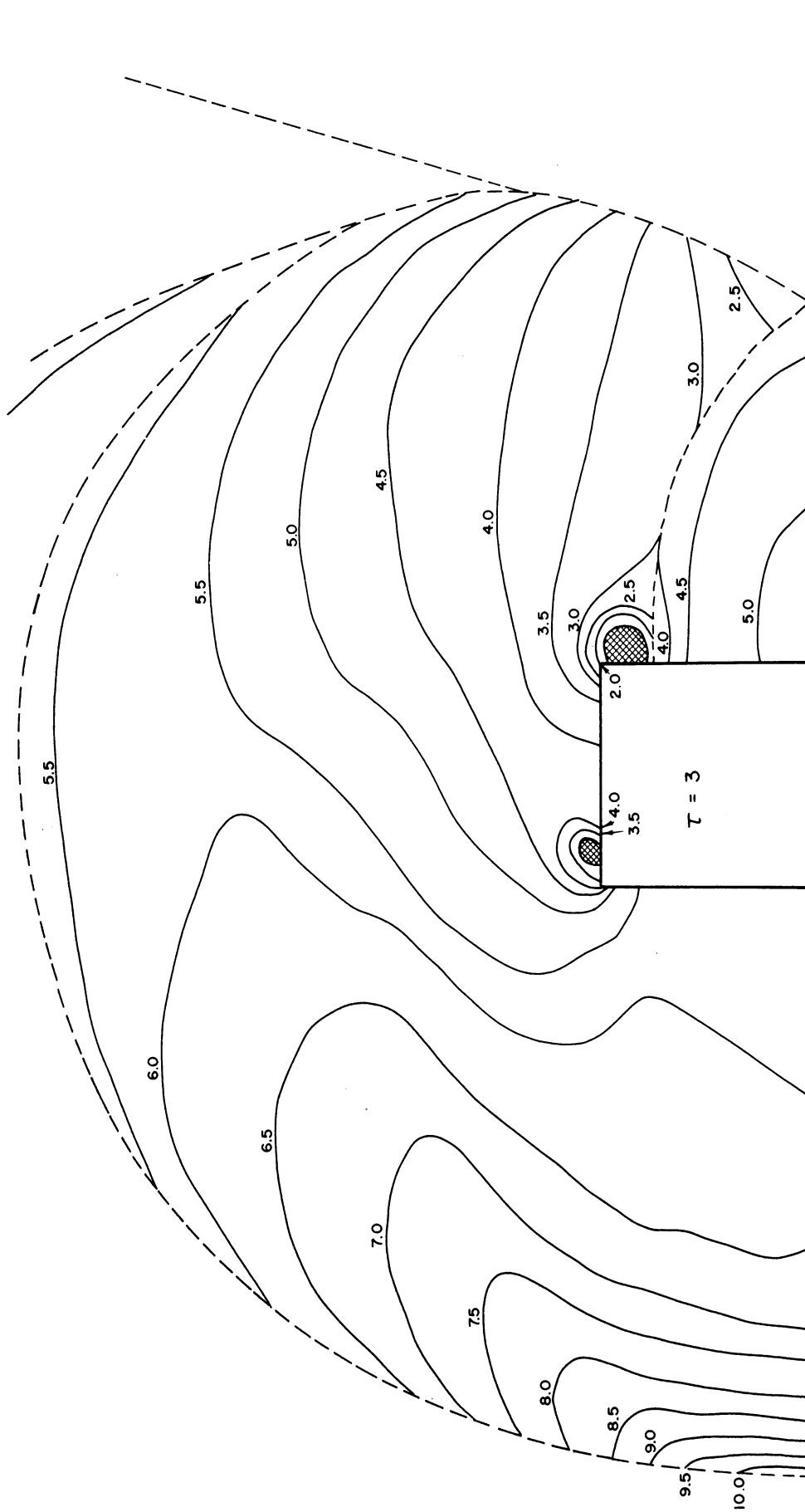


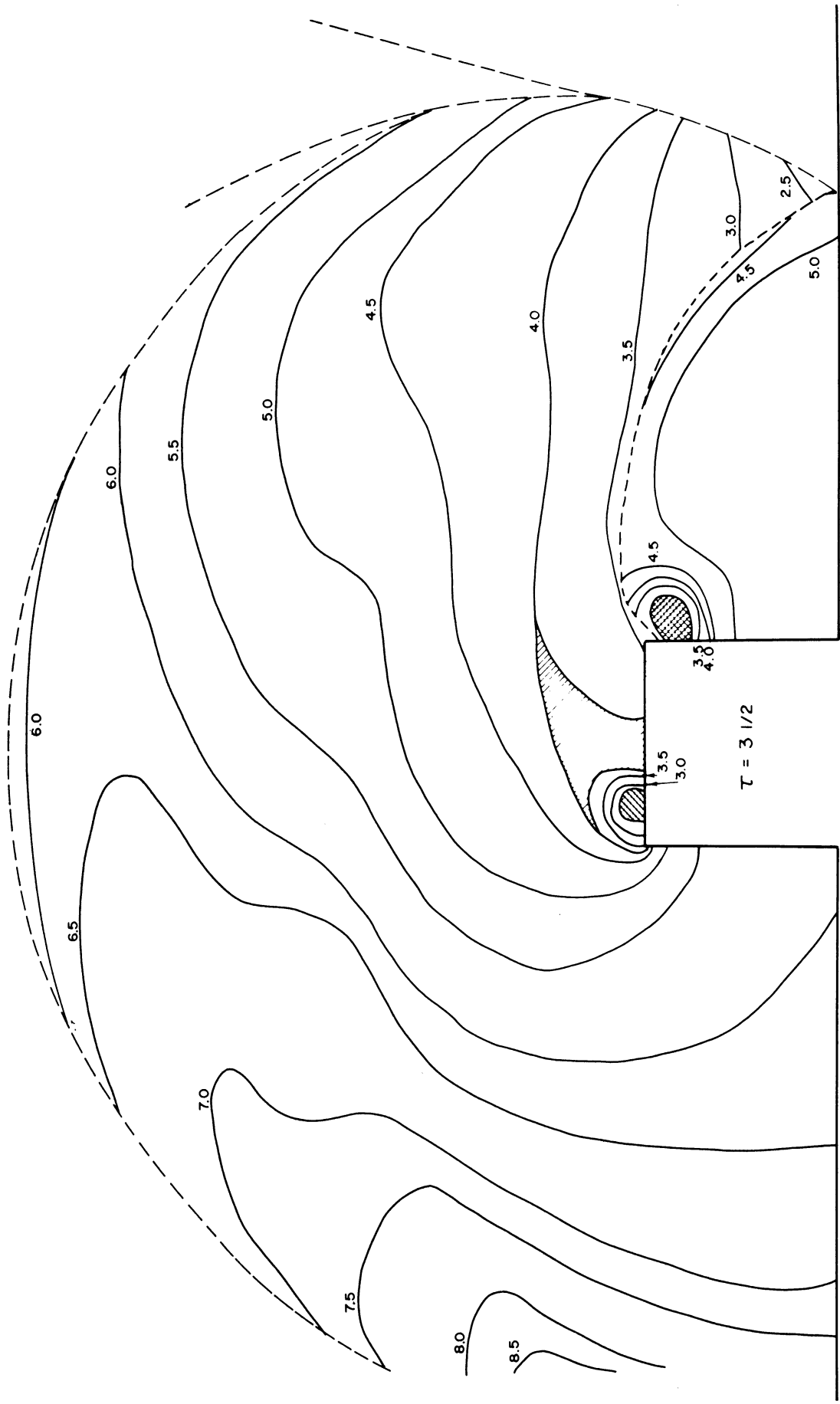


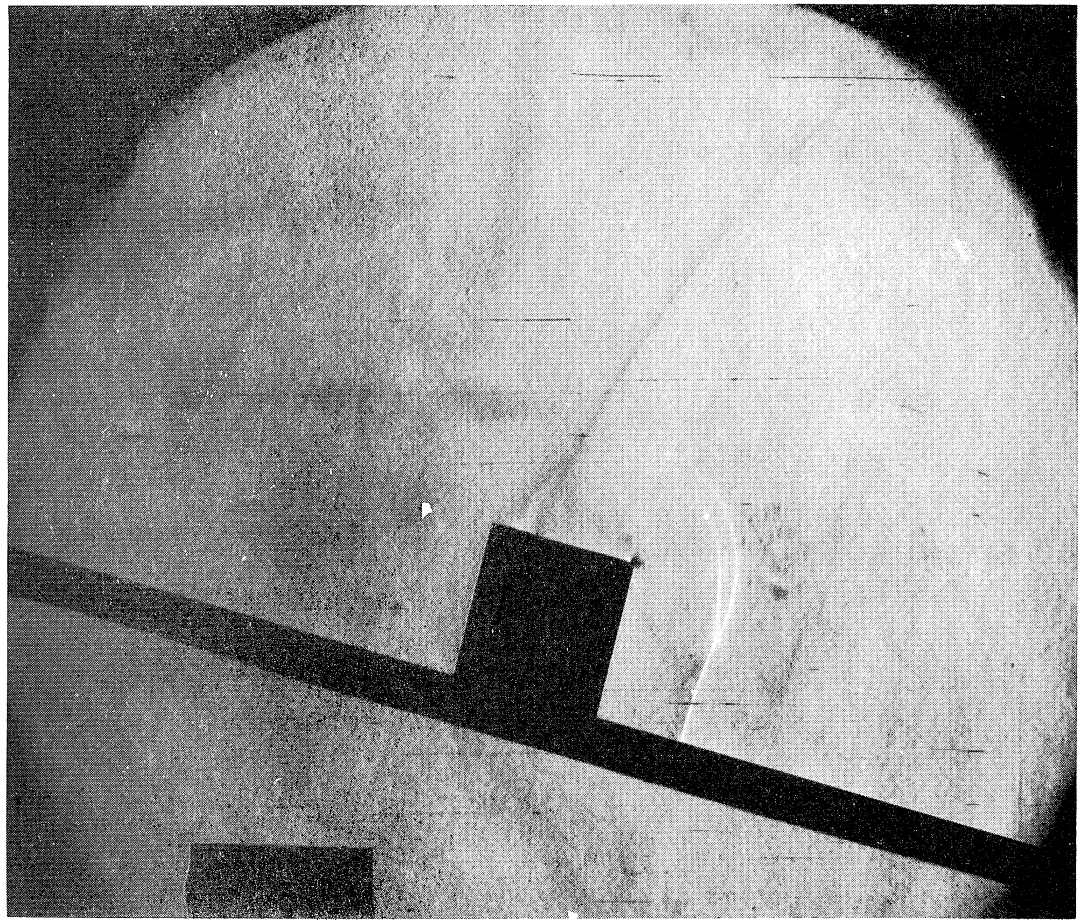
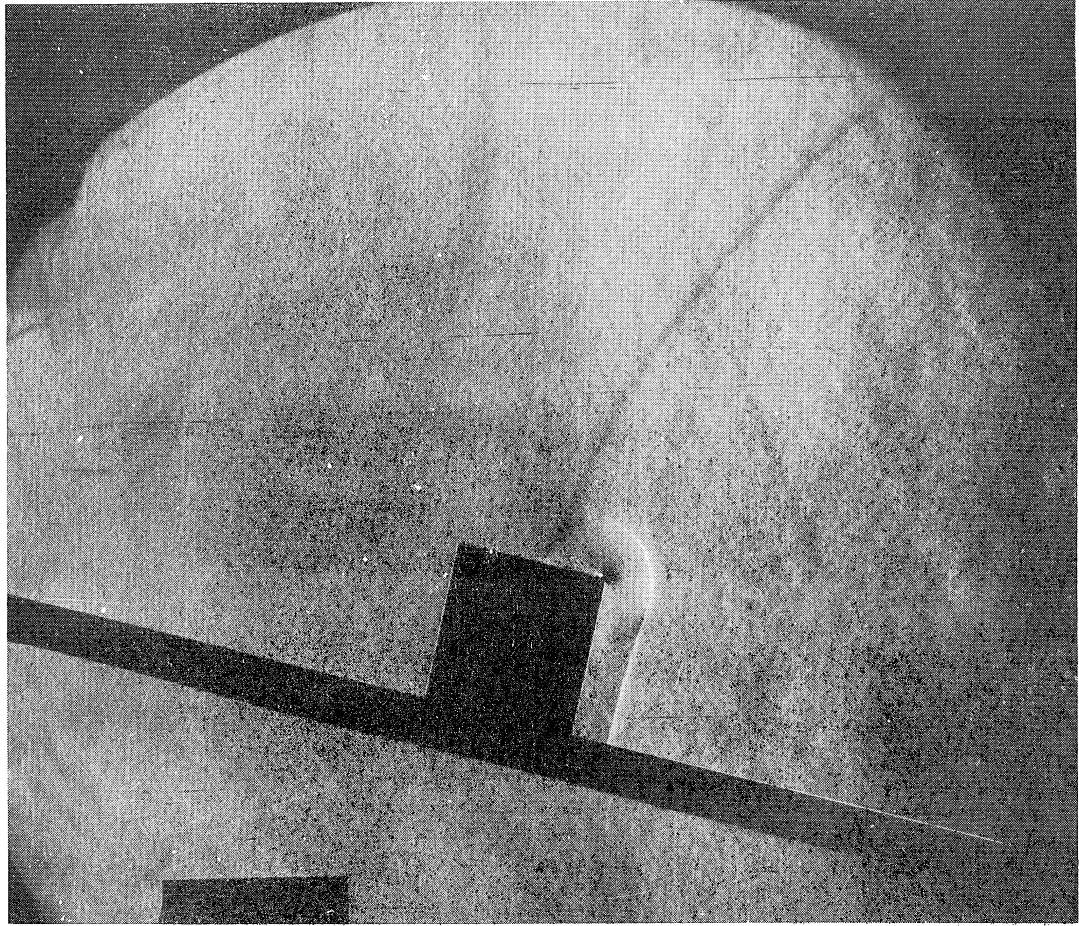


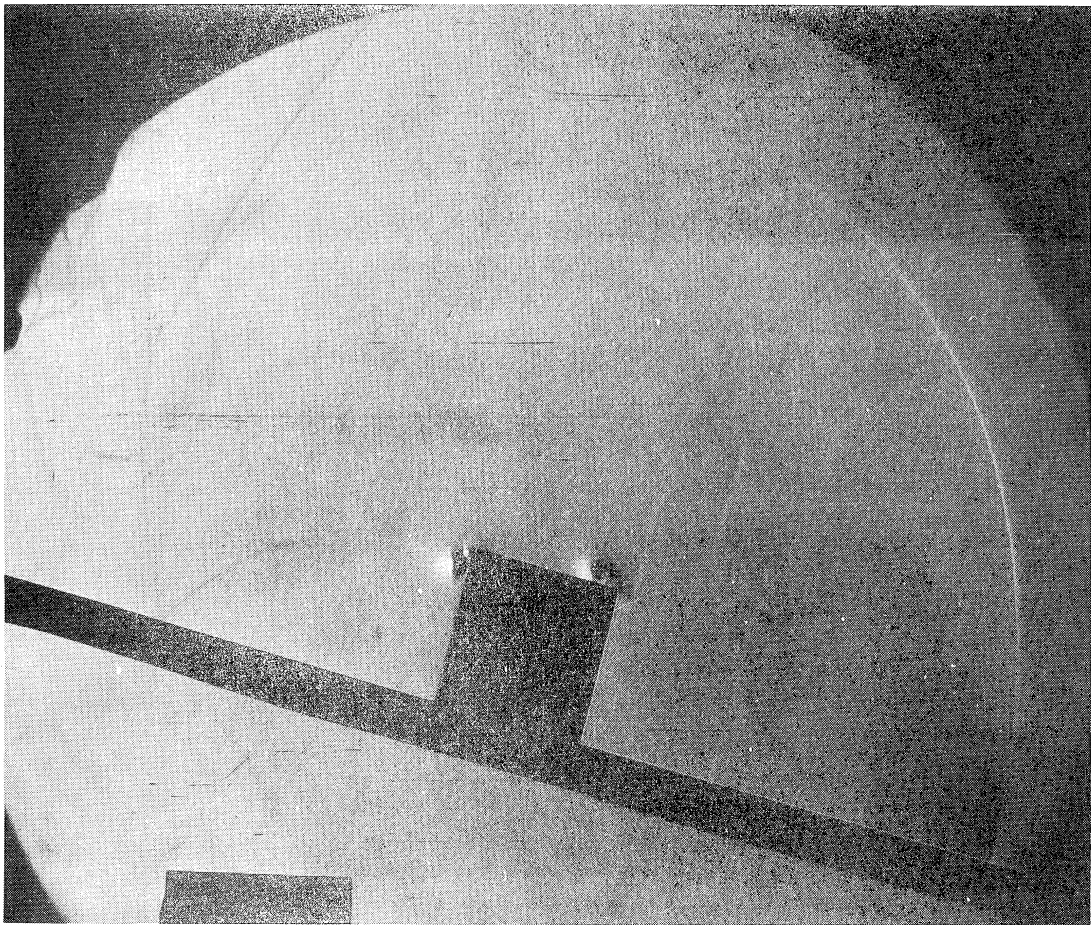
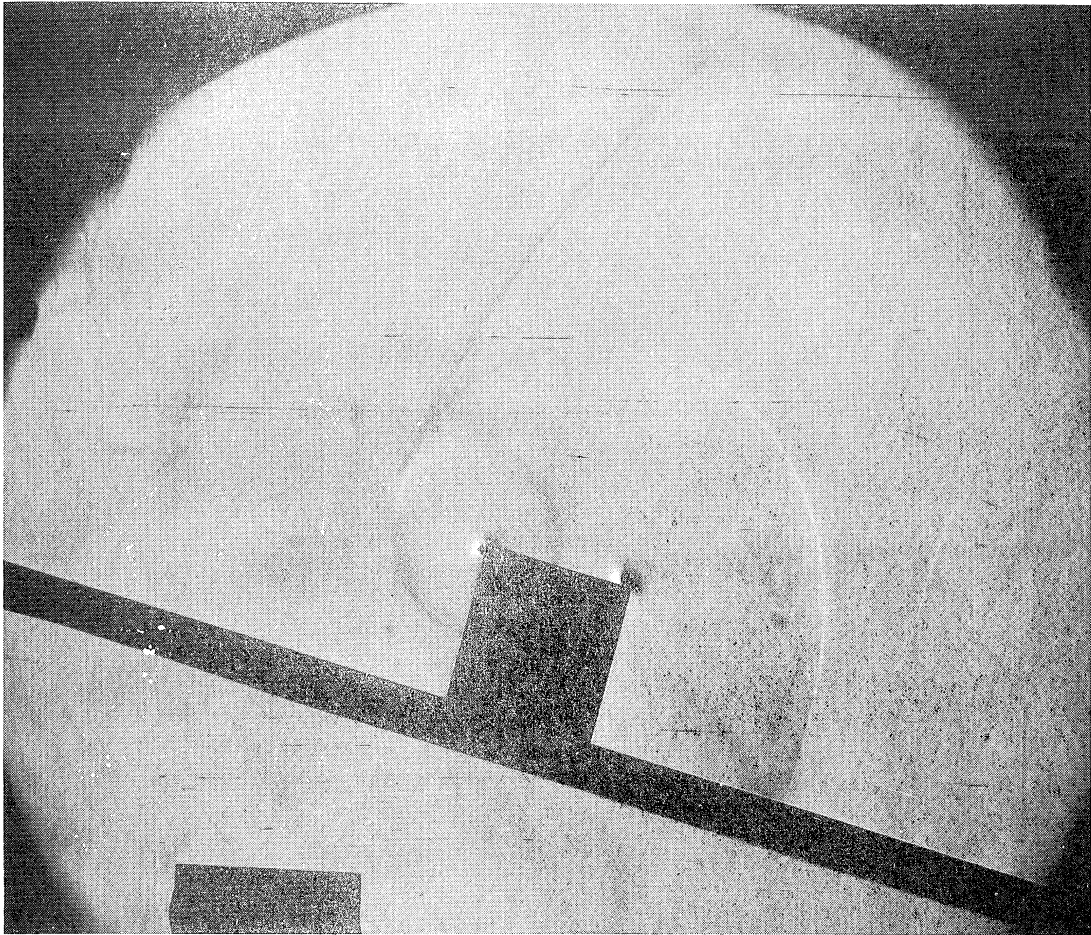












SERIES V

Shock strength..... $\gamma = 1.224$

Mach stem height..... 2

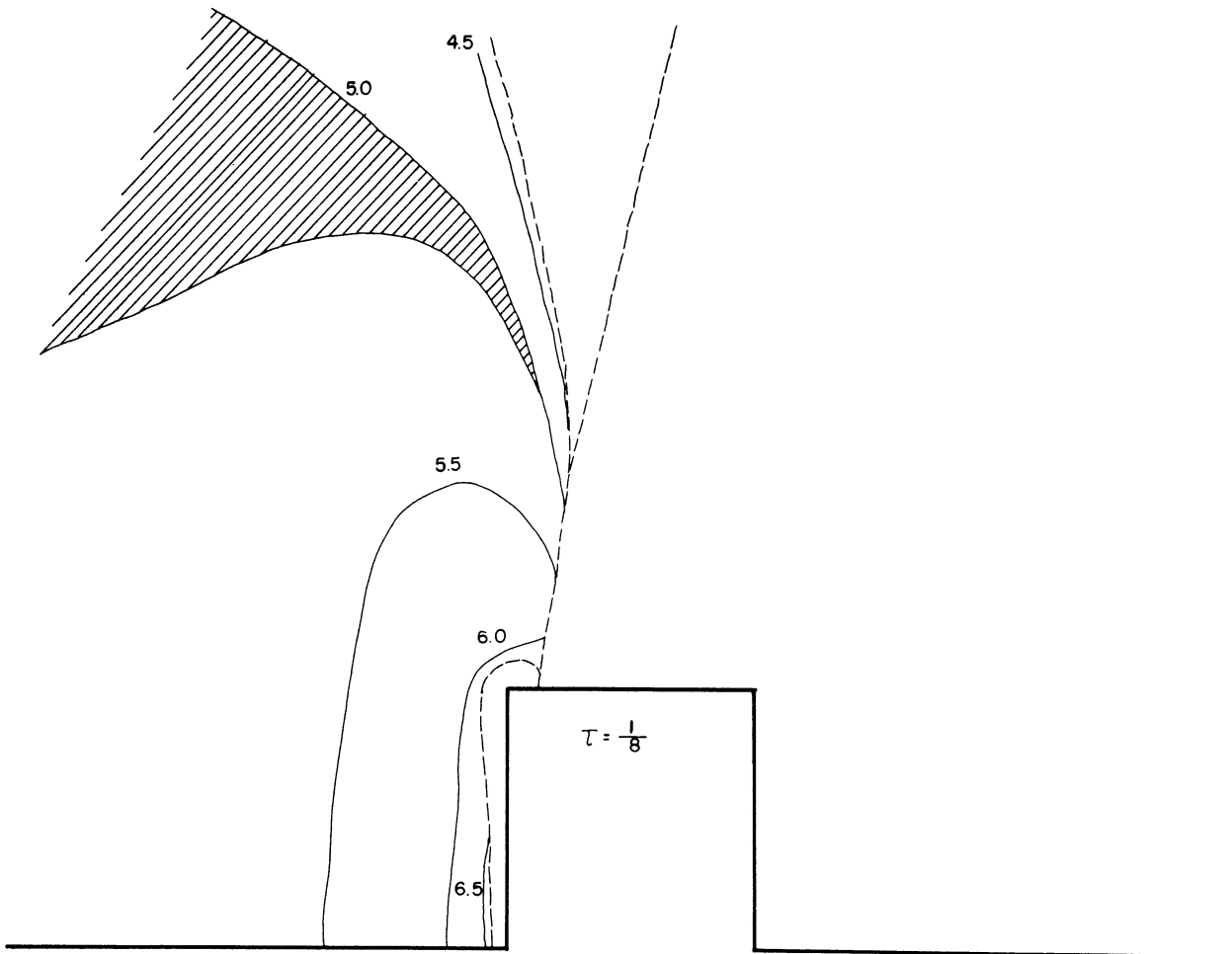
Block height..... $3/4$

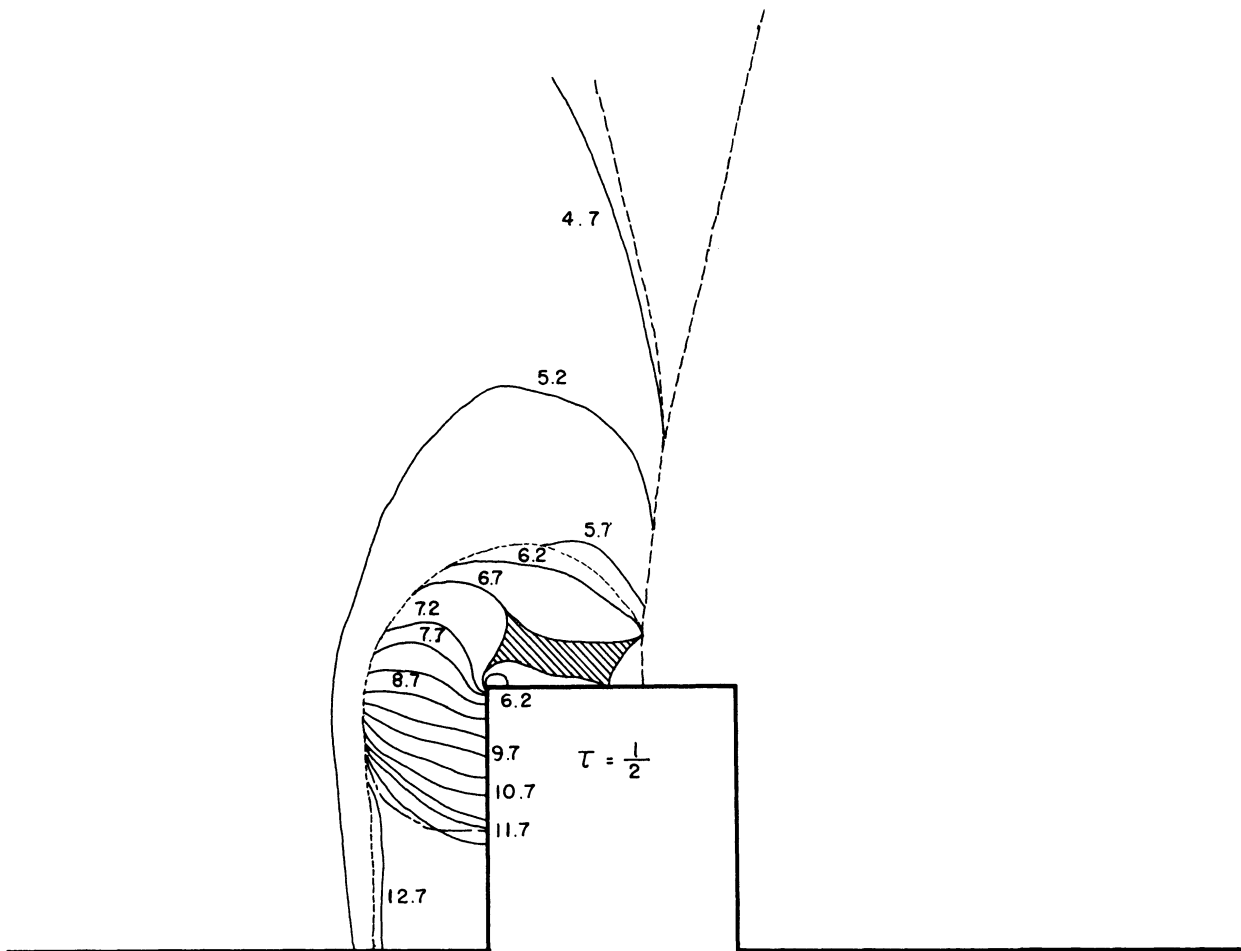
Angle of incidence..... 75°

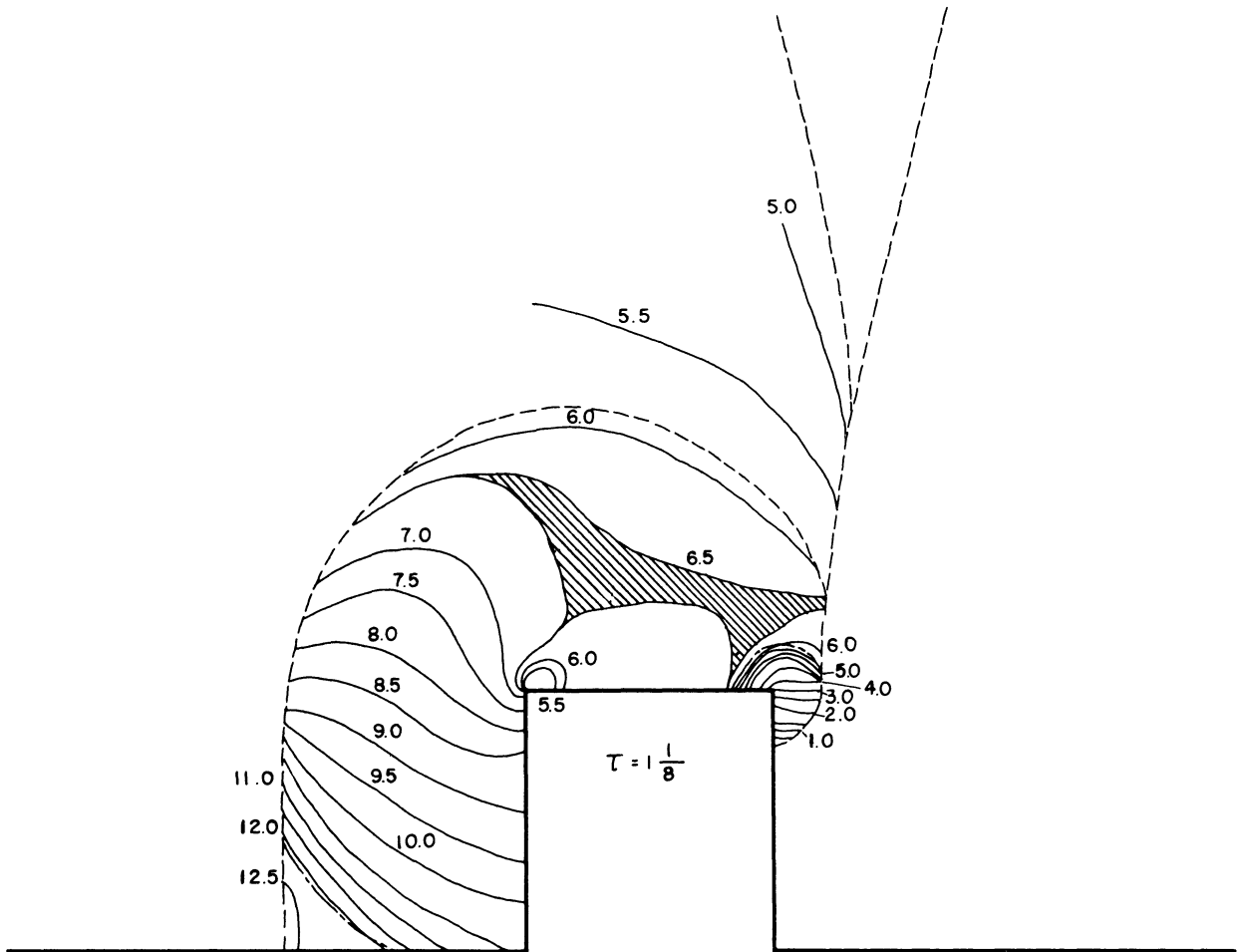
Density ratio..... $\frac{\rho_1}{\rho_0} = 1.154$

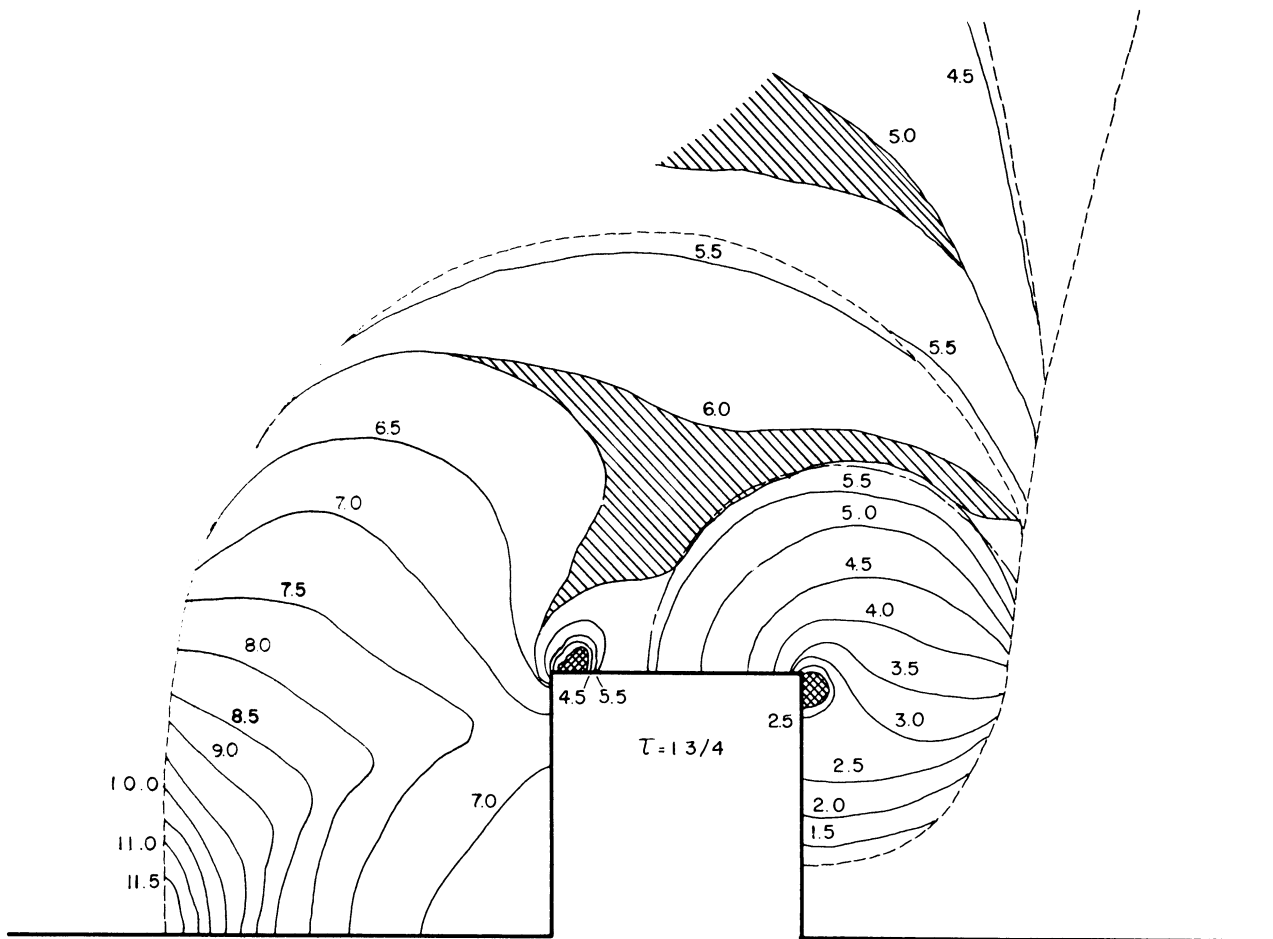
Pressure..... $P_0 = 736$ mm Hg.

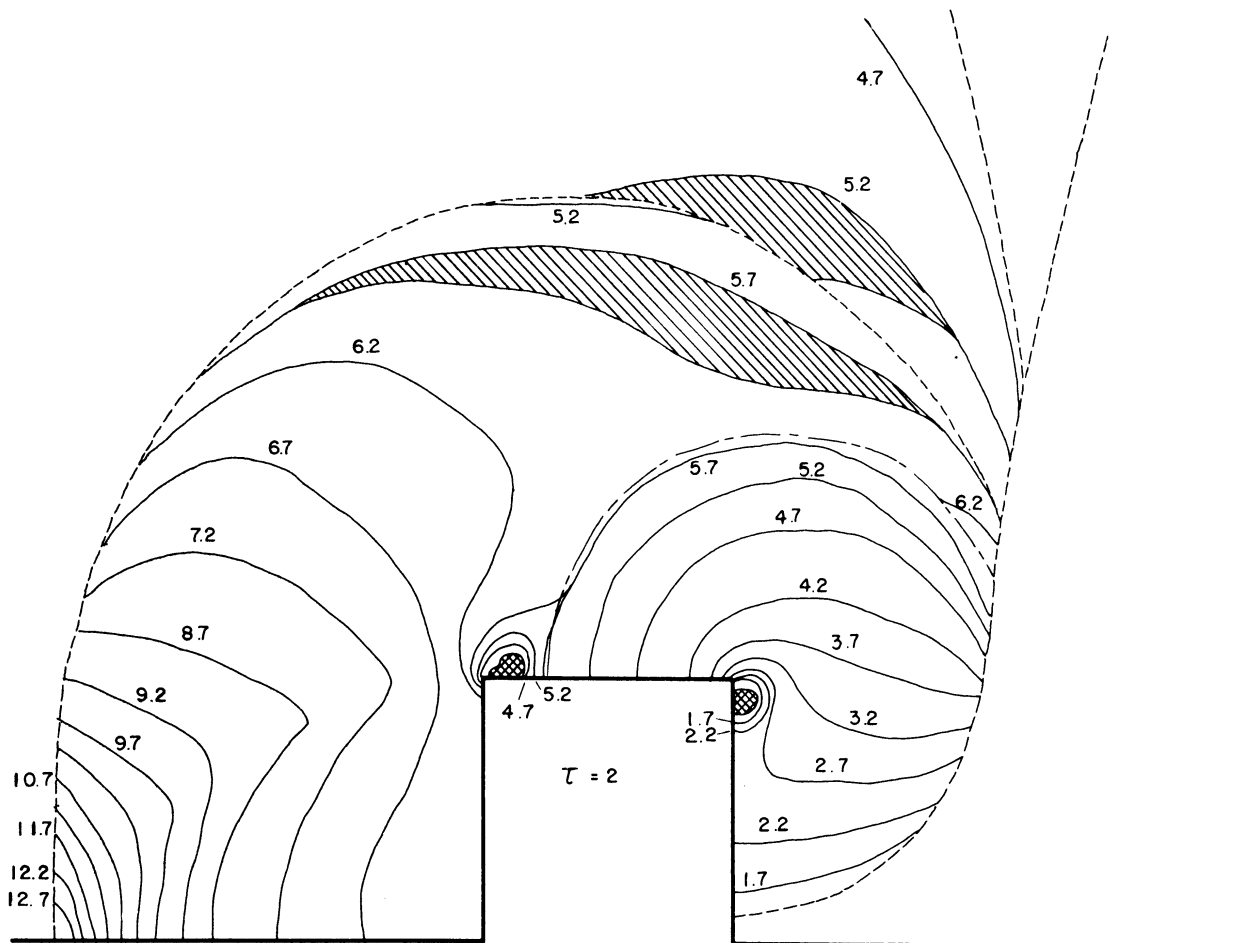
Shift across incident shock... $n_1 = 4.06$

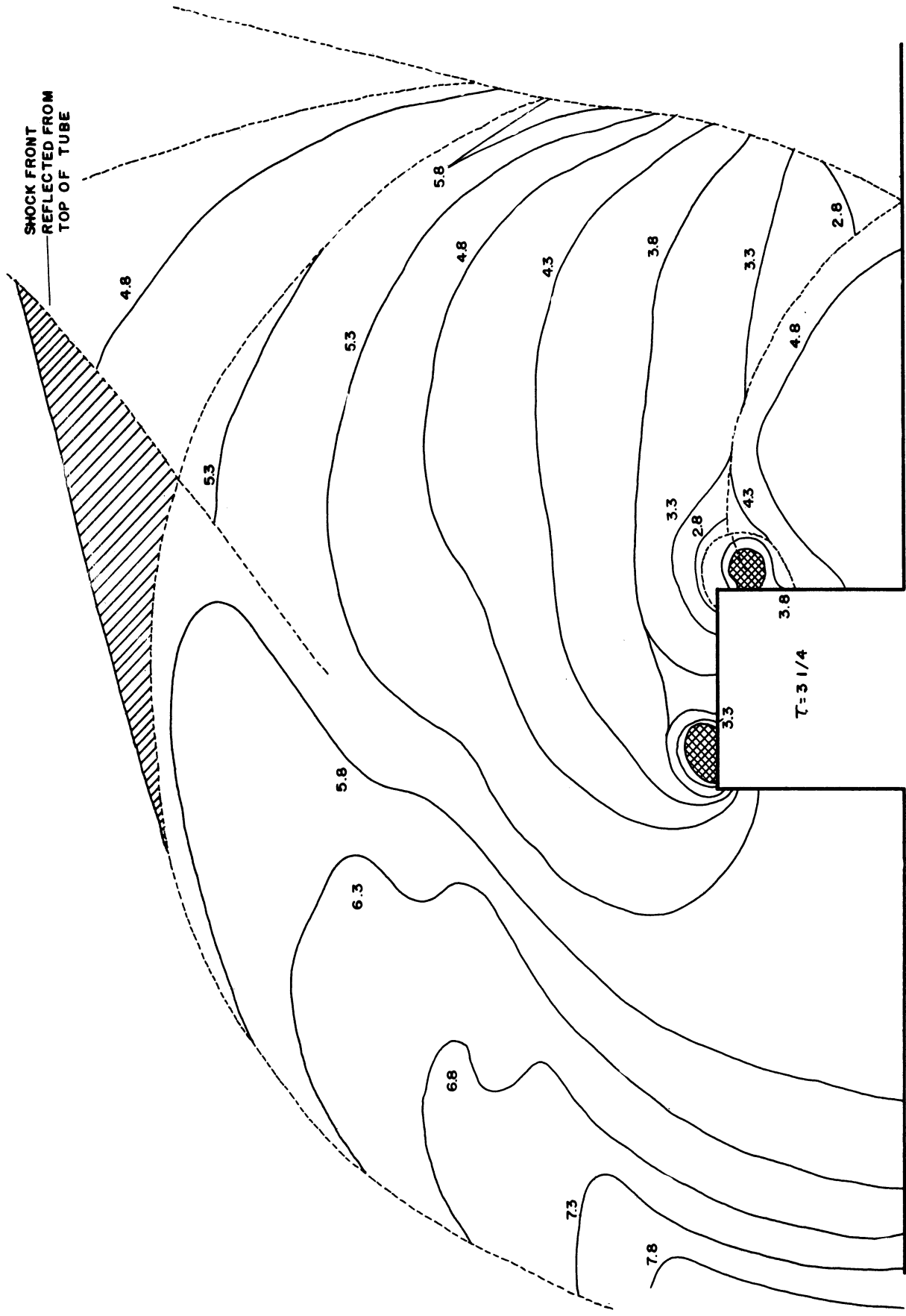


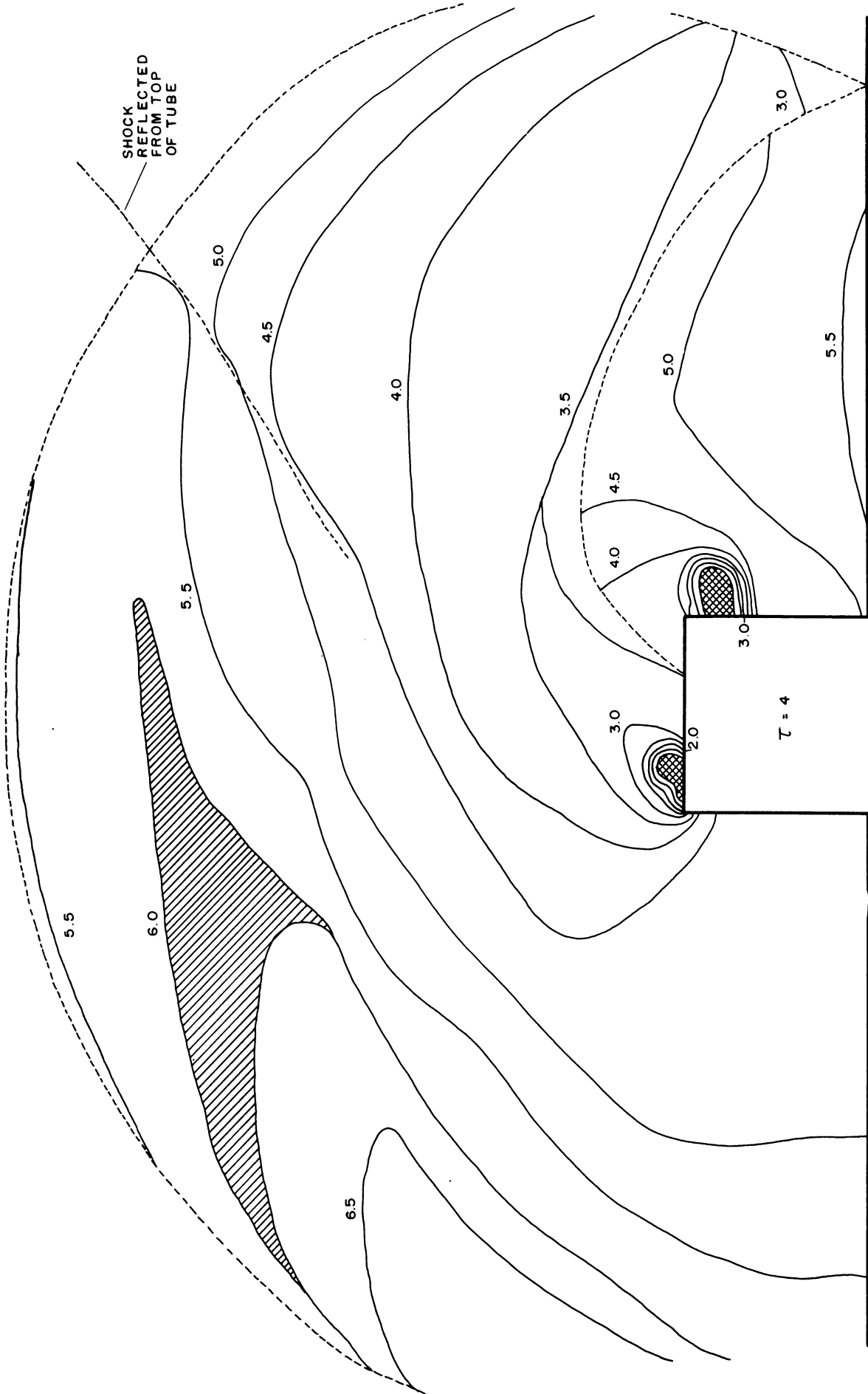


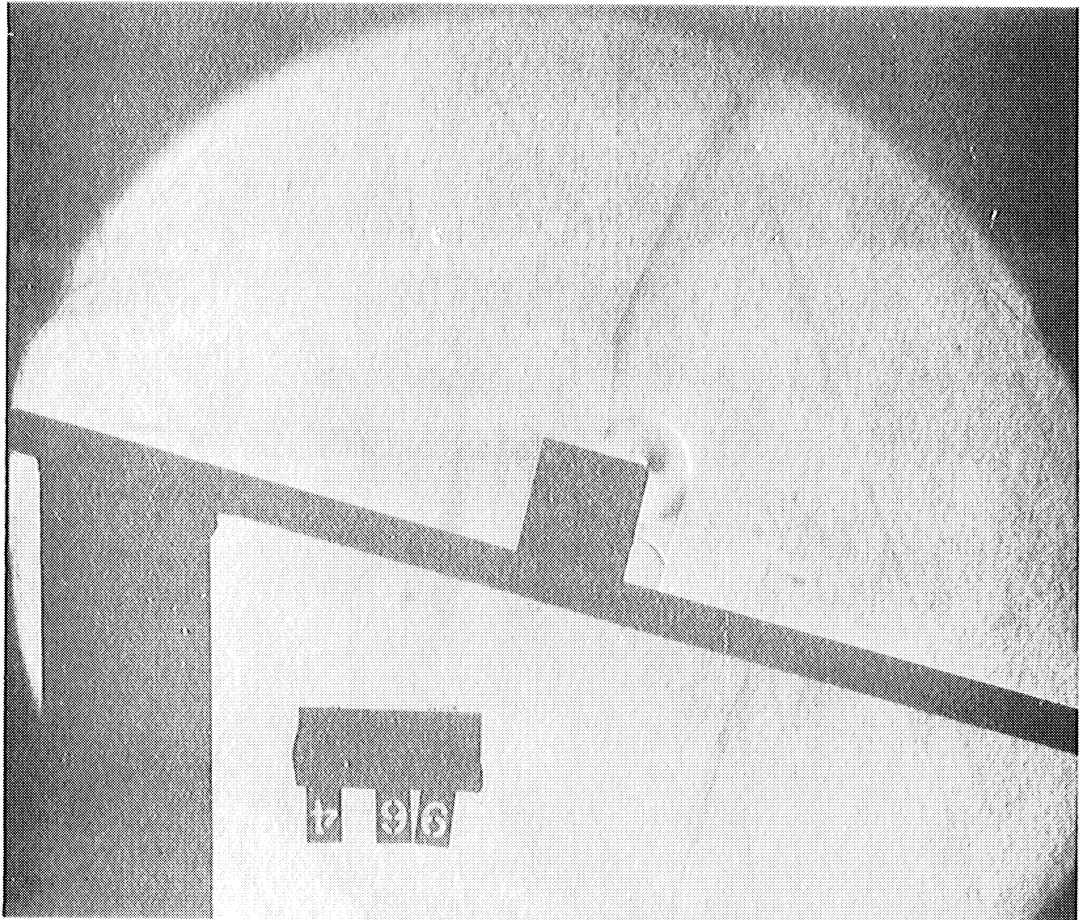
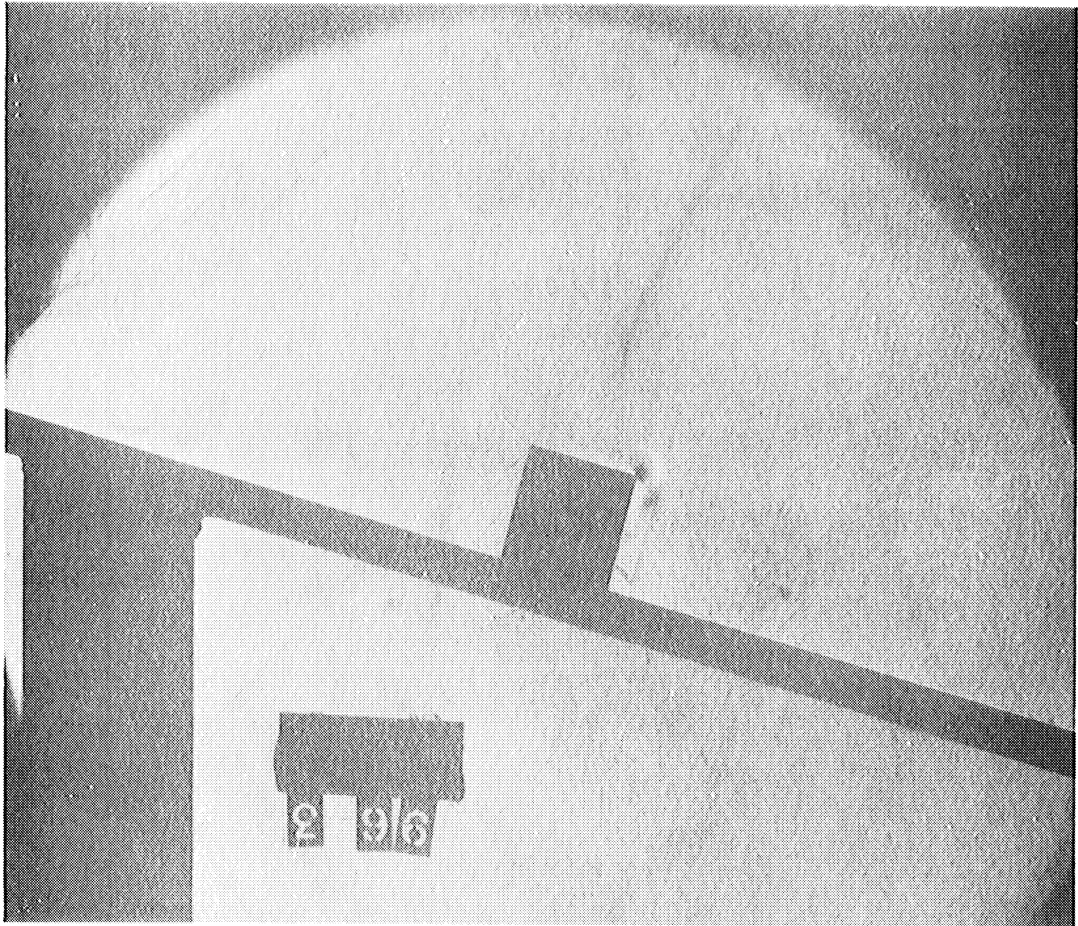


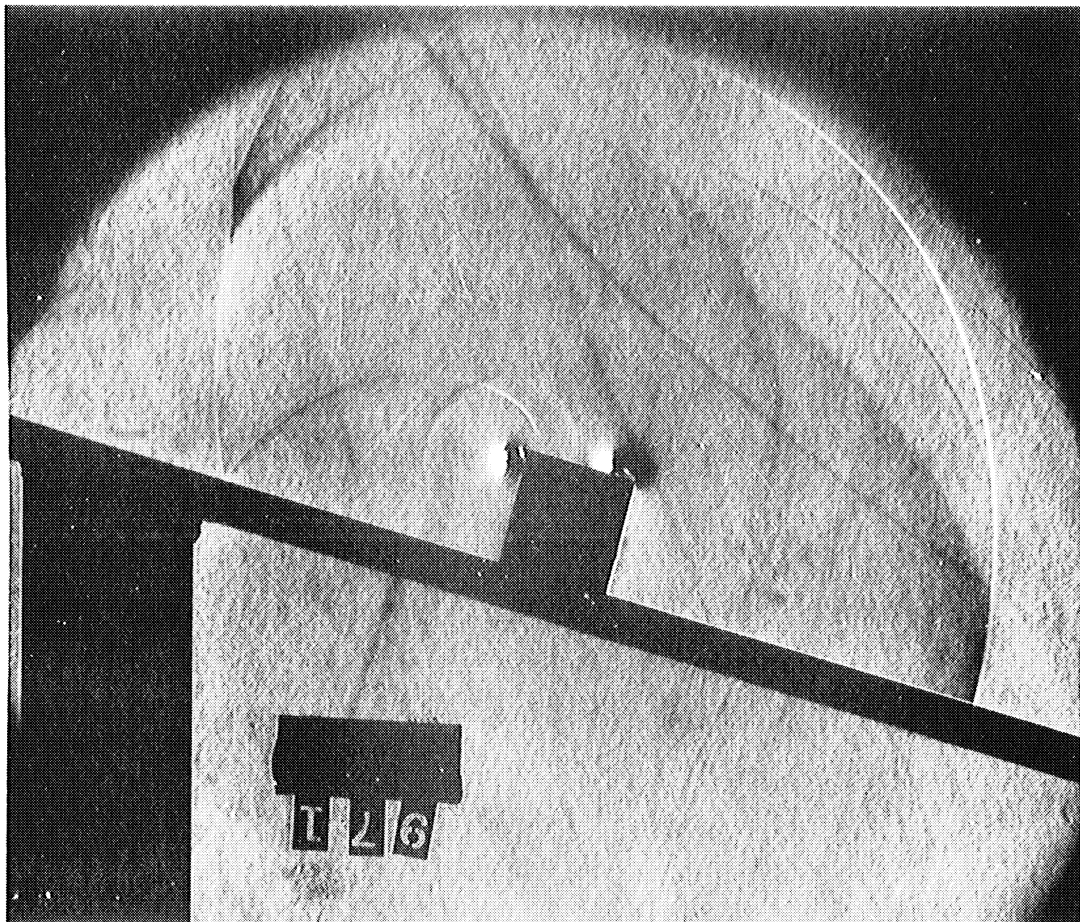
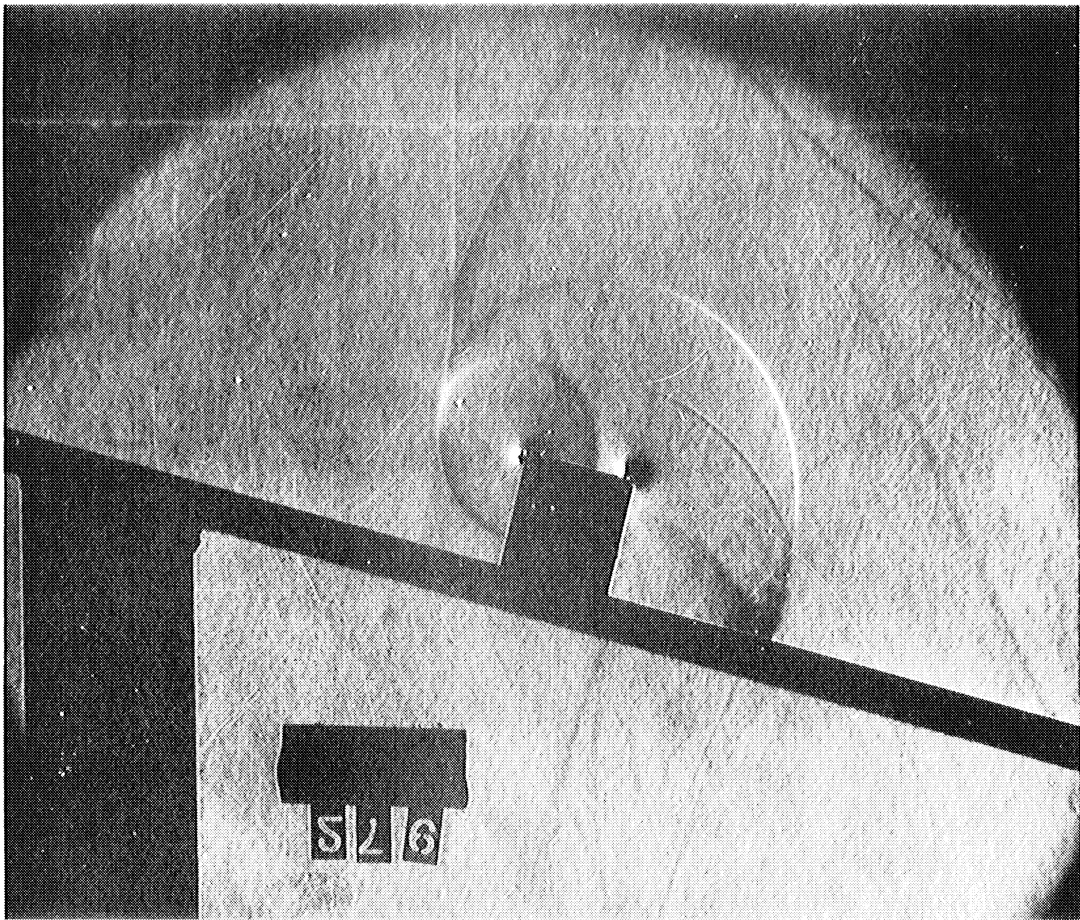












SERIES VI

Shock strength..... $\gamma = 1.33$

Mach stem height..... $1/2$

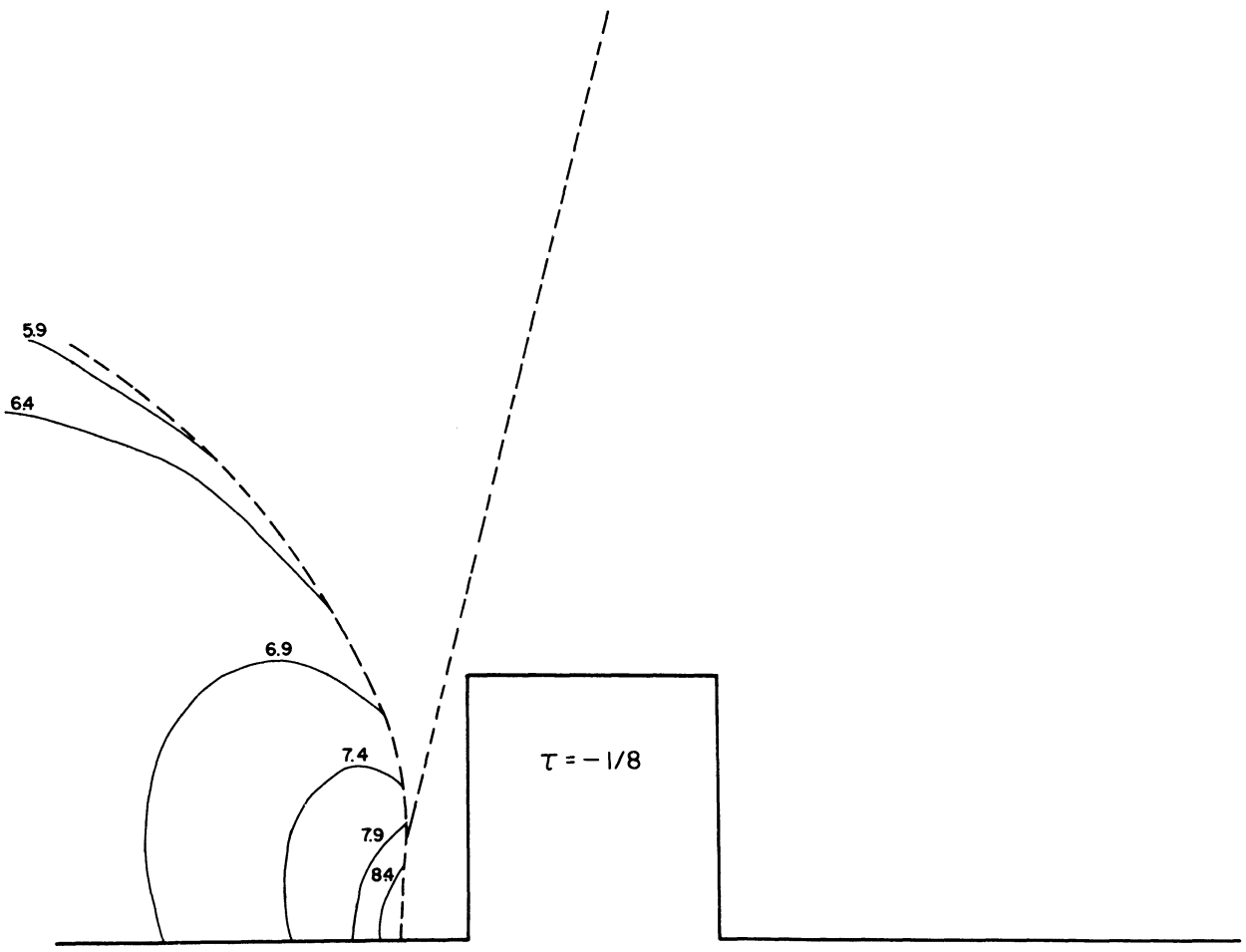
Block height..... 1

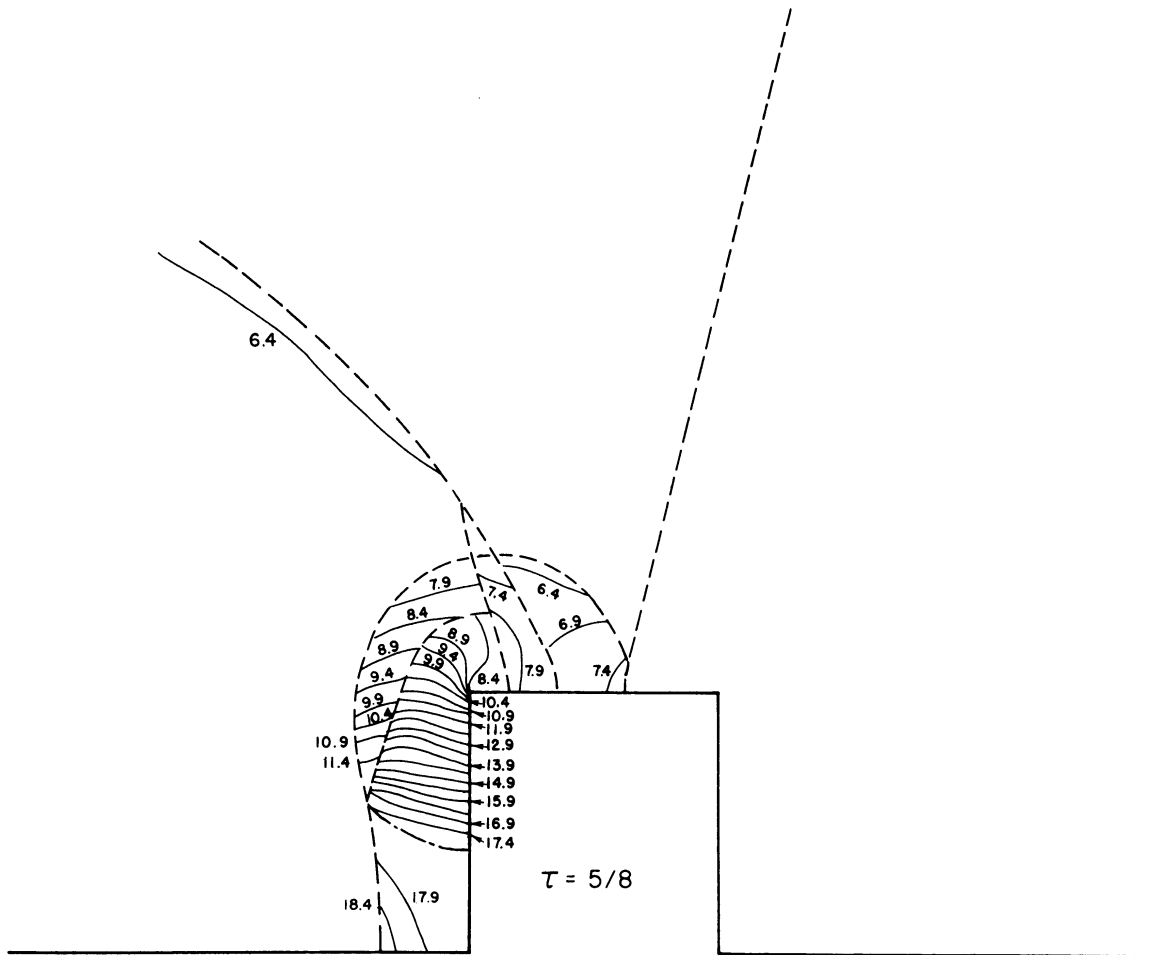
Angle of incidence..... 75°

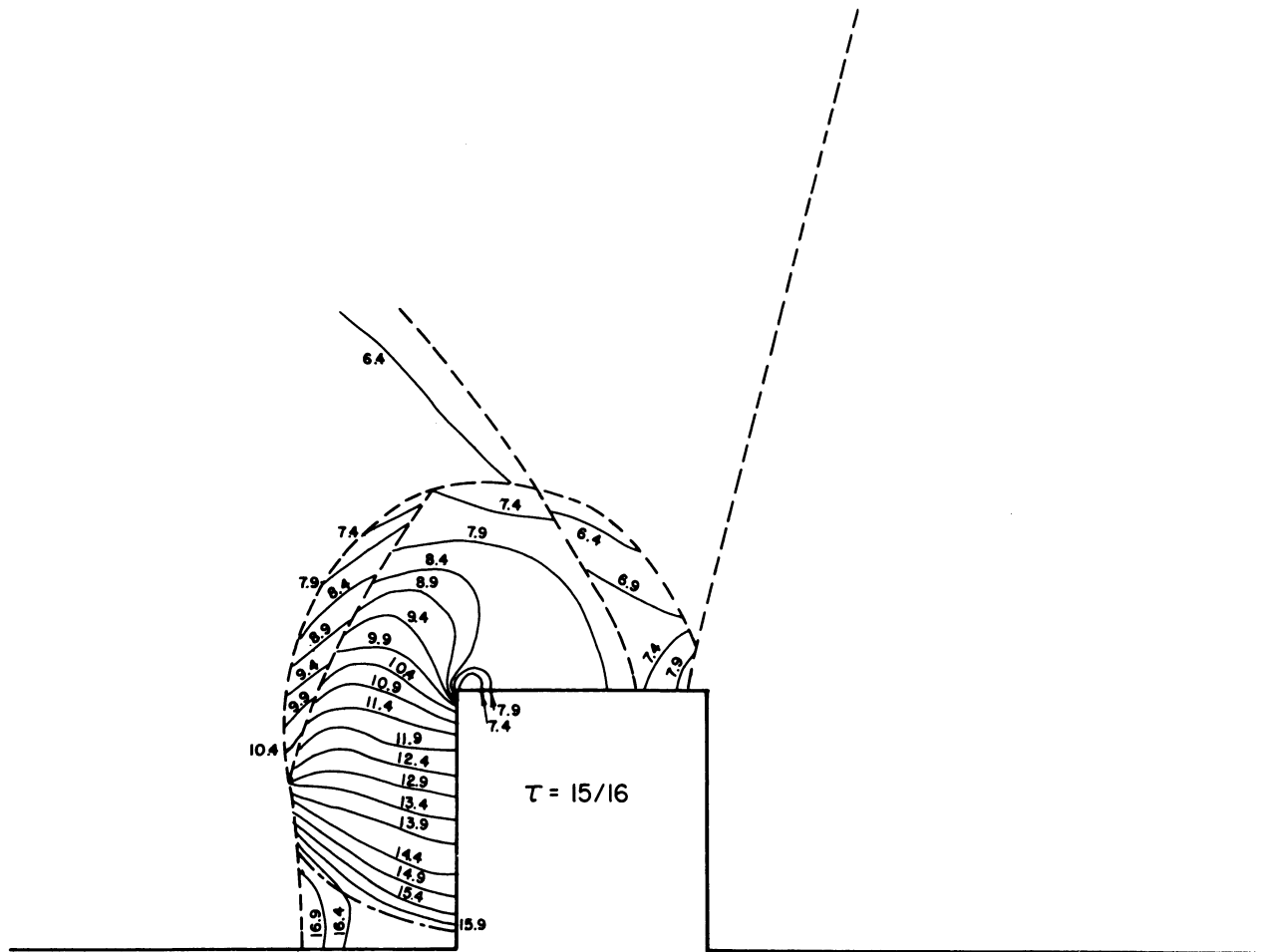
Density ratio..... $\frac{\rho_1}{\rho_0} = 1.223$

Pressure..... $P_0 = 733$ mm Hg.

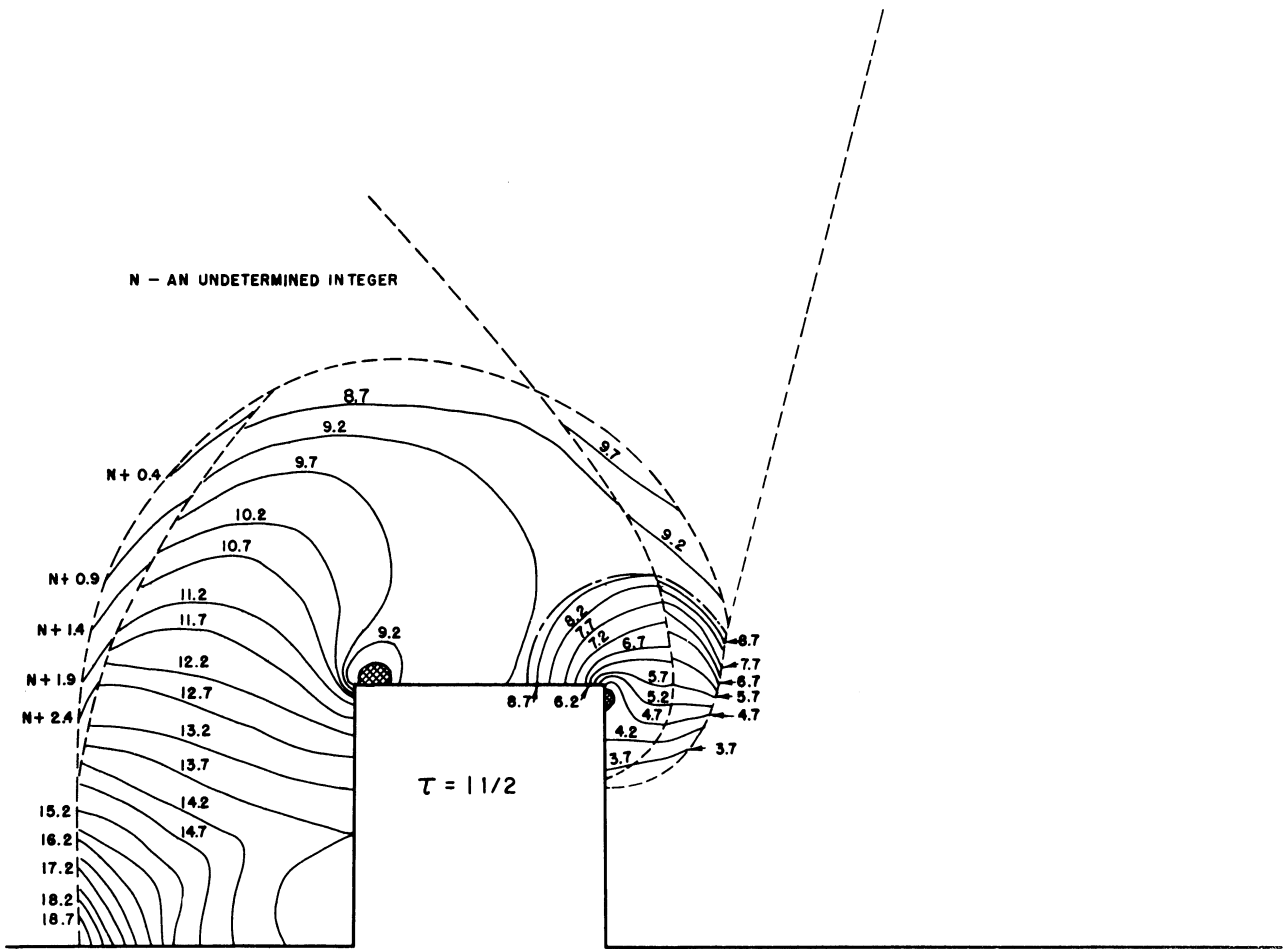
Shift across incident shock... $n_1 = 5.75$



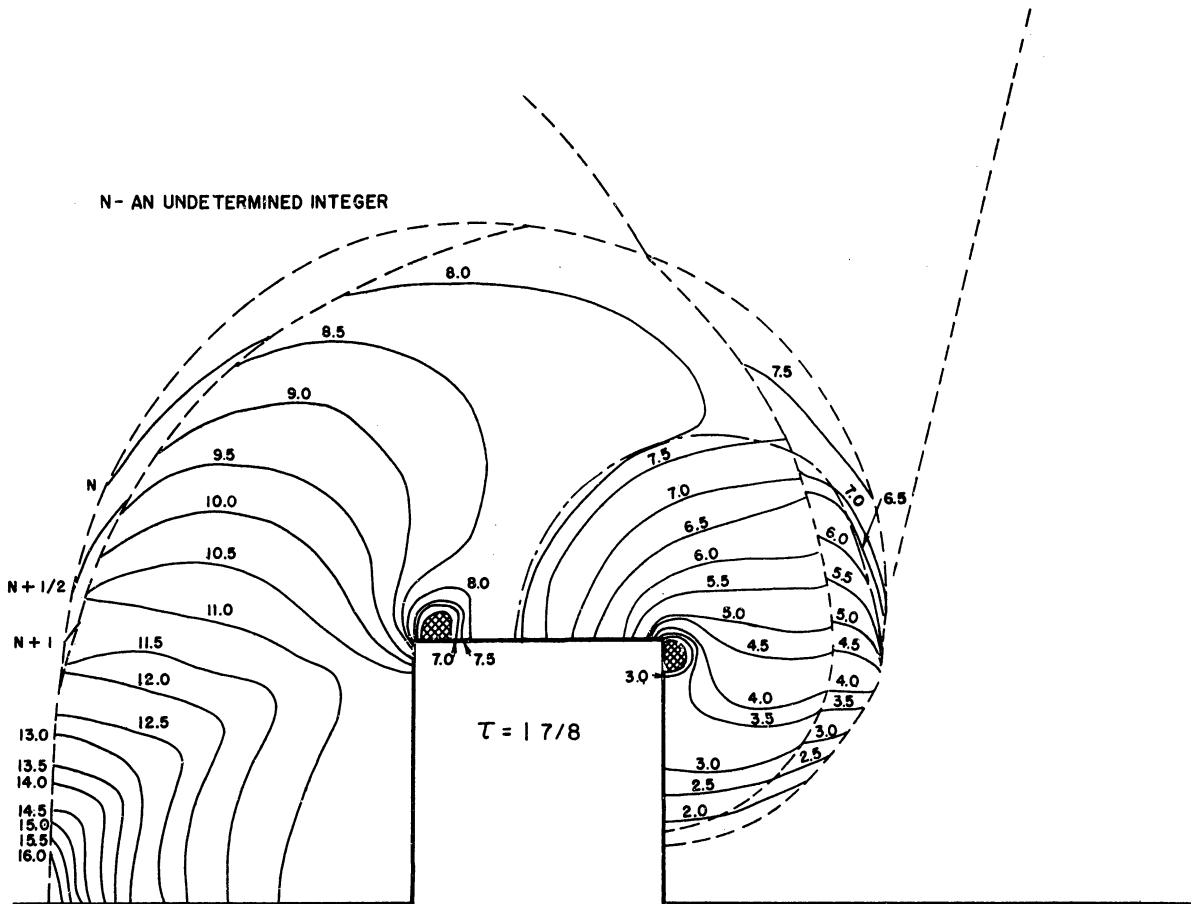


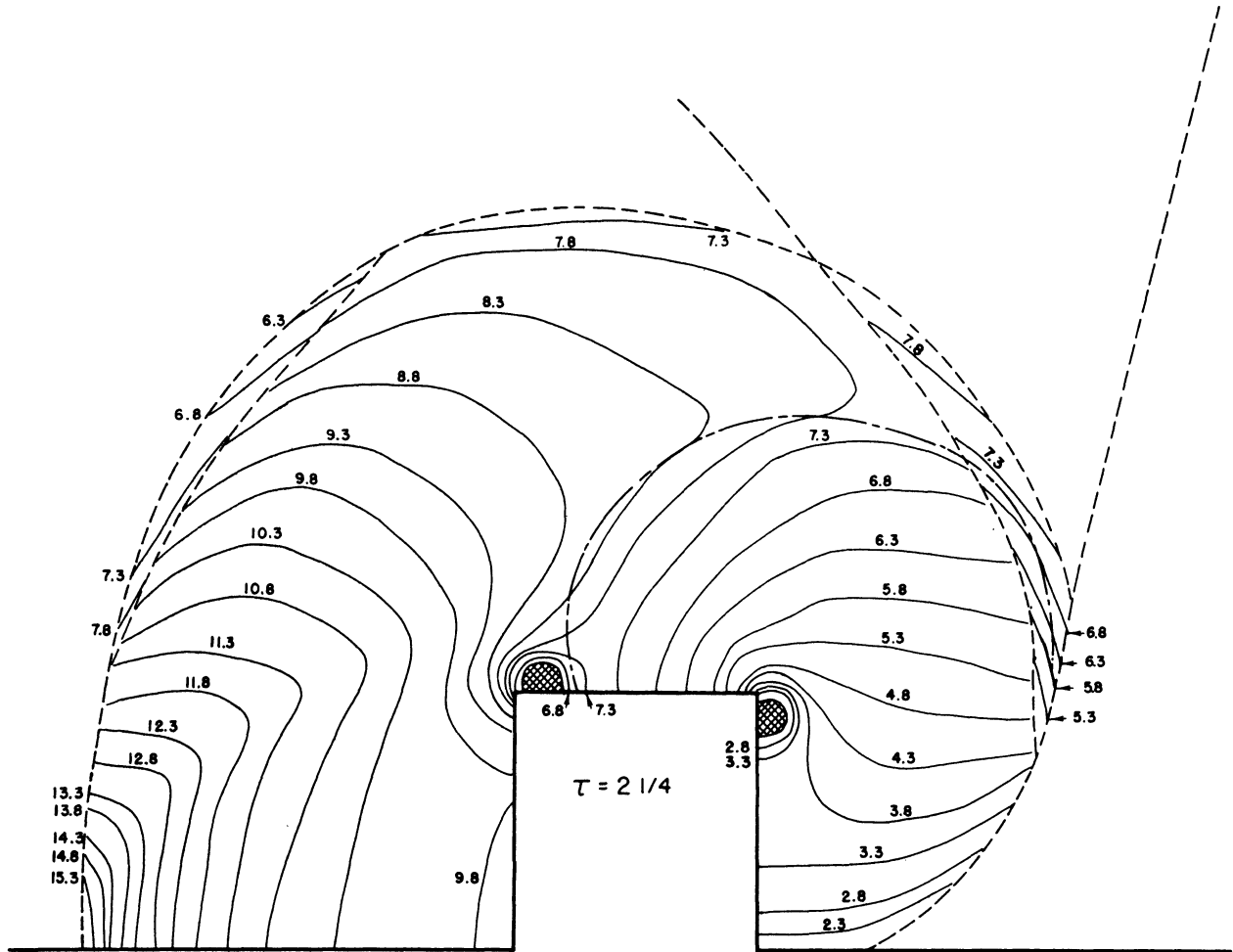


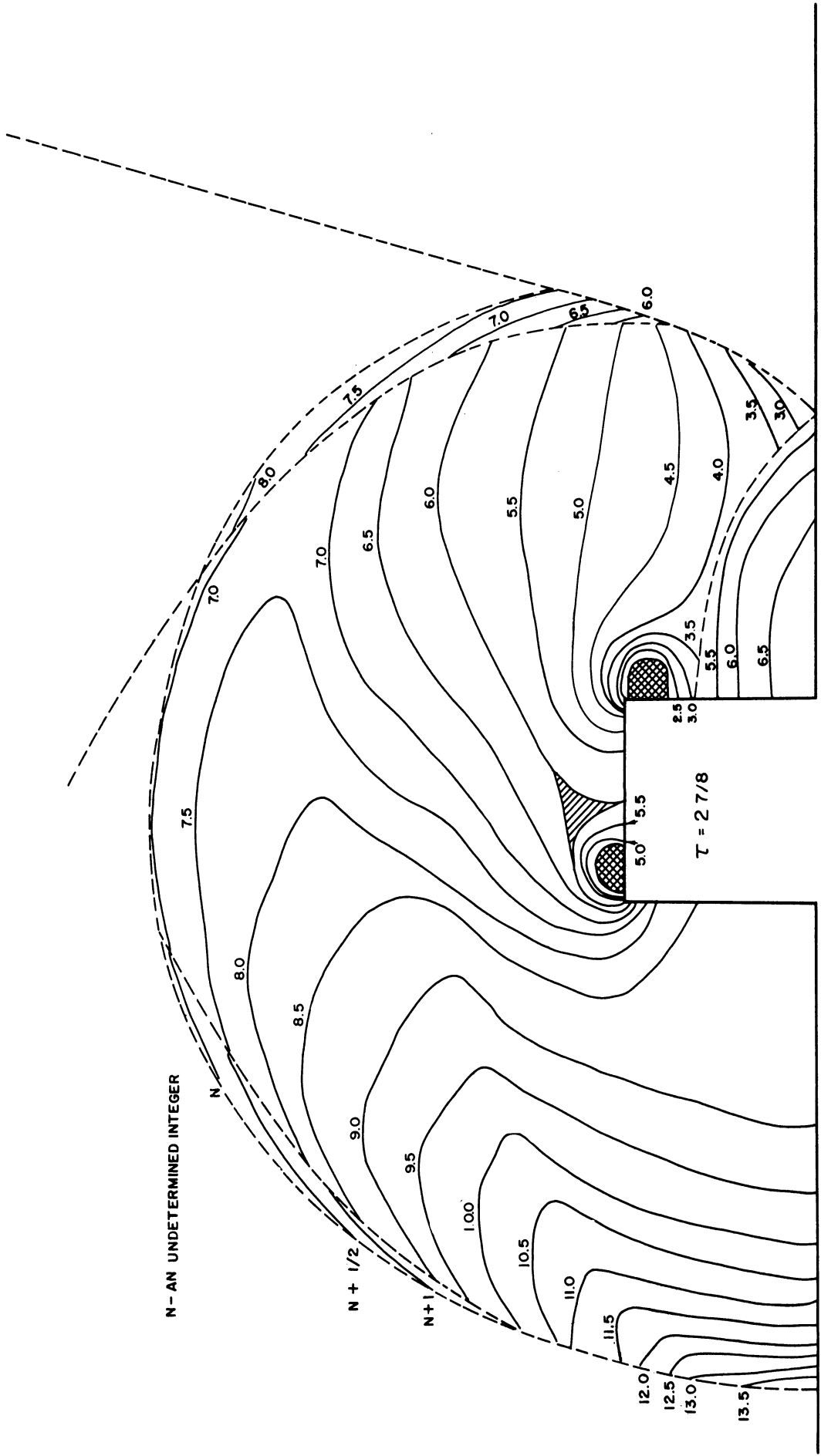
N - AN UNDETERMINED INTEGER



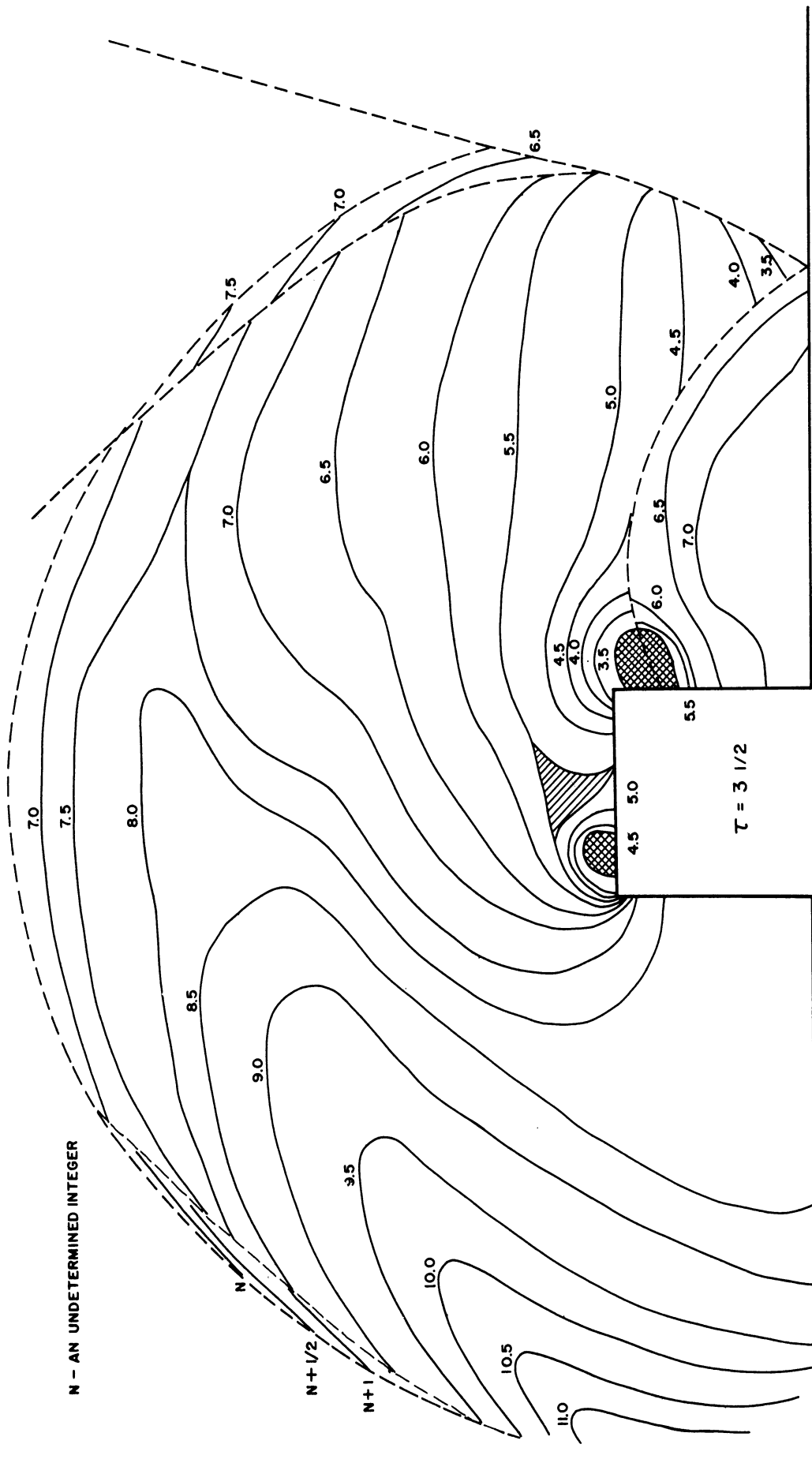
N - AN UNDETERMINED INTEGER





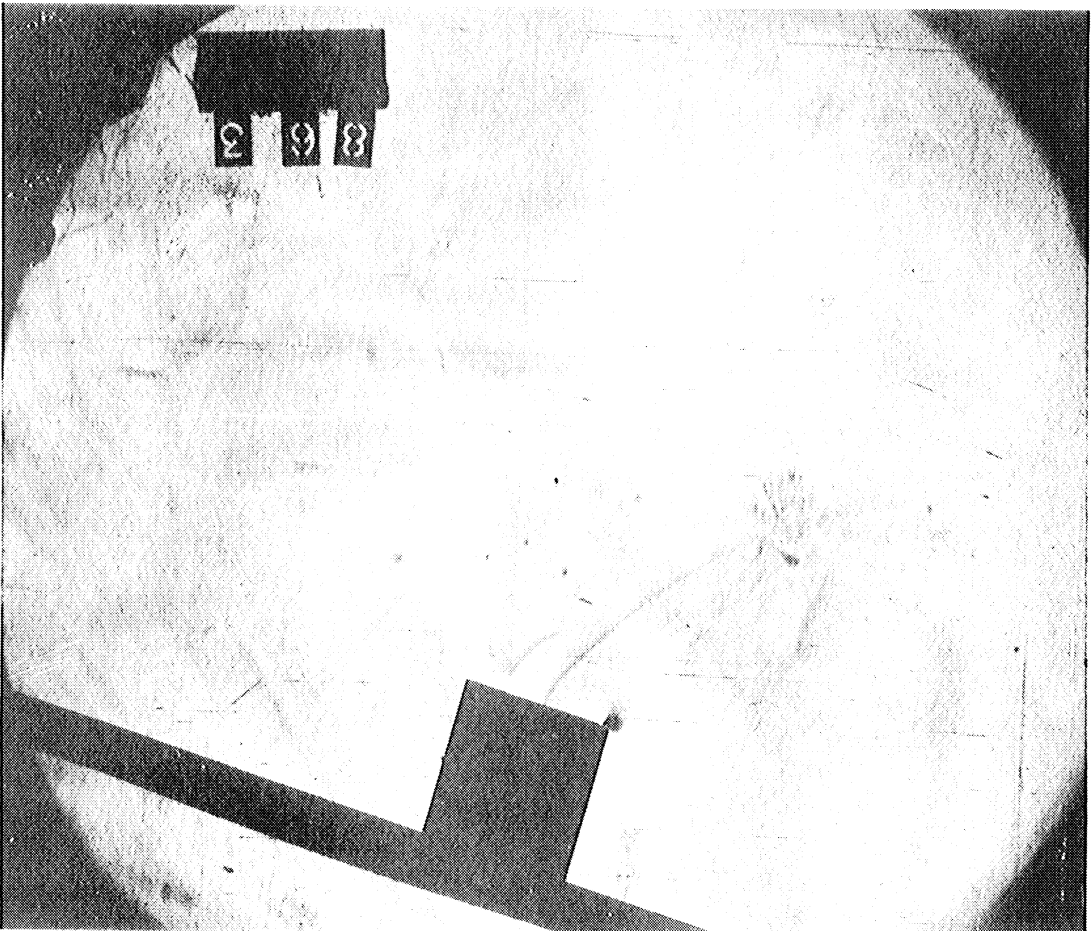
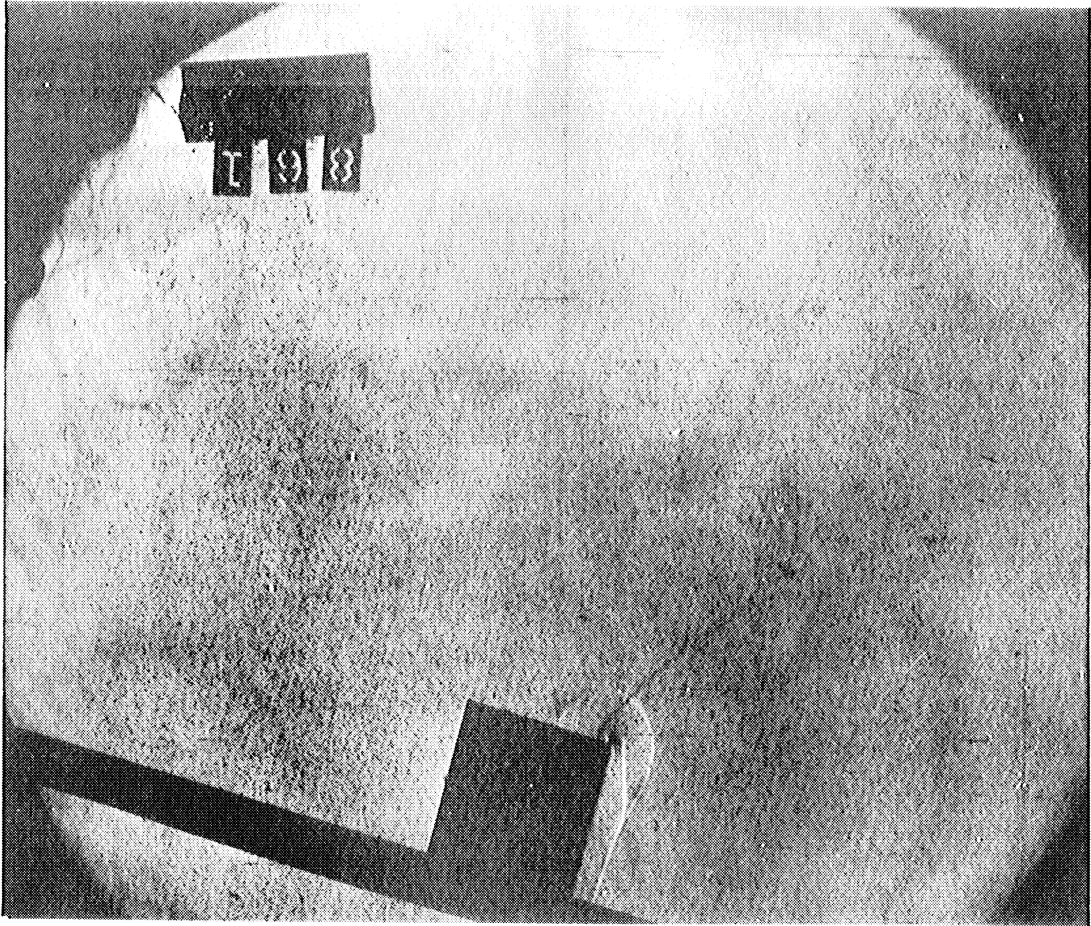


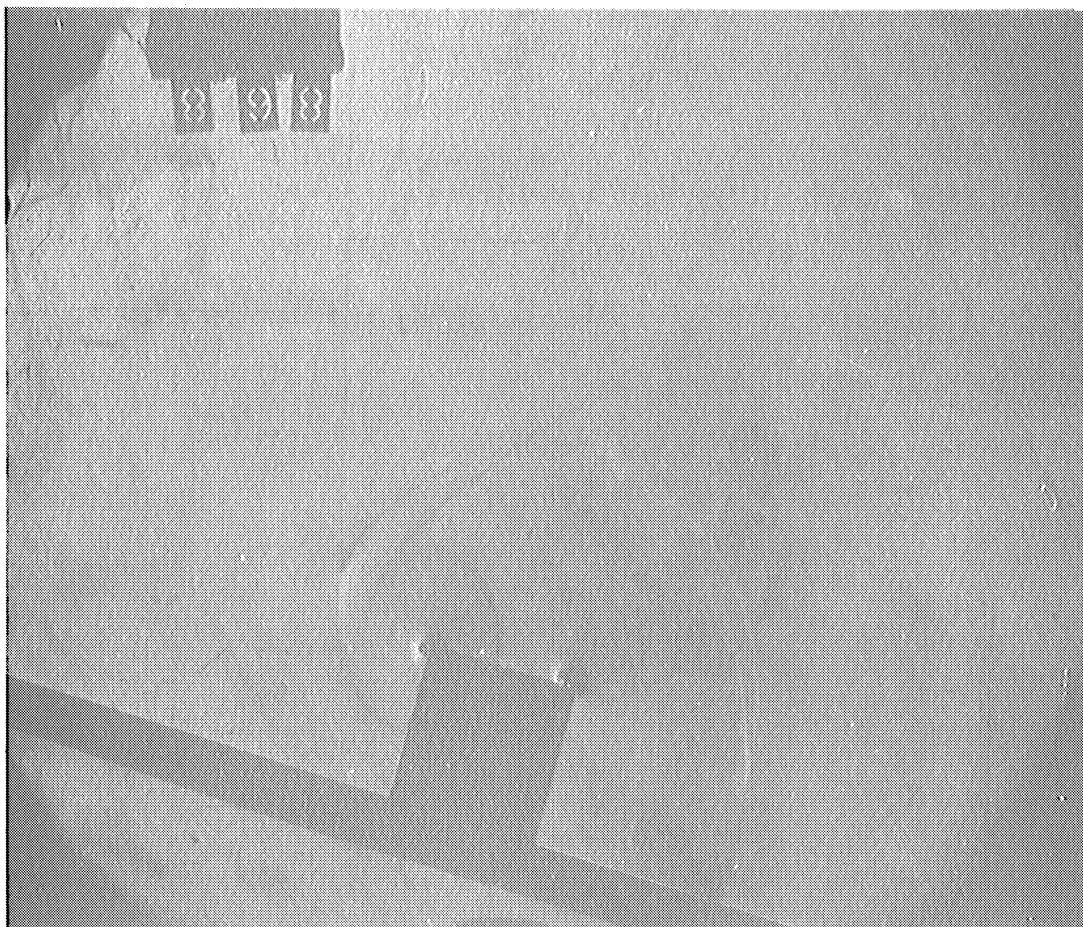
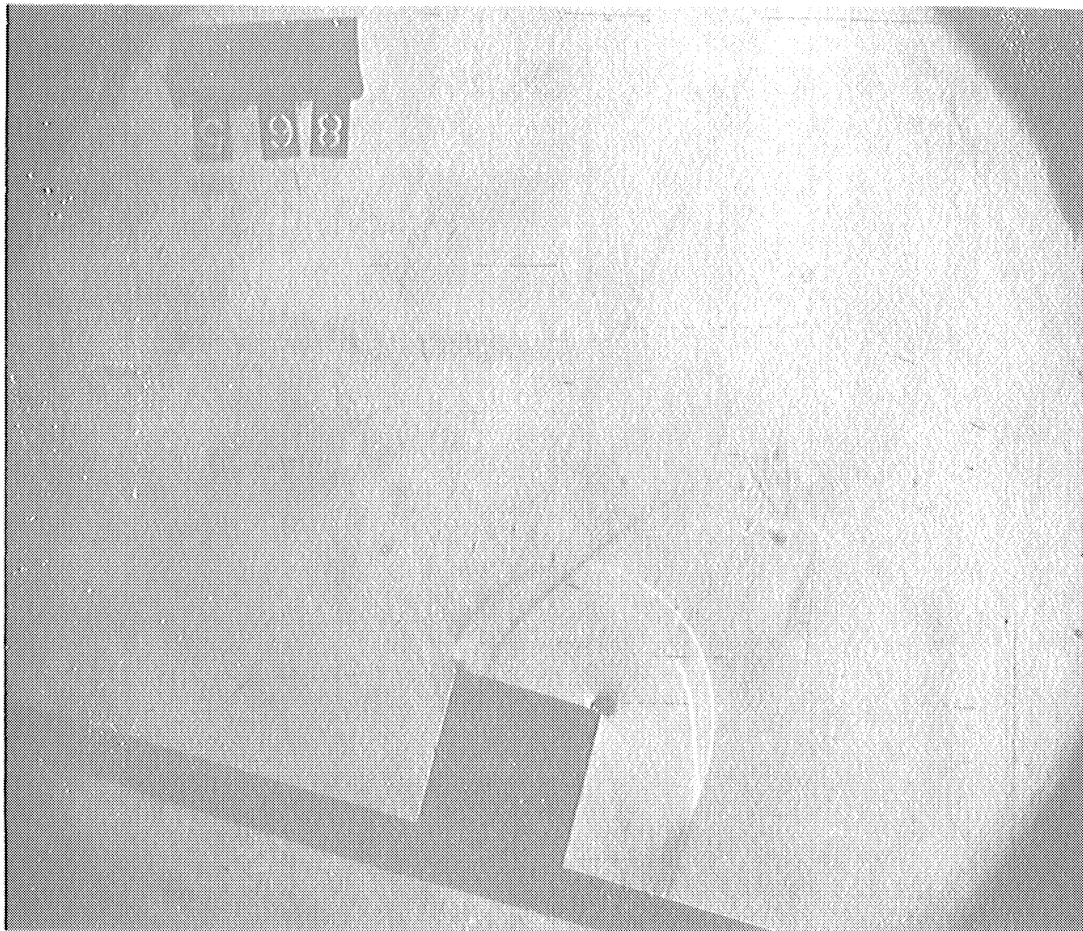
N - AN UNDETERMINED INTEGER



N - AN UNDETERMINED INTEGER

N
 $N + 1/2$
 $N + 1$





SERIES VII

Shock strength..... $\gamma = 1.33$

Mach stem height..... 1

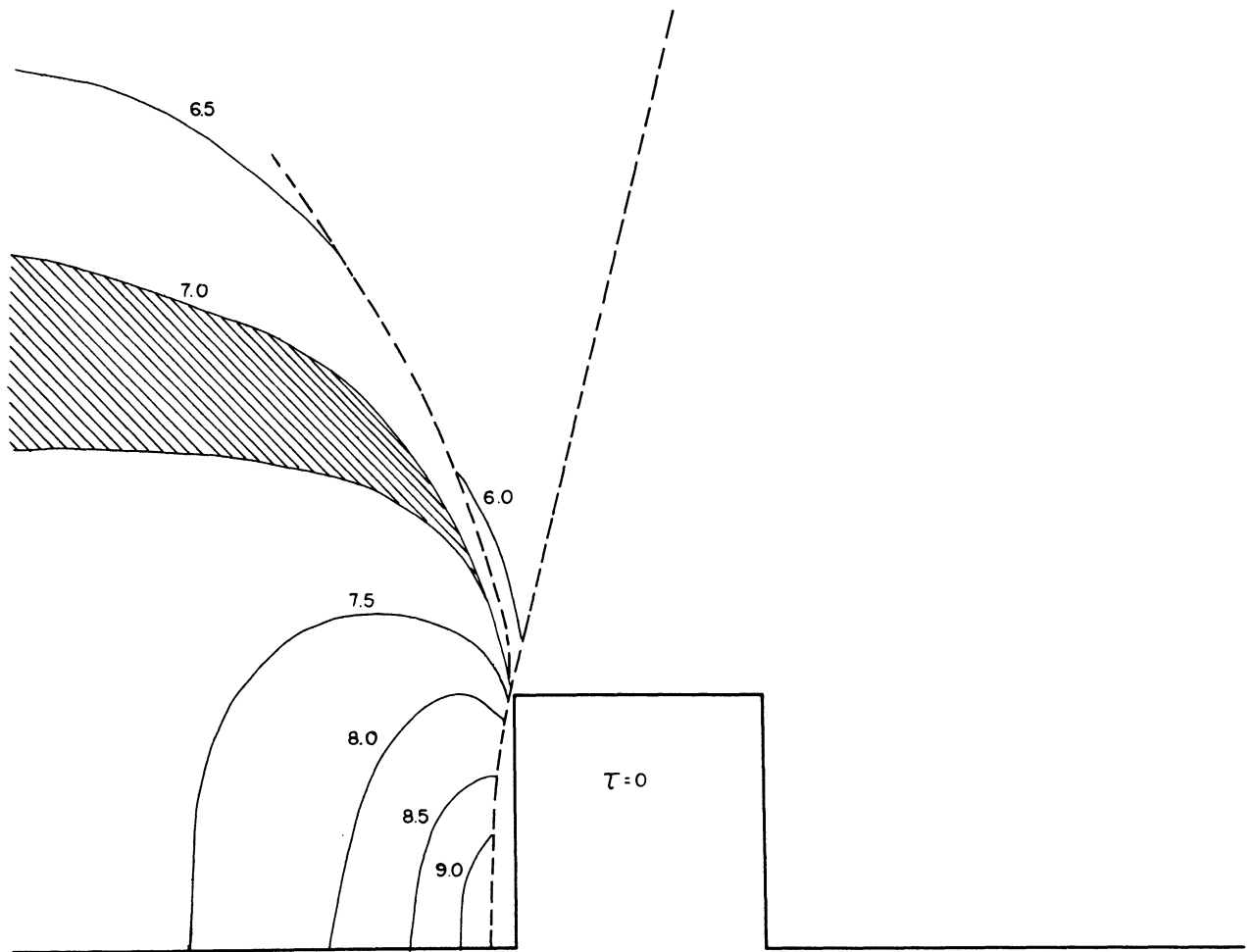
Block height..... 1

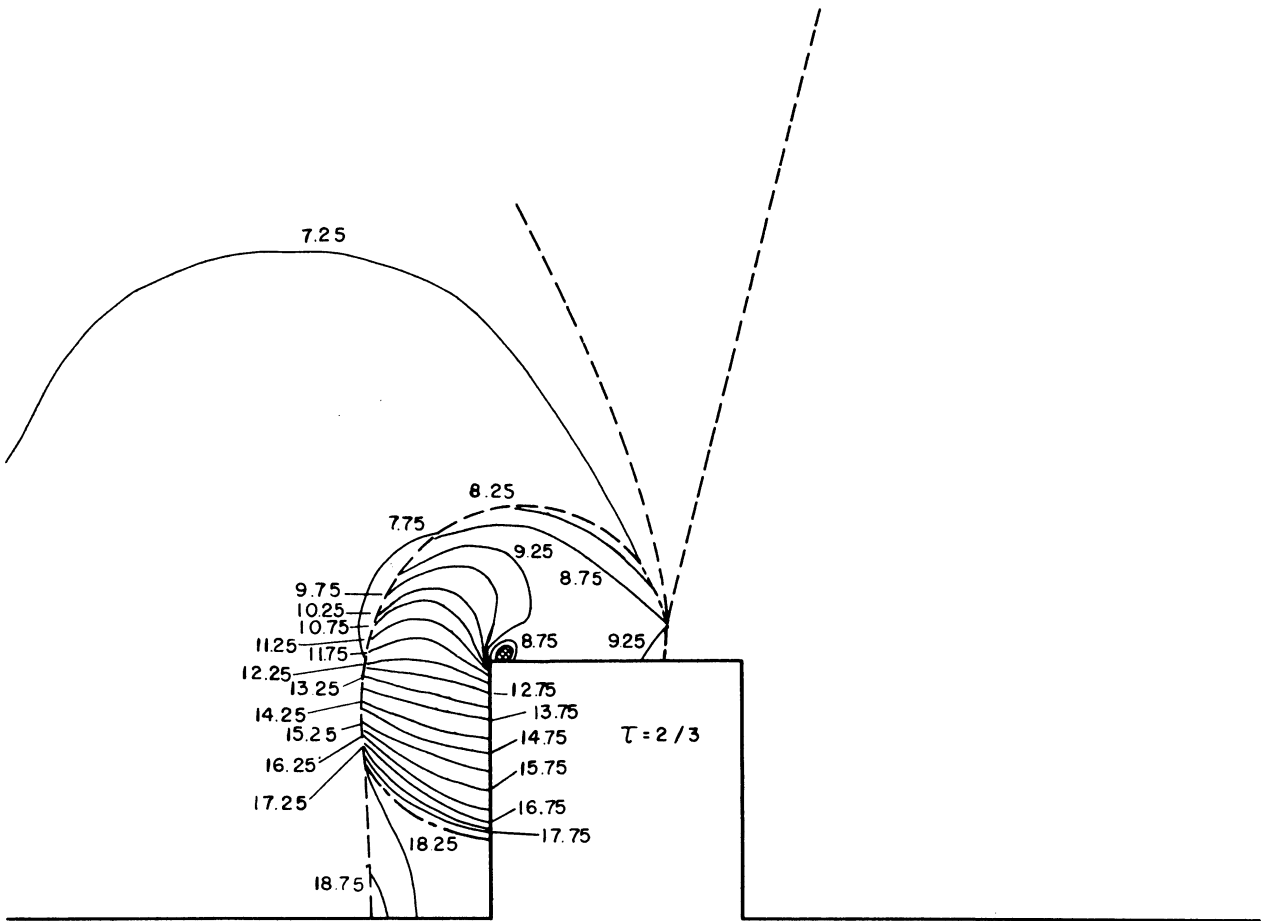
Angle of incidence..... 75°

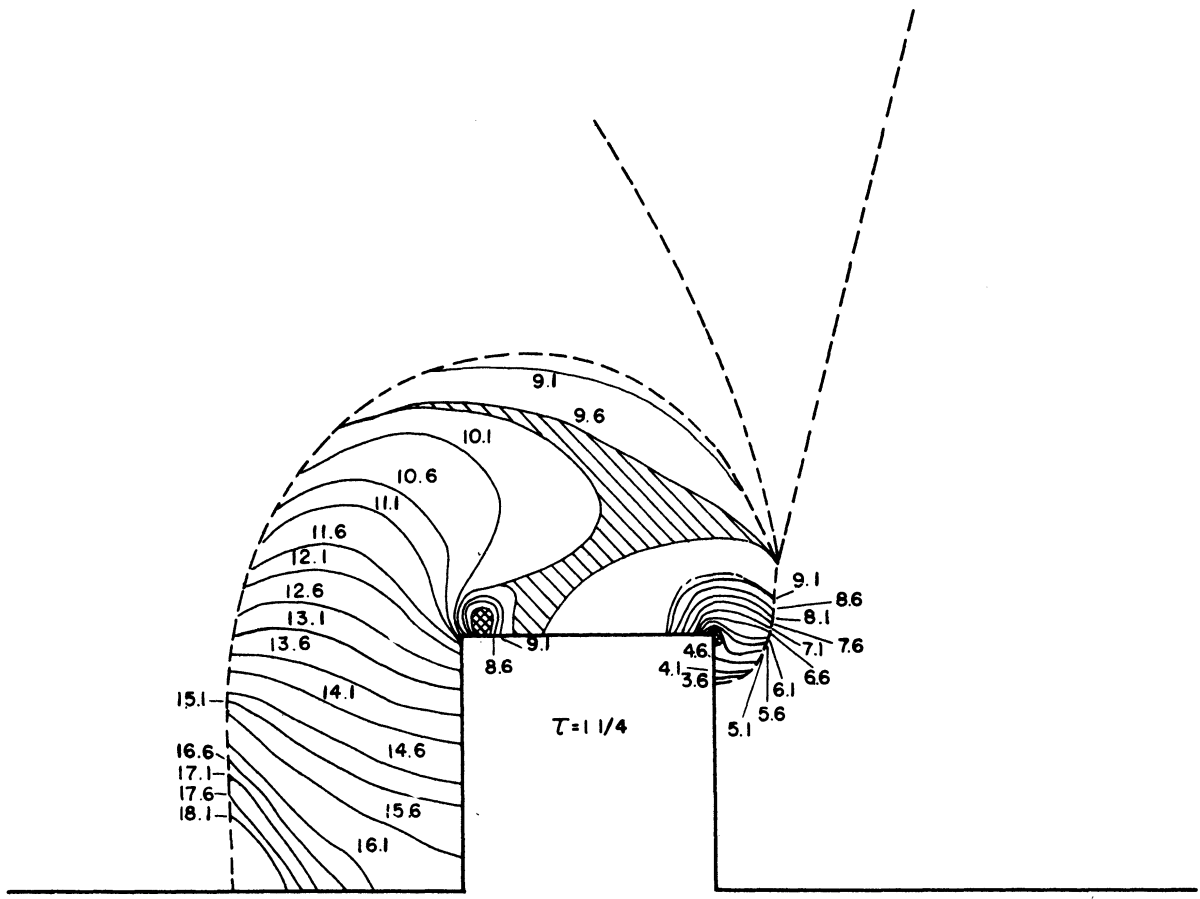
Density ratio..... $\frac{\rho_1}{\rho_0} = 1.223$

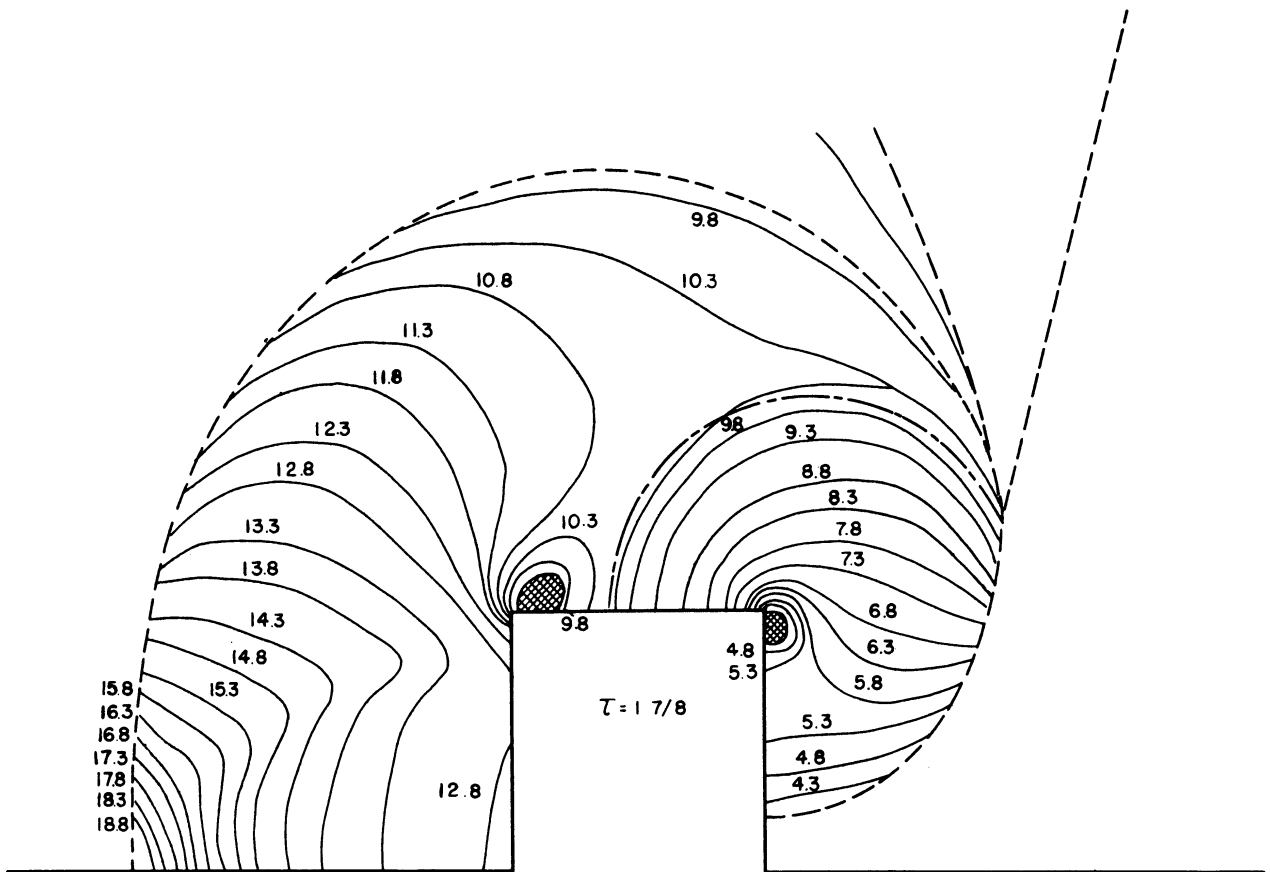
Pressure..... $P_0 = 737$ mm Hg.

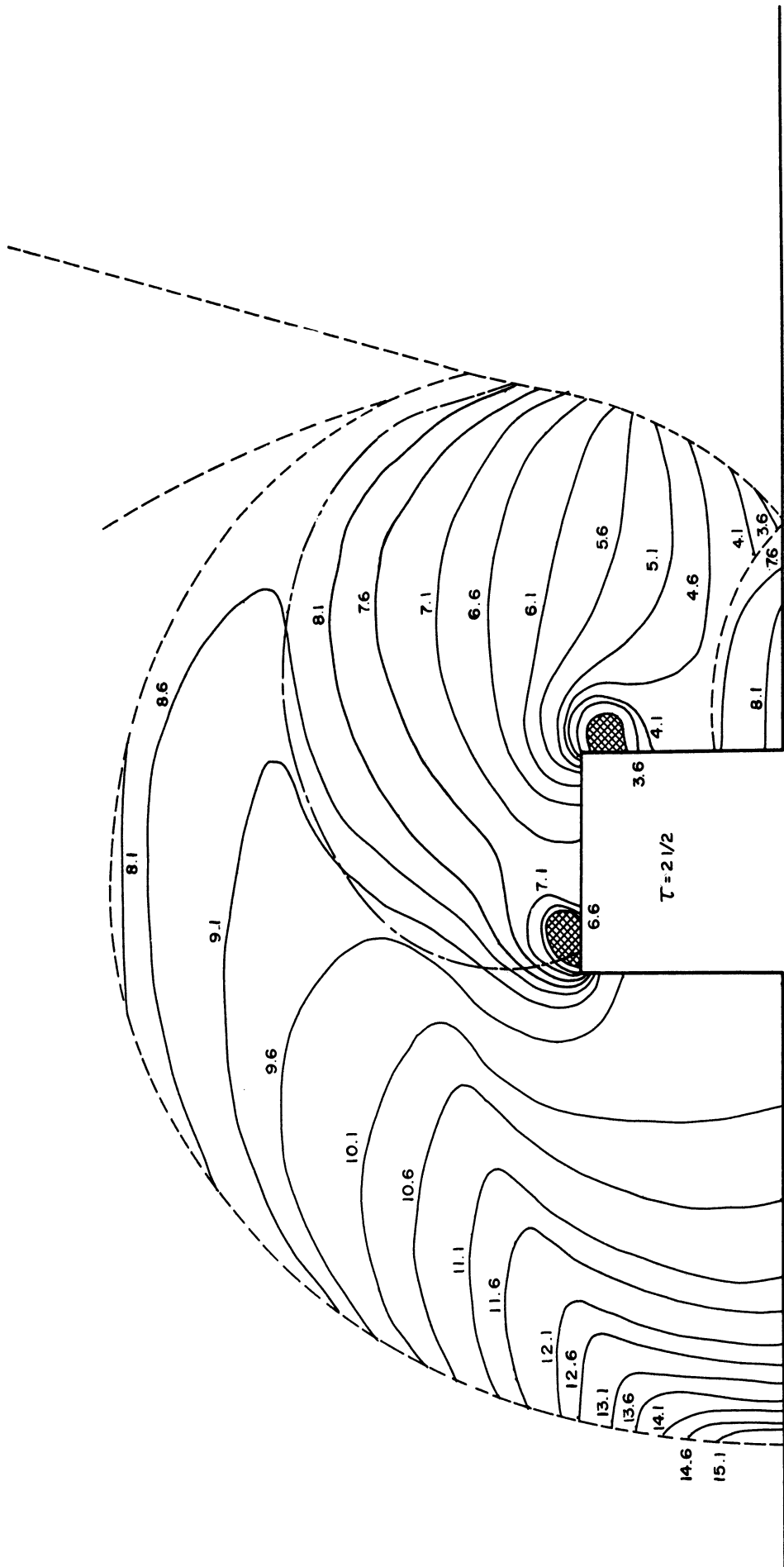
Shift across incident shock... $n_1 = 5.75$

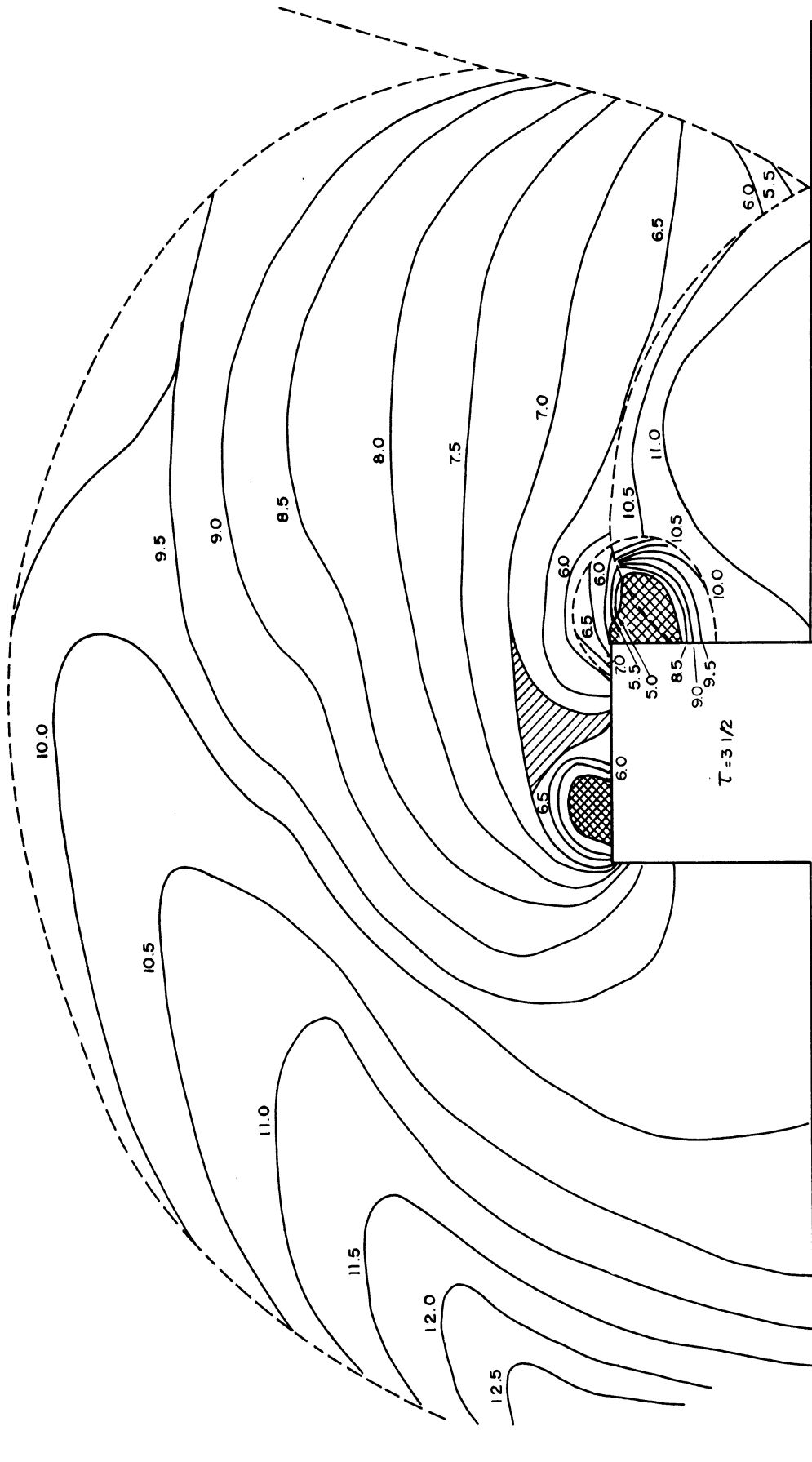


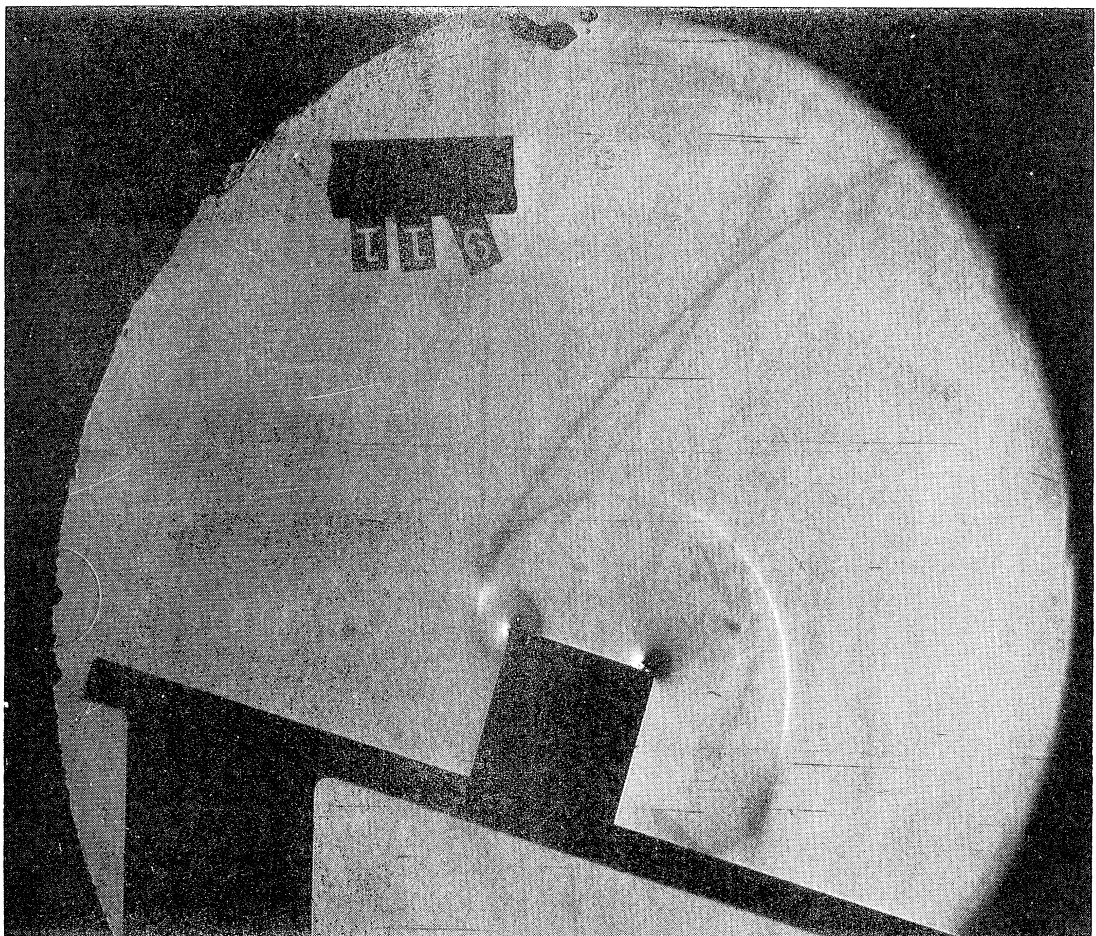
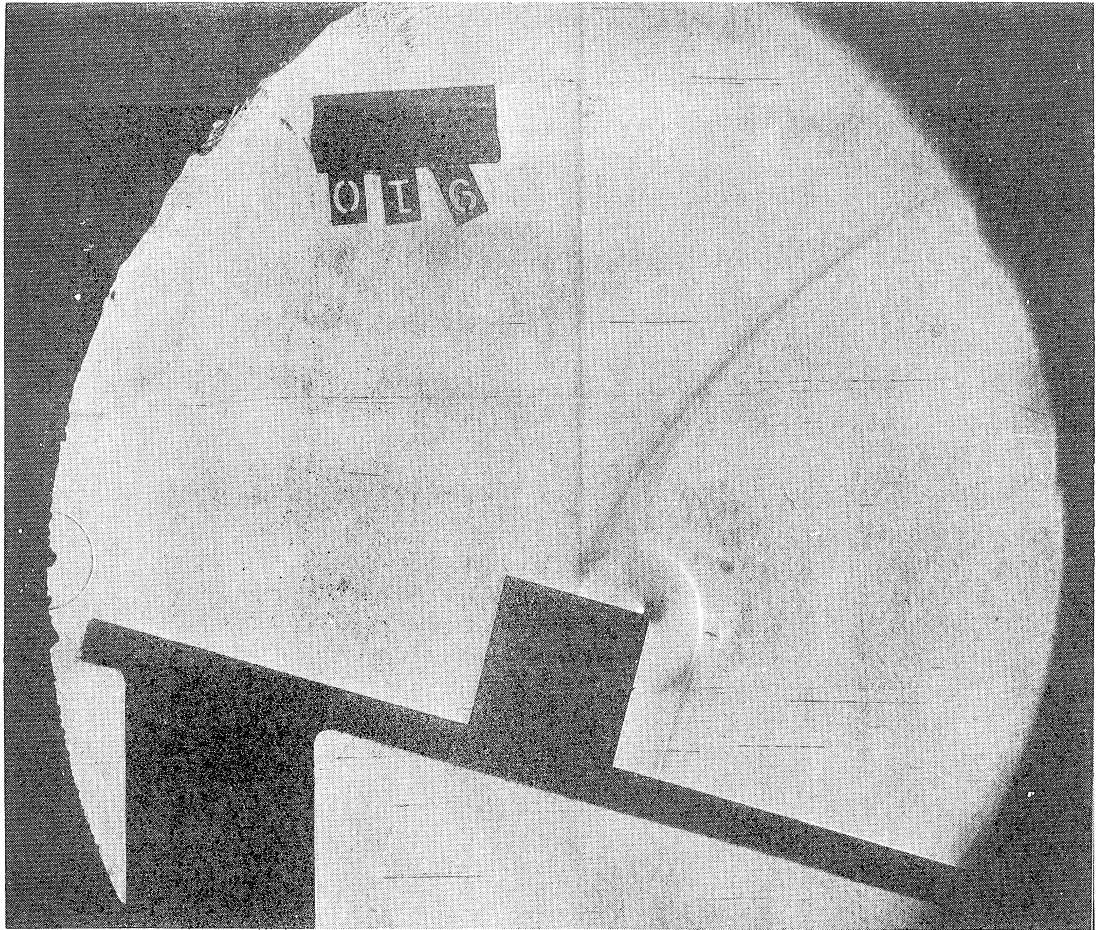


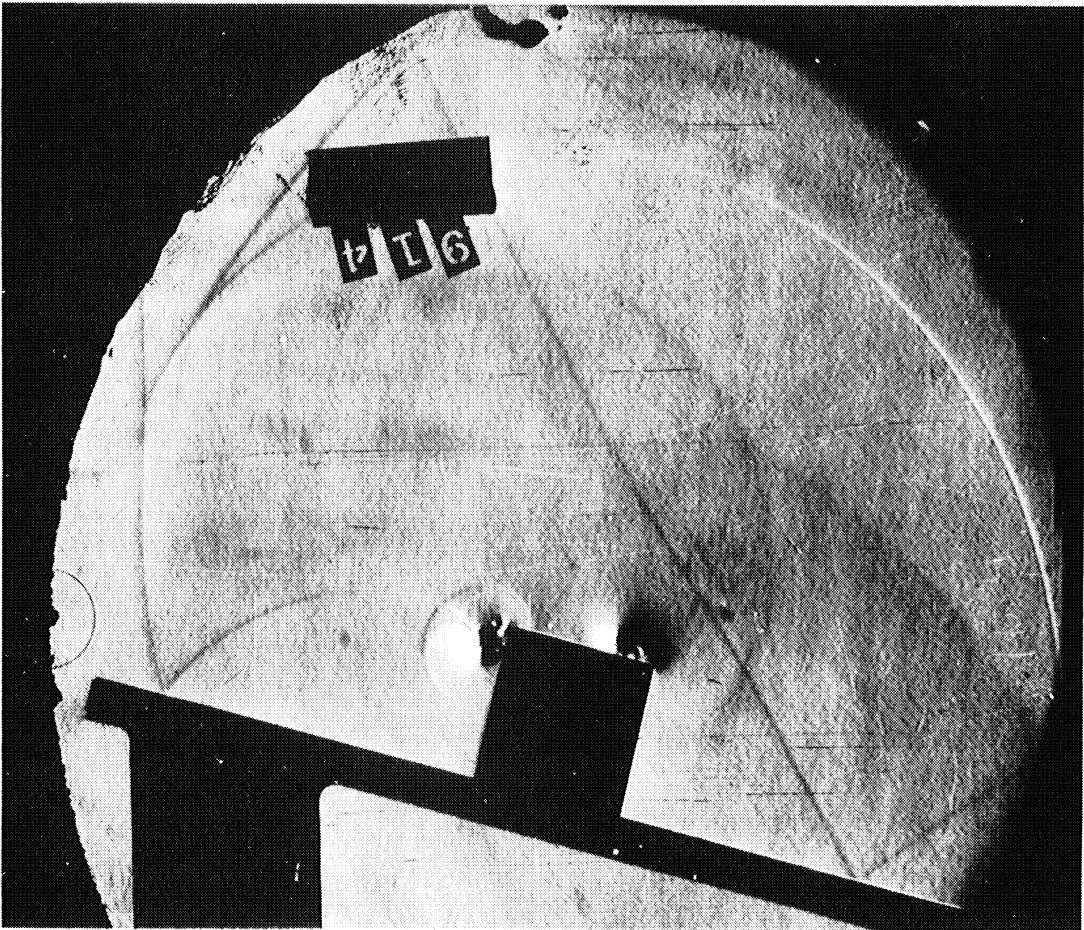
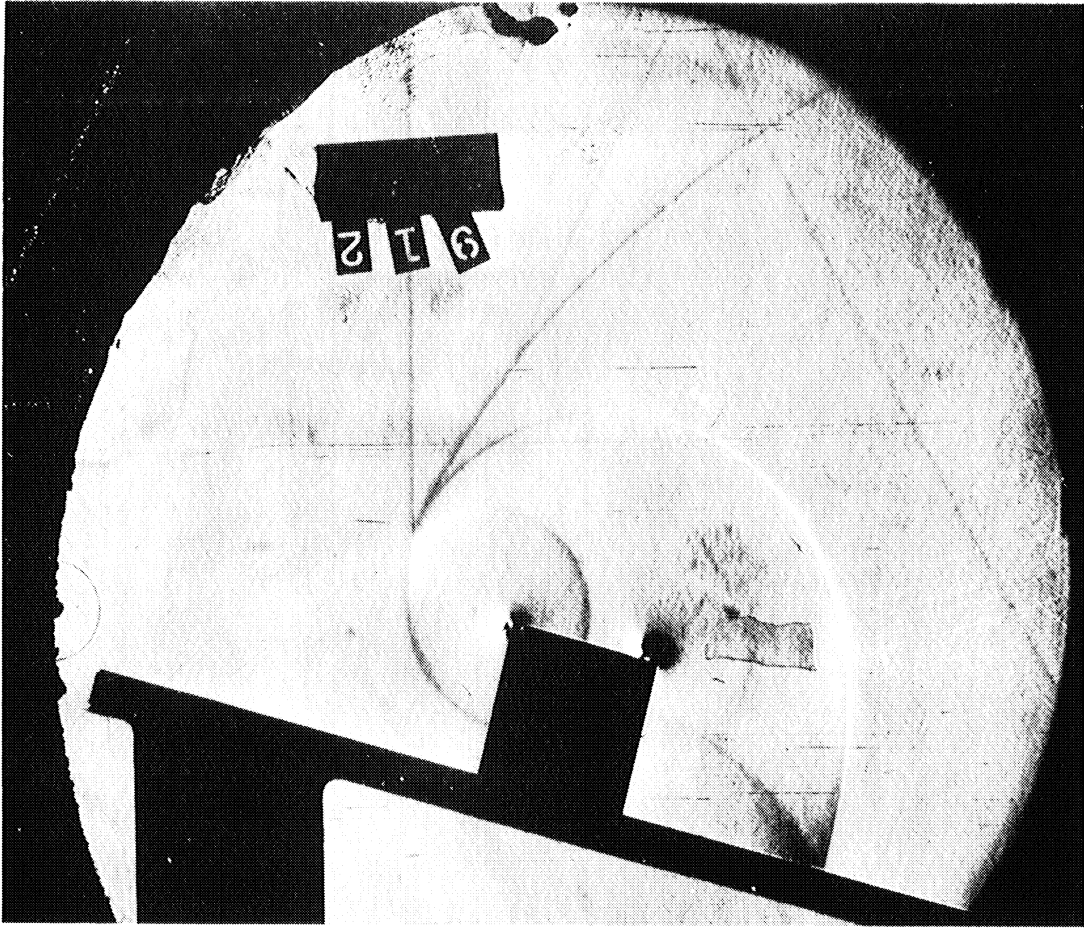












SERIES VIII

Shock strength..... $\gamma = 1.33$

Mach stem height..... 2

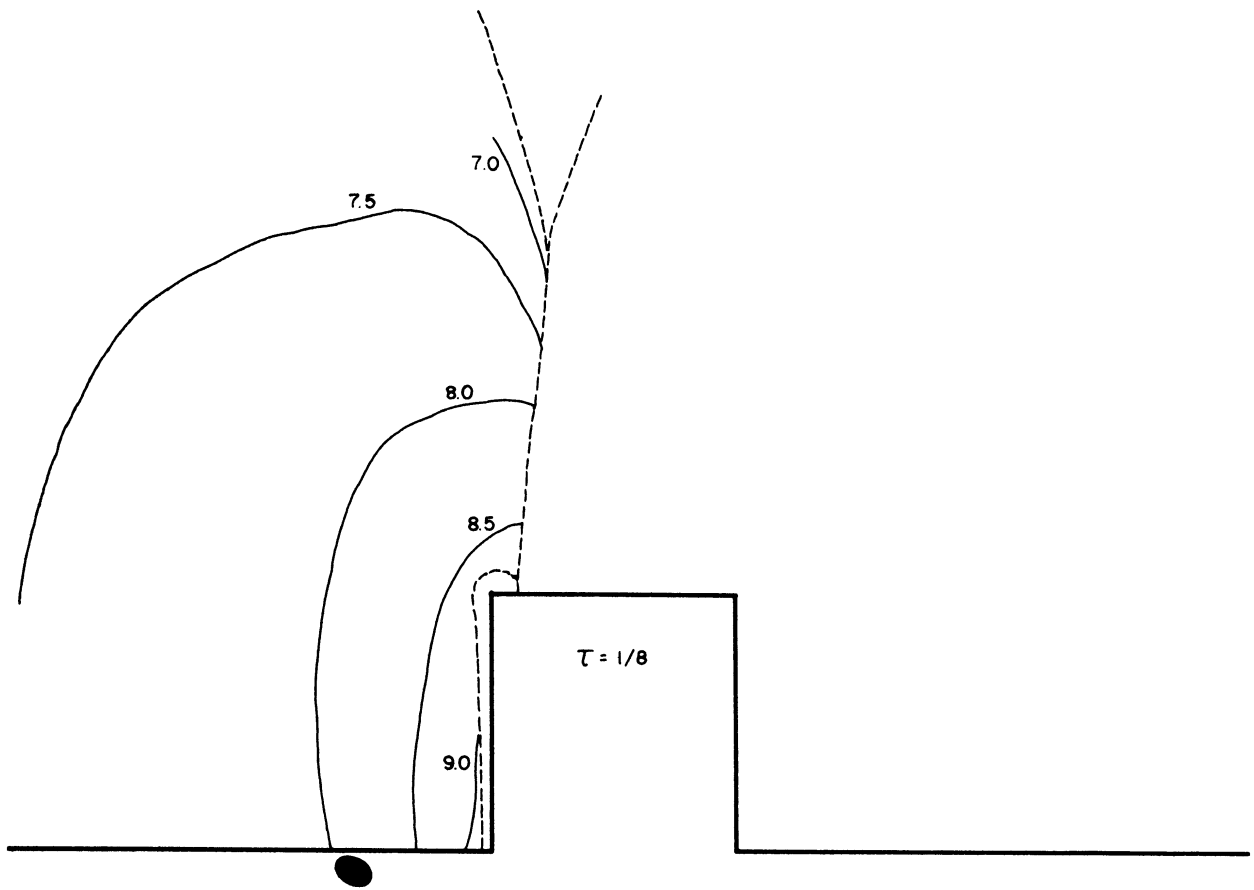
Block height..... $3/4$

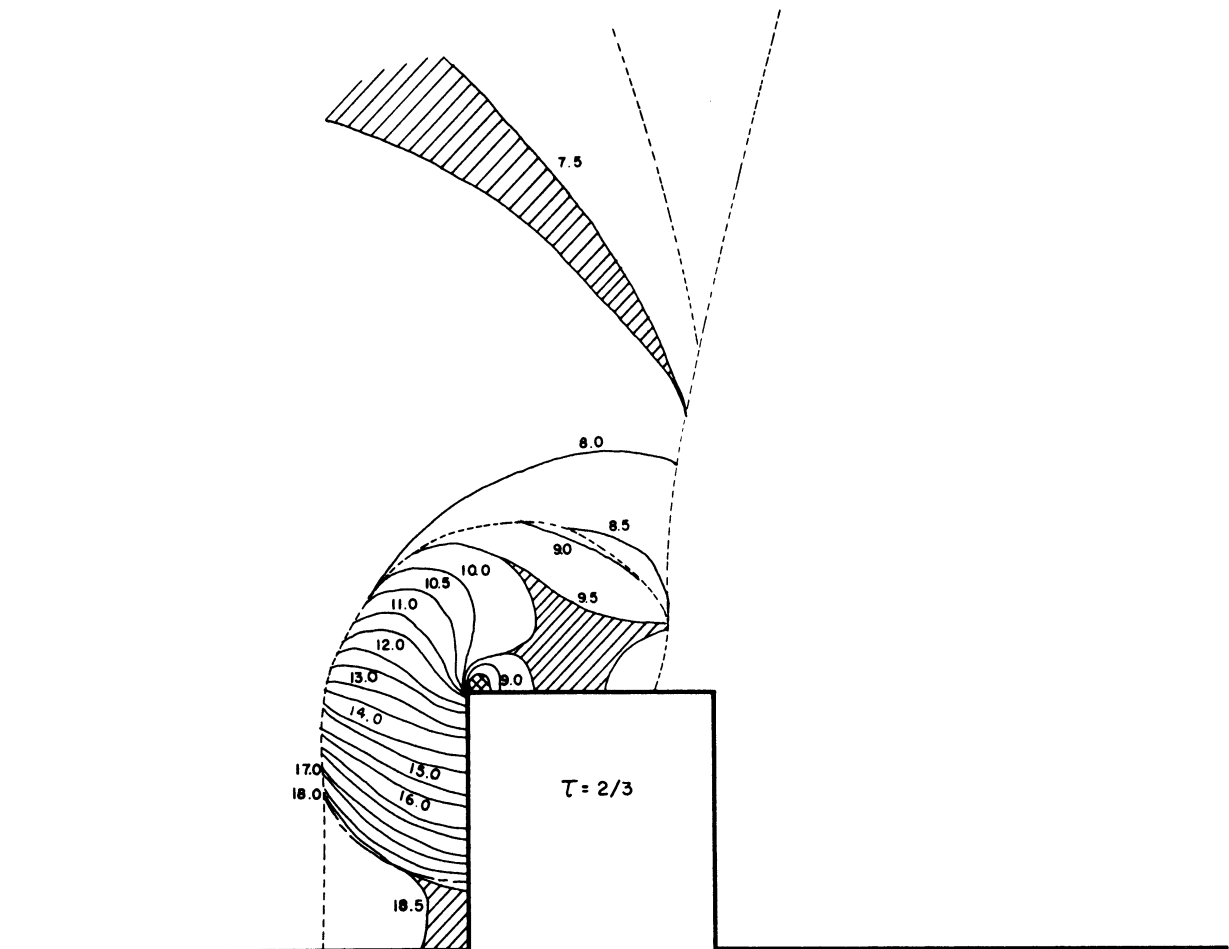
Angle of incidence..... 75°

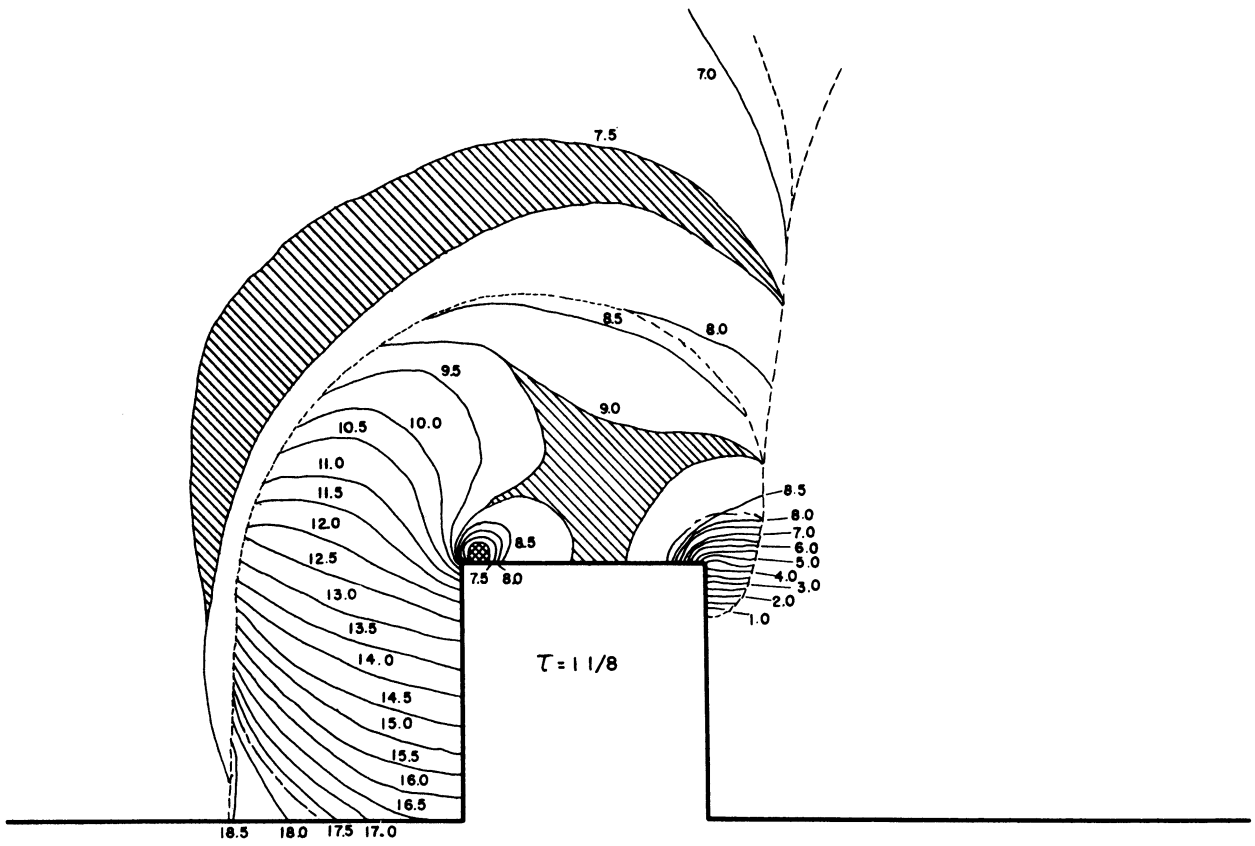
Density ratio..... $\frac{\rho_1}{\rho_0} = 1.223$

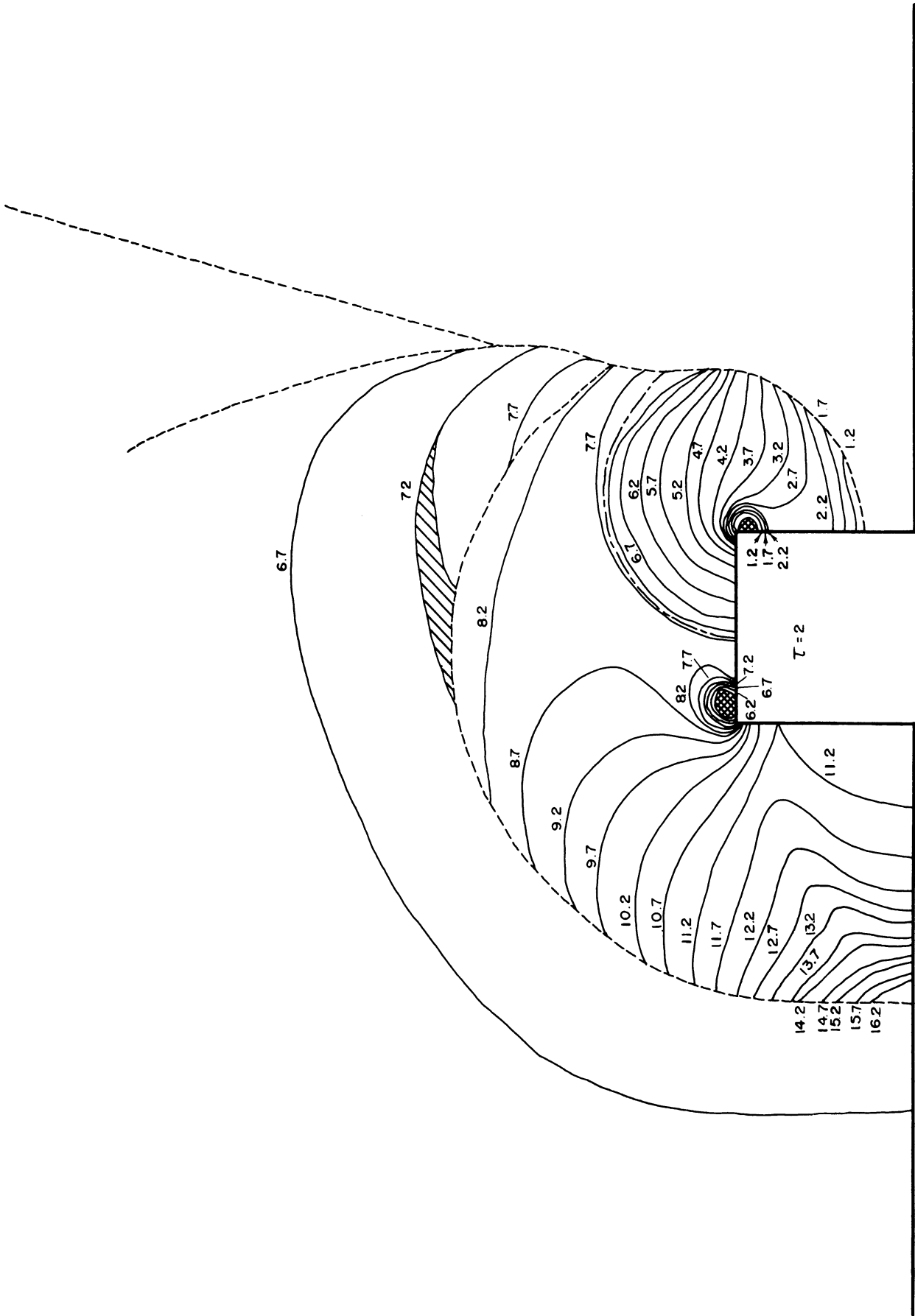
Pressure..... $P_0 = 743 \text{ mm Hg.}$

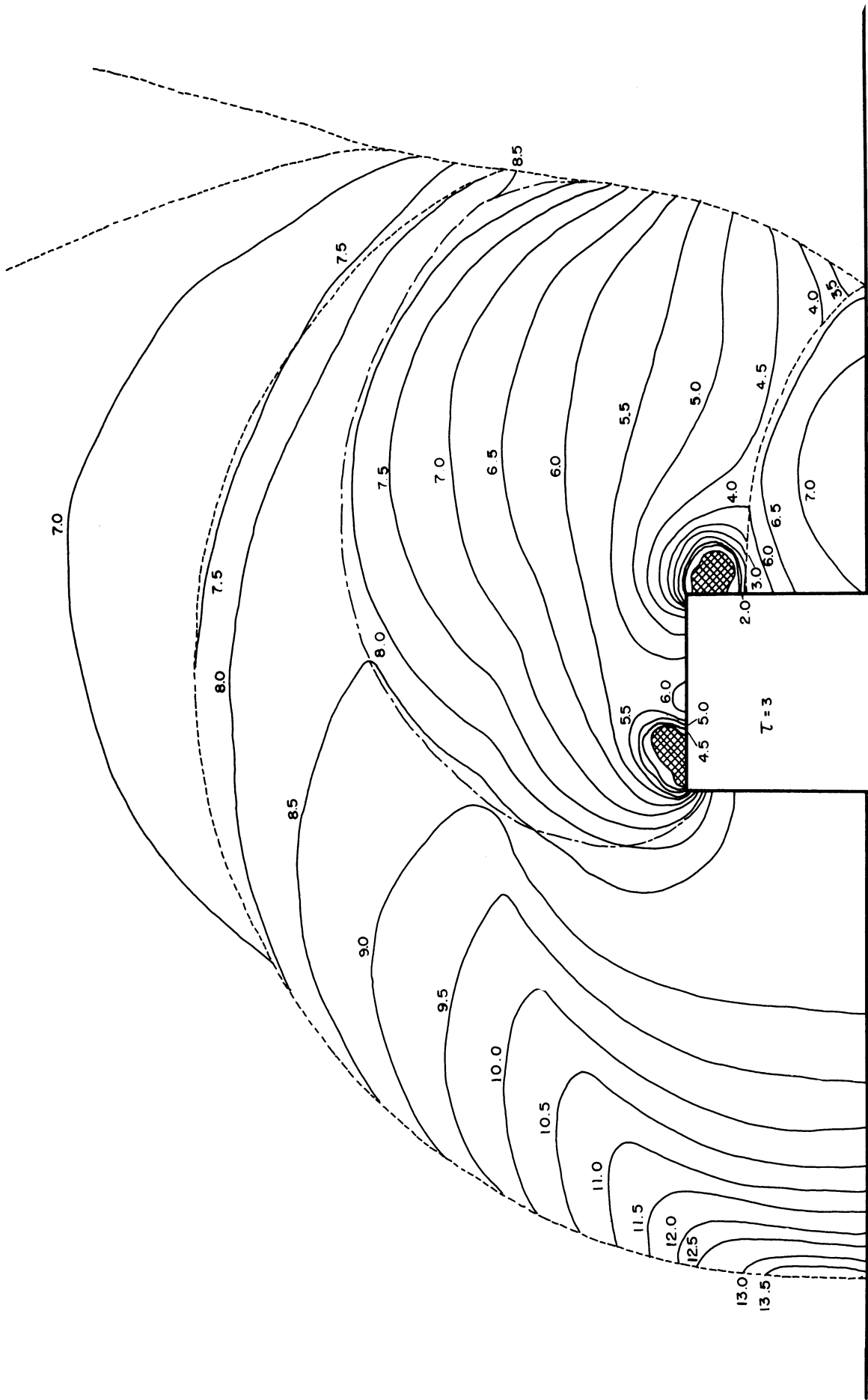
Shift across incident shock... $n_1 = 5.75$

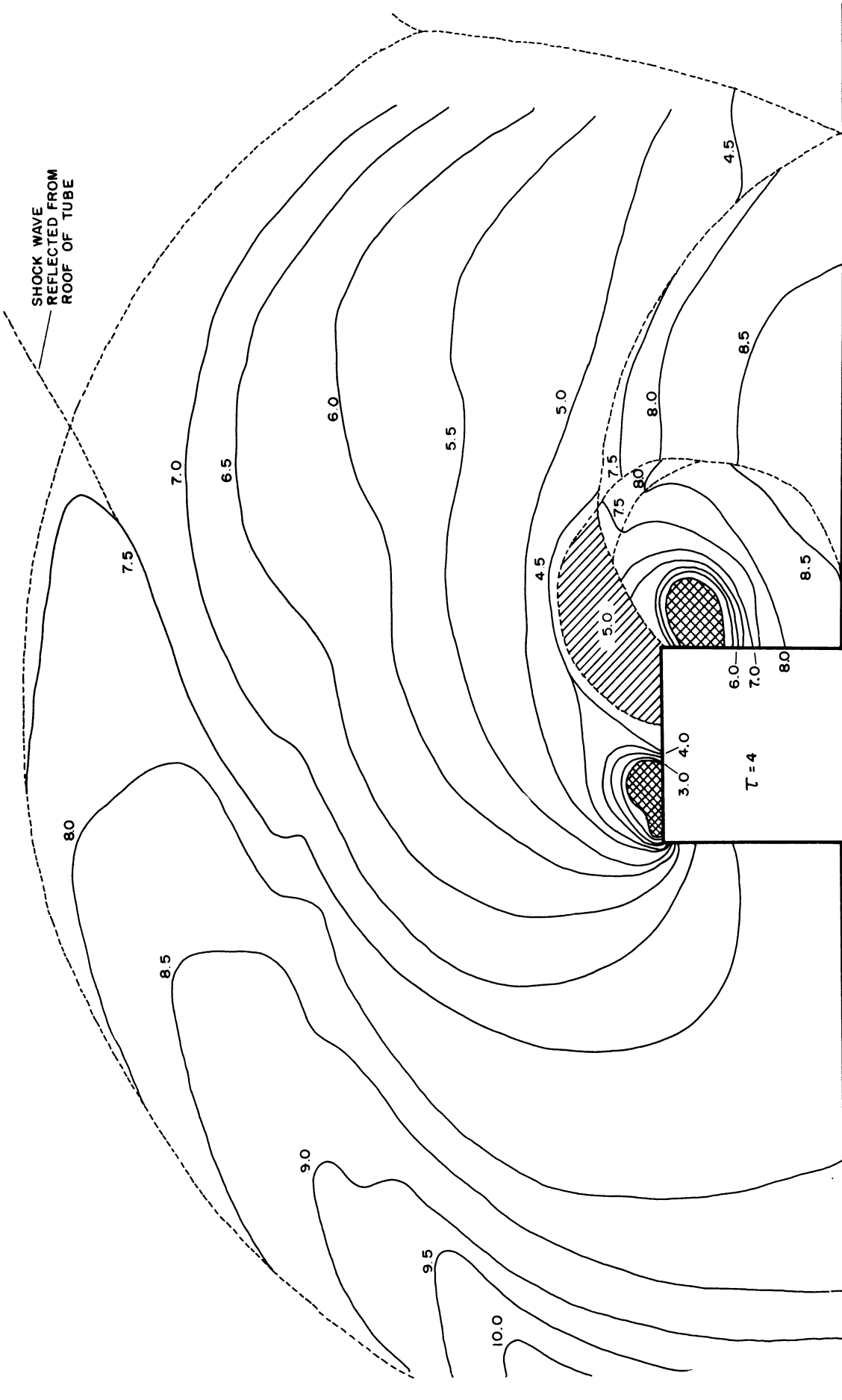


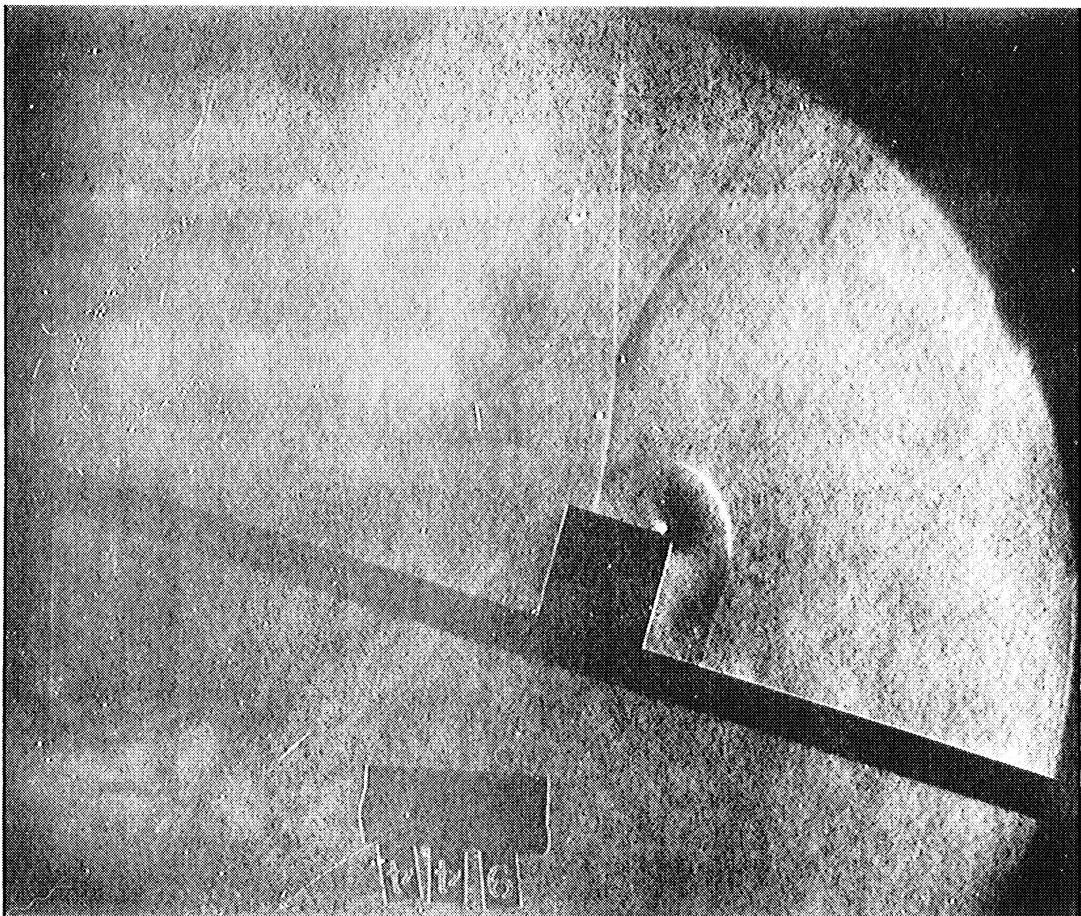
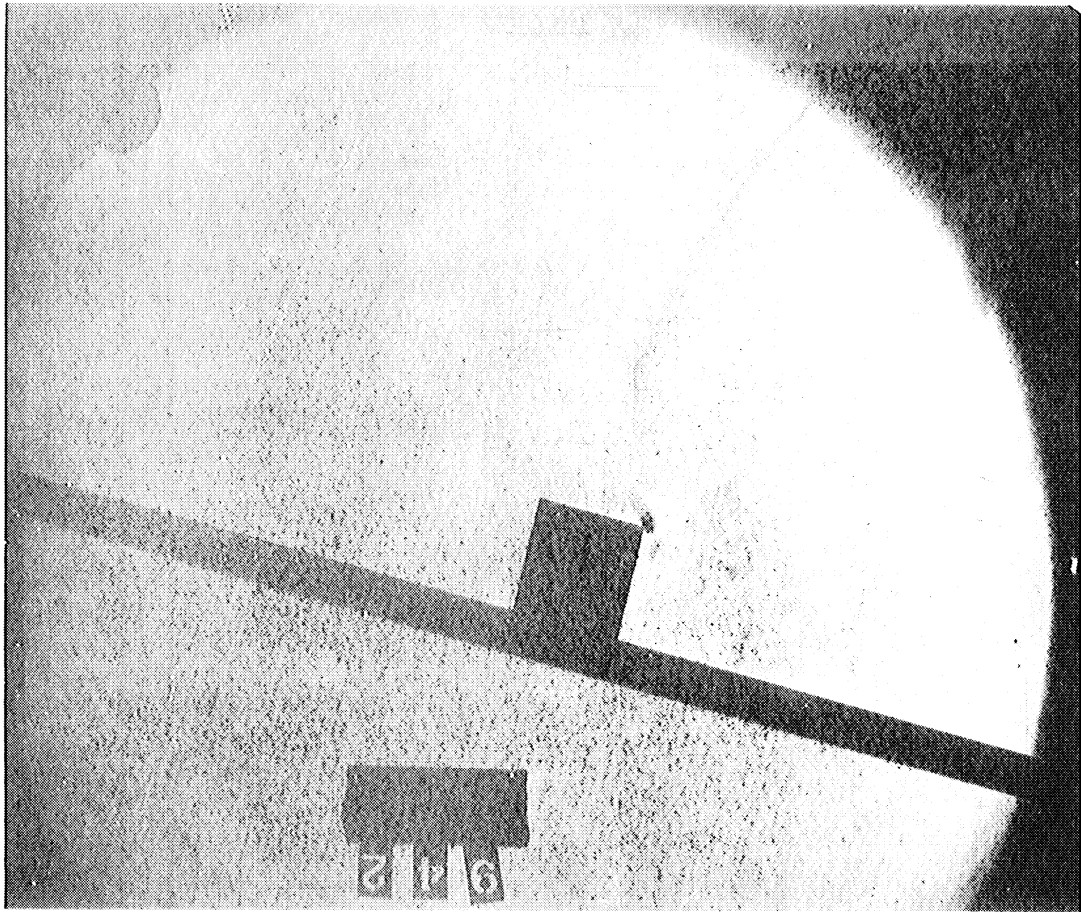


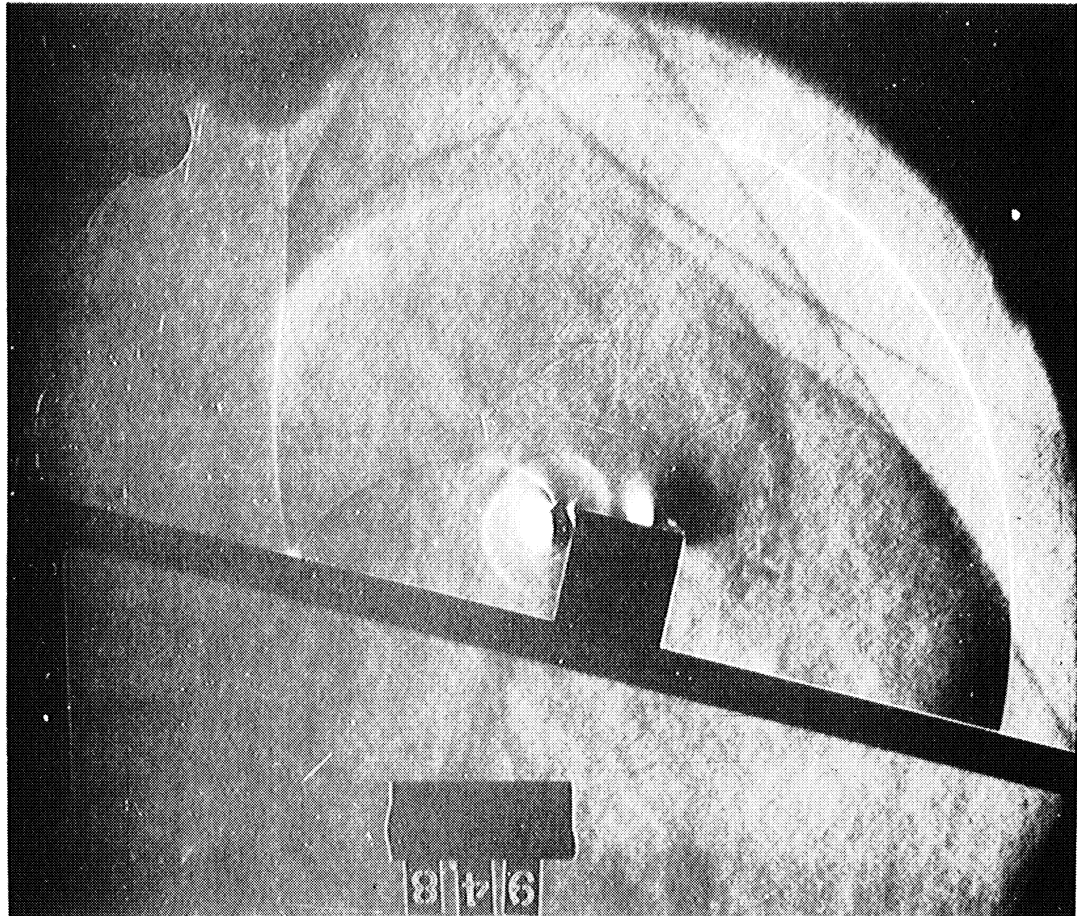
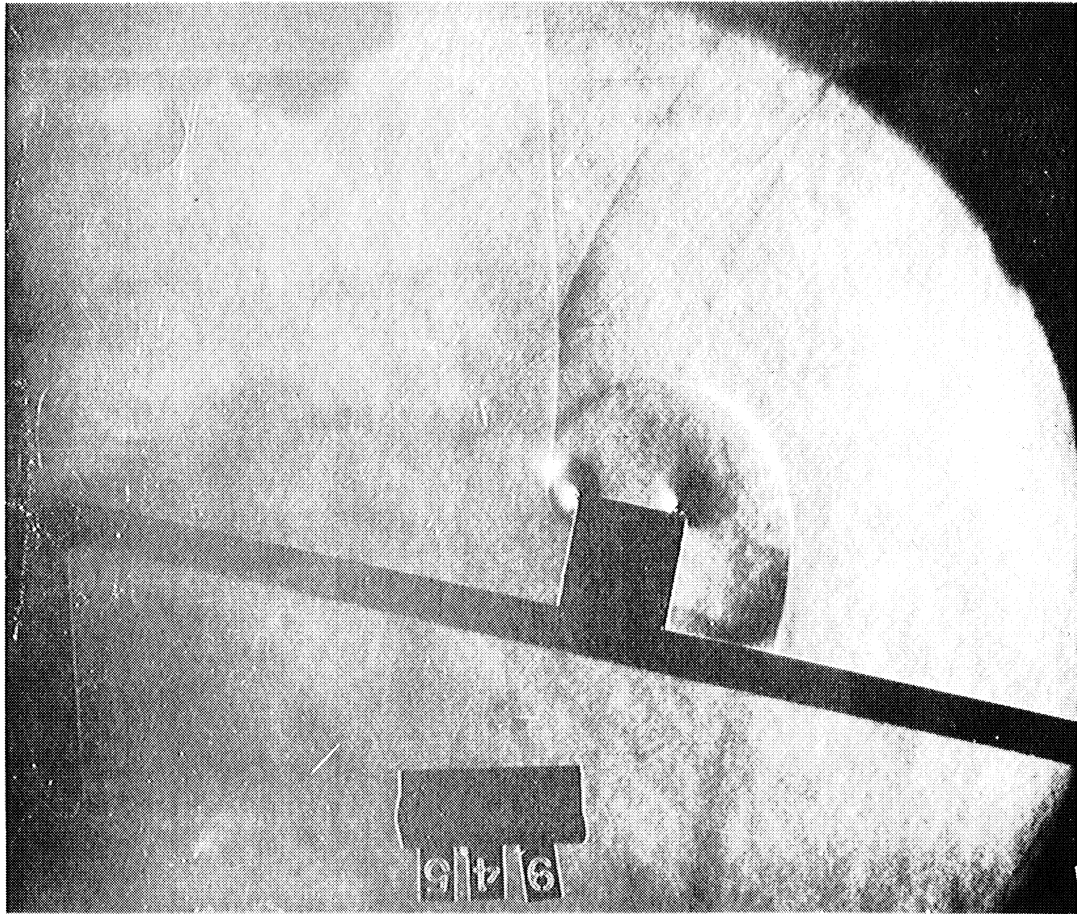












SERIES IX

Shock strength..... $\gamma = 2.02$

Mach stem height..... $1/2$

Block height..... 1

Angle of incidence..... 60°

Density ratio..... $\frac{\rho_1}{\rho_0} = 1.630$

Pressure..... $P_0 = 500$ mm Hg.

Shift across incident shock... $n_1 = 11.56$

